



UNIVERSITA' DELLA CALABRIA

Dipartimento di Ingegneria Informatica, Modellistica, Elettronica e
Sistemistica

Dottorato di Ricerca in
Ambiente, Salute e Processi Ecosostenibili

XXVII Ciclo

Modeling of mixing and drying processes in pasta production

S. S. D.

ING-IND/24 PRINCIPI DI INGEGNERIA CHIMICA

Coordinatore: Ch.mo Prof. Bruno de Cindio

Firma 

Supervisore/Tutor: Ch.mo Prof. Noemi Baldino

Firma 

Dottorando: Dott./ssa Ilaria Carnevale


Firma 

Table of contents

Introduction I

Chapter I – Dough of durum semolina 1

1. Introduction 1

2. Durum wheat composition..... 2

 2.1 Starch 3

 2.2 Wheat proteins 4

 2.3 Other components 6

3. Dough development..... 7

4. Factors affecting dough during mixing 9

5. Dough making process..... 13

6. Phase transition 19

REFERENCES 22

Chapter II – Small strain characterization of durum semolina dough 27

1. Introduction..... 27

2. State of art 28

3. Materials and methods 30

 3.1 Dough preparations and mixing..... 31

 3.2 Samples preparation..... 31

4. Rheological characterization: oscillatory tests 33

5. Weak gel model 34

6. Results and discussions..... 35

 6.1 Effect of time mixing..... 36

 6.2 Effect of temperature mixing..... 44

 2.3 Effect of temperature measure 51

REFERENCES 55

Chapter III – Large-deformation properties and microstructure of durum wheat dough.....58

1. Introduction58

2. State of art59

3. Data interpretation63

4. Extensional rheological theory64

5. Materials and methods67

6. SEM Analysis69

7. Results and discussions.....70

 7.1 Uniaxial elongation test70

 7.2 SEM Analysis results.....81

8. Conclusions85

REFERENCES86

Chapter IV 4 – Drying process: mathematical modeling90

1. Introduction90

2. State of art92

3. Physical phenomena94

4. Geometry of system96

5. Balance equation of system96

6. Boundary and initial conditions97

7. Thermodynamic and transport properties99

 7.1 Activity water99

 7.2 Transport of coefficients.....101

8. Material parameters103

 8.1 Properties of air.....103

 8.2 Properties of dough.....104

9. Shrinkage106

10. Method of calculation108

11. Results and discussion109

| | |
|---|------------|
| 11.1 Sensitivity Analysis | 110 |
| REFERENCES | 114 |
| Chapter V-Thermo elasto-viscous stresses | 117 |
| 1. Introduction | 117 |
| 2. Mariotte Analysis | 118 |
| 3. Material and methods | 122 |
| 4. Relaxation mechanism | 125 |
| 5. Result and discussion | 126 |
| REFERENCES | 133 |
| Conclusion | 134 |
| Proceeding of Italian Conferences..... | 136 |
| Activities | 136 |

I. Carnevale (2014), Modeling of mixing and drying processes in pasta production, Ph.D. Thesis

Keywords: gluten network; mixing stage; rheology; durum dough and texture.

Introduction

In the present PhD thesis has as purpose the study of mathematical modeling, experimental validation and optimization of transport phenomena that occur during the drying process in the production of dry pasta, as well as the study of the best process conditions to be used in the mixing step and drying of the dough according to the different operating parameters (time of mixing, the initial amount of protein, water temperature, mixing, etc.).

The aim of this thesis is to obtain a more accurate and predictive of the process and therefore an improvement in the quality of the final production.

This PhD thesis is the result of the project between the laboratory L.A.R.I.A. of the University of Calabria and the company RUMMO S.p.A (Benevento, Italy).

Pasta is made from a mixture of water and semolina. Semolina is a coarse-ground flour from the heart, or endosperm, of durum wheat, an amber-colored high protein hard wheat that is grown specifically for the manufacture of pasta.

The industrial process of drying pasta can be divided in seven steps: dosage, mixing, kneading, rolling, extrusion, drying and packaging.

Mixing and drying stage are considered a critical step of pasta production process.

The mixture that is obtained has a lower extensibility than the dough flour and water and a higher tenacity, has higher protein content and shows a greater capacity for water absorption.

Semolina dough strength is related to mixing condition and gluten composition. Gluten is a complex protein constituted by gliadin and disulfide-linked glutenin polymers. Gliadin contributes to dough extensibility and glutenin contributes to dough elasticity. The water is distributed among semolina particles to obtain the gluten network. In the early stages of mixing, glutenin this is arranged in a random and disordered. Subsequently, the appropriate hydration of gliadin and starch present, leads to an alignment of the fibers of glutenin and to the formation

of a fibrous mass and filamentous. The process of "unfolding" and "relaxing" continues throughout the mixing process allowing to achieve a more ordered structure. It has thus between the different chains, the formation of new and more regular bonds (cross-links) that stabilize and extend the structure. During the mixing stage, the interactions between the polymers cross-link became stronger and, as a consequence, dough strength, resistance to extension and restoring force after deformation increase.

These ties increase the resistance of the dough and its elasticity and the optimum time of mixing, the elasticity and the resistance of the dough reach their maximum value. A mixing time greater than the optimum time leads to the breaking of these bonds and the formation of a sticky dough and with low elasticity, while a shorter time leads to the obtaining of a more inconsistent and not developed.

The gluten network is characterized by: time to reach the maximum dough consistency, temperature of mixing and relative fraction of proteins in dough. In these study, semolina with different fraction of protein are analyzed.

Six samples of durum semolina with different protein content are analysed.

For each semolina is added the appropriate amount of water in order to obtain a mixture with 34% moisture on a wet basis. The mixing phase has a total duration of 35 minutes. In order to characterize the behaviour of the dough of the tests were carried out for different mixing times and for different temperatures of the process.

Dough rheological properties are measured with the dynamic oscillatory test (chapter 2) and in uniaxial extension (chapter 3) with the main purpose to investigate the optimum network formation for high quality pasta dough during mixing. The oscillatory tests have been revised according to the parameters A and z. Dates are fitting with the model of weak-gel (chapter 2). Instead, the tests in uniaxial elongation have been restated by the index of strain hardening. Experimental dates are fitting the equation of Hollomon (chapter 3).

In order to verify what has been obtained by the tests in uniaxial elongation, the tests were performed of scanning electron microscopy, using SEM analysis (chapter 3).

In order to optimize the time industrial drying of the paste and, simultaneously, increase the quality and production of the same, avoiding an excessive volume of waste, successive stages of drying and tempering, which avoid the problems of breakage, caused by the fact that the outer layers, placed in contact with the fluid desiccant, show a more rapid contraction compared to the inner layers, which exchange matter with difficulty.

This has been carried out writing of a mathematical model of the process that requires writing the balance equations of momentum, of energy and matter coupled with the appropriate boundary conditions, which through the use of appropriate dimensionless analysis, can be explained in terms of transport coefficients, as it is discusses in the chapter IV.

In the simulation program, in the chapter V, is introduced the stress within pasta format laundry during the drying, the piece was treated as a tube of thin wall thickness δ , which contains in its interior a material elasto-viscous and treat the problem with analysis of Mariotte.

Chapter I

Dough of durum semolina

1. Introduction

Pasta is made by mixing of semolina and water under energy application at controlled temperature and moisture conditions.

The major use of durum wheat is for pasta and their final end-products quality is related to the durum grain, which, in turn, is mainly determined by the genotype, but also by the environment (weather and nutrition) and crop management [Troccoli et al., (2000)].

The wheat preferred for making pasta is durum *Triticum turgidum L.* subsp. *turgidum conv. durum* [Sissons, (2008)].

Durum is obtained from the endosperm of durum wheat and has an amber colour and high protein level that is grown specifically for the manufacture of pasta.

Three parts constitute the grain seed: the endosperm, the bran and the germ, as illustrated in Figure 1.

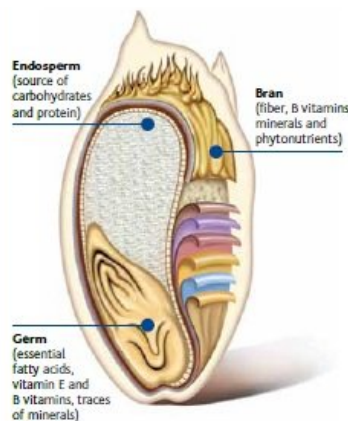


Figure 1. The grain seed structure: endosperm, bran and germ.

The endosperm represents the major part (80–85% by weight) of the kernel and consists of an intimate mixture of proteins and starch. The proteins are present as discrete particles and as interstitial material. Many different proteins are present in the endosperm, but the four main groups of proteins are the gliadins, glutenins, albumins and globulins. They represent the storage proteins of the wheat and usually make up about 10–14% of the weight of the kernel [Cornell, (2003)].

The wheat and endosperm are very rich in glutamine (30%) and proline (10%), while leucine (6.5%) is the next important amino acid. All the other amino acids are at levels between 1% and 5% of the wheat.

The external layers and the internal kernel of the grain have their own specific chemical and morphological characteristics. In the external layers of the caryopsis, the chemical characteristics are given by the concentration of cellulose, minerals and proteins. In the internal kernel, there is the starch and, finally, the germ is rich in fats that can easily go rancid.

2. Durum wheat composition

Dry pasta, a traditional cereal-based food product, recently increases its popularity in worldwide because of its accessibility, palatability, and high nutritional quality. Durum semolina is acknowledged as the most appropriate raw material for pasta production due to its inimitable colour, flavour and cooking quality [Feillet & Dexter, (1996)].

The pasta consumption in Italy was about 3,024,000 tonnes in 2004 and, specifically speaking, pasta made with durum semolina represented about 88% of the whole production (2,736,800 tonnes).

The Italian pasta industry confirms its leadership with a many manufacturing structure: 152 industrial establishments, of which 121 are specialized in the production of dried pasta, 18 in the production of industrial fresh pastas and 13 covering both types of productions. The industry production is estimated at 4,600,000 tonnes per year, with capacity utilization of about 68% (Data from U.N.I.P.I, Unione Industriali Pastai Italiani).

The most important components of pasta made with semolina are starch, protein,

lipids, pentosans and enzymes.

2.1 Starch

One of the major components of durum wheat is the starch (74-76% dry basis). Starch is deposited in the plastid of higher plants in the form of granules within membrane-bound organelles called amyloplasts in cereals and comprises 70% w/w of the endosperm in wheat [Stone (1996)].

Intact starch granules are almost insoluble in water, but, when heated in excess water, it gelatinises. The starch gelatinization causes the granules swell and eventually the rupture. This change is detected by microscopy and differential scanning calorimetry (DSC) in a ranging gelatinisation temperature of ~50-70°C. Upon heating, starch loses its rigid structure, becomes rubbery passing its glass transition and can readily absorb water.

This causes an increase in viscosity as the granules swell and release soluble material from the granule.

Starch is a polymer of α - linked glucose residues and is comprised of two molecules, amylose and amylopectin.

Amylose is a lightly branched polymer, with molecular weight of about 10^5 - 10^6 .

In wheat it typically represents about 25% of the starch granule, but in some genotypes this can vary greatly from 0 to 40%. Amylopectin is a highly branched polymer with MW of 10^7 - 10^8 . The amylose polymer can form complexes with lipids. This amylose-lipid complex resists leaching from the starch granule and also prevents entry of water into the granule.

Durum and other wheat have biphasic granule distributions, as illustrated in Figure 2: small spherical B-type granules (average diameter 2-3 μ m) and larger lenticular A-type granules (average diameter 25-40 μ m) [Buleon et al. (1998)].

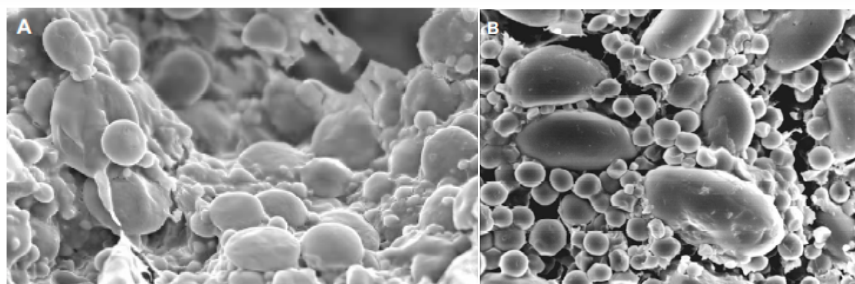


Figure 2. Starch: biphasic granule distributions, large (A-type) and small (B-type) granules. A-types are lenticular and B-types are spherical [Sissons, (2008)].

B-starch granules make up about 25-30% of the total starch volume but about 90% of the number of starch granules [D'Appolonia and Gilles (1971)].

When the percentage of B-granules are increased in durum starch, the dough absorbs more water, because the smaller B-granules have a higher surface to volume ratio and are able to hydrate and swell more efficiently and bind more water than A-granules. Therefore an increase of B-granule content should increase flour water absorption [Soh et al. (2006)].

The high demand of water by B-granule starch might create a disproportion of water distribution in the dough resulting in weaker dough. Soh et al. (2006) found that an increased dough resistance up to 32% B-granules, followed by a decrease at B-granule above 40% whereas in another study using granules with size 6.5-19.5 μm decreased resistance to extension [Sebecic (1995)].

Park et al. (2005) proposed that more small granules could interact more intimately as filler particles with the continuous gluten phase in dough, which causes a corresponding increase in resistance to mixing [Sisson (2008)].

2.2 Wheat proteins

Proteins can be classified into albumin (water-soluble), globulin (soluble in salt solution), gliadin (extractable in aqueous ethanol solution) and glutenin (soluble in dilute acid), conforming to Osborne's protein classification (1907). The proteins include enzymes, enzyme inhibitors, lipoproteins, lectins and globulins of unknown function.

The major fraction (80%) of durum semolina proteins is gliadins and polymeric glutenins, while minor fractions (20%) are albumins and globulins. The group of

proteins in wheat that exert the most influence on the strength and elastic properties of dough are the glutenins and gliadins. The polypeptide complex composed of glutenin, gliadin and lipid is defined as the viscoelastic mass remaining after removal of the starch.

Specifically speaking, the glutenin function is able to form an extensive three-dimensional network of molecules through disulphide bonding, hydrogen bonding and hydrophobic interactions. All contribute to the formation of cohesive elastic dough. The gliadin is also important in this network of reactions. Proteins, such as those in gluten, are denatured by heat and extreme changes in pH.

Hence, in order to retain its strong viscoelastic properties, wet gluten should be dried carefully. Figure 3 shows a model of the function of glutenin and gliadin in dough.

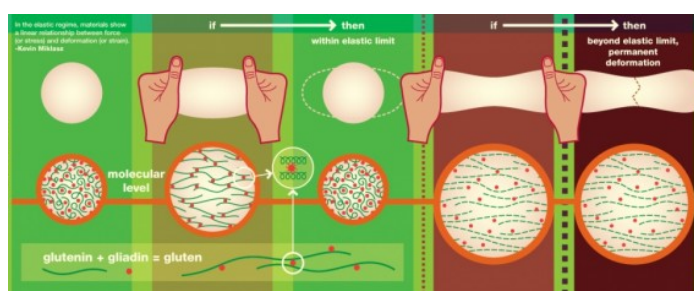


Figure 3. Structure of gluten.

Glutenins are constituted of different subunits linked together by disulphide bonds and their molecular weight can be high and/or low [Greenwell and Schofield, (1986)]; they have varying size ranging from about 500000 to more than 10 million [Wieser et al., (2006)].

Gliadins are present as monomers; they were initially classified into four groups in order of decreasing mobility at low pH in gel electrophoresis α -, β -, γ -, ω -gliadins.

Gliadins can be grouped on the basis amino acid composition and MWs into four groups: ω 5-, ω 1,2-, α/β -, and γ -gliadins [Wieser, (1996)].

ω -Gliadins are characterized by the highest contents of glutamine, proline and phenylalanine which together account for around 80% of the total composition.

ω 5-Gliadins have higher MWs (50000) than ω 1, 2-gliadins (40000).

Most ω -gliadins lack cysteine, so that there is no possibility of disulphide crosslinks. These proteins consist almost entirely of repetitive sequences rich in glutamine and proline. α/β - and γ -gliadins have overlapping MWs (28000-35000) and proportions of glutamine and proline much lower than those of ω -gliadins. They differ significantly in the contents of a few amino acids.

The distribution of total gliadins among the different types is strongly dependent on wheat variety and growing conditions (soil, climate, fertilization), it can be generalized that α/β -, and γ -gliadins are major components, whereas the ω -gliadins occur in much lower proportions [Wieser and Kieffer, (2001)].

The predominant protein type is LMW glutenin subunits (LMW-GS), their proportion amounts to 20% according to total gluten proteins [Wieser and Kieffer, (2001)]. HMW glutenin subunits belong to the minor components within the gluten protein family.

2.3 Others components

Non-starch components such as protein and lipids influence starch behaviour in food applications. Lipid is constituent of wheat notwithstanding being only 1-3% of the grain. In durum semolina free lipids represent 64% of total lipids.

The two main groups of polar lipids are galactosyl glycerides and phospholipids, which affect final pasta quality. It affects water absorption and hence gelatinization properties. Lipids are important in regulating the colour of pasta due to pigments and lipoxygenase. The pigments establish in the endosperm consist of primarily xanthophylls. A bright yellow colour is wanted in pasta products, which develops from the pigments in the endosperm although some diminution in colour can occur during pasta processing.

Other lipids in durum wheat involve hydrocarbons, sterols, glycerides, fatty acids, glycolipids and phospholipids. Hydrocarbons are a minor component 0.036% of dry weight. Lipid content does not show to decrease during pasta processing, but it is less easily extracted from pasta than semolina, suggesting that under mechanical stress of extrusion, lipids undergo chemical changes or are complexes

with proteins and carbohydrates. Lipid altered the interactions between proteins and it weight pasta quality such as an increase in stickiness of pasta and cooking loss [Sissons, (2008)].

The water-soluble fraction of durum contains albumins and globulins too.

Enzymes linked to pasta quality are lipoxygenase, peroxidase, polyphenoloxidase and amylase. Lipoxygenase is present in many tissues of higher plants and animals and catalyzes.

Finally, grains are good sources of insoluble fiber. Pentosans, non-starch polysaccharides, are only 2.2-2.8 % fractions in durum wheat semolina. This fraction plays an important role in binding 25% of the total water contributes to the structure and properties of the dough.

3. Dough development

Pasta process consists of different stages, but the first one, the mixing stage, is the most important. Generally, the durum wheat semolina is mixed with water in a paddle mixer, fed into an extruder, then compressed and extruded through a die. The rheological behaviour of dough after extrusion is related to gluten development matrix [Belton, (1999); Letang et al., (1999)]. In fact, the rheological properties of polymers reflect the degree and type of cross-linking of the polymers as shown in Figure 4.

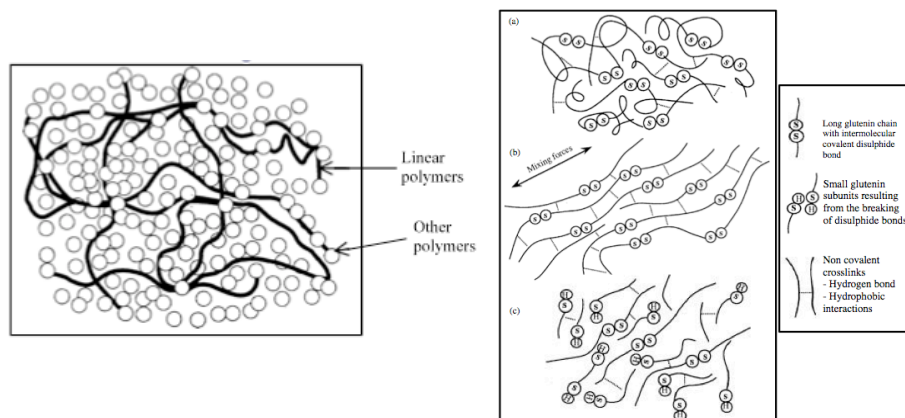


Figure 4. Model for the disulphide-bonded structure of glutenin.

At the early stage of mixing, the water is distributed among the semolina particles.

The water is added to rich final moisture content of about 33% on a wet basis.

At the initial mixing time, glutenins, which are the long polymeric proteins, are folded and the chains are in random orientation, but, as mixing proceeds, more protein becomes hydrated and the glutenins tend to align, because of the shear and stretching forces imposed by the paddles.

For the network development, during mixing, it is very important the balance of gliadin and glutenin and the chemical bonds developed.

As a matter of fact, the optimum dough structure involves bonds like disulphide and hydrogen bonds and crosslinks involving dityrosine [Tilley et al. (2001)].

In fact, as reported in the literature, adding hydrogen bond breaking agents, it is possible observe a drastic effect on dough rheology and the strengthening effect of heavy water compared to ordinary water [Tkachuk and Hlynka (1968)]. Another unique feature of hydrogen bonds is their ability to interchange under stress and thereby facilitate re-orientation of gluten proteins. Hydrophobic bonds result from the interactions of non-polar groups in the presence of water.

Their functionality is similar to that of hydrogen bonds, but the overall effect is much smaller.

Hydrophobic bonds contribute significantly to the stabilization of the gluten structure. They are different from other bonds, because their energy increases with increasing temperature; this can provide additional stability during the dry pasta process.

Disulphide bonds play a key role in the formation and development of dough. They form strong cross-links within and between polypeptide chains, thereby stabilizing hydrogen bonds and hydrophobic interactions. The interchange reaction requires a “mobile” sulfhydryl-containing substance to initiate the series of disulphide interchanges [Edwards et al., (2003)].

The total number of S-S bonds does not change; only their location in the glutenin molecule is altered [Wall, (1971)]. When the durum is hydrated and well mixed, the monomeric proteins, gliadins, form a matrix within the long polymer networks and contribute to resistance to extensions and between protein polymers increases gluten viscous resistance and resistance to extension.

Glutenins, and particularly omega-gliadins, seem to interact with the glutenins during dough processing through non-covalent interactions [Kuktaite et al. (2004)].

Then, when the dough is at the optimum mixing time the gluten network has a maximum cross-linking of protein with disulphide bonds, the interaction between the polymers cross-link are becoming stronger, and, as a consequence a maximum resistance to extension and restoring force after deformation can be observed.

On the contrary, when the dough is mixed longer past its optimum development, the cross-links begin to break due to the breaking of disulphide bonds [Zaidel Abang et al., (2010)]. The glutenins become depolymerised and the dough is overmixed. The presence of smaller chains in the dough makes the dough sticky [Zaidel Abang et al., (2010)].

The polymeric protein (glutenin) is mainly responsible for the elasticity of the dough, whereas the monomeric gliadins are the extensibility-related characters. Thus the ratio of glutenin to gliadin can be directly related to the balance of dough strength and extensibility [Wrigley et al. (2006a-2006b)]. It is accepted that weak and inelastic gluten promoted poor pasta cooking quality, but how much strength is optimal is not known. To increase gluten strength in durum semolina, blending with higher strength semolina is a commonly employed strategy by millers in Italy, which enhances pasta texture [Marchylo et al. (2004)].

4. Factors affecting dough during mixing

Rheological properties of dough and gluten during mixing are affected greatly by the durum wheat composition (i.e. low or high protein content), processing parameters (mixing time, energy, temperature and speed rate) and ingredients (as example water and salt). Different durum semolina have different optimum mixing time [Hoseney (1985)].

Mixing time and energy input are normally used to change dough properties.

The widespread belief is that stronger dough requires longer mixing time and more energy input. In order to achieve optimum dough development, the mixing time and work input must be above the minimum critical level [Angioloni and

Dalla Rosa (2005)], and also the mixer design, operation conditions and water level influence the final quality. In fact, An optimum in work input and mixing time have been related to optimum breadmaking performance [Skeggs, (1985)], which varies depending on mixer type, semolina composition and ingredients [Mani et al., (1992)].

Sliwinski et al. (2004) have reported a correlation between dough mixing time and the percentage of glutenin protein in flour. Water addition and gluten protein content are correlated with rheological properties as a function of mixing time. Moreover, they have found a positive correlation between stress at a chosen strain and the percentage of polymeric protein of large size and a negative one between the strain rate-dependency of the stress and the percentage of the high molecular weight glutenin subunits on total protein.

Elongation rheology of HMW proteins is a sensitive indicator of changes in secondary molecular structure. For stability of polymers undergoing large deformation, it is used strain hardening index, which is sensitive to the degree of entanglement and long chain branching (LCB) of the polymer. In fact, it was found that LCB raises the strain-hardening index. This structure contributes to resistance and to extension under large deformation. The HMW branched polymer behaviour is described by the pom-pom model, proposed by McLeish et al. (1998). An increase in mixing time and work input above the optimum level induces the changes in mechanical properties of dough [Cuq et al. (2002)].

The flow properties of wheat flour dough are evaluated by using a piston-driven capillary rheometer and are conducted using the classical Bagley approach considering linear functions between pressure drop and L/D ratio. The experiments are performed at increasing shear rates corresponding to increasing plunger speeds. The capillary behaviour of wheat flour dough is characterized by the value of entrance pressure drop, P_0 .

High P_0 value indicates a large contribution of elongational flow and it correlates to branch number. For short mixing times, the structural changes in dough during mixing are from the formation of the gluten network through SS bonds and chain entanglements. Over the development time, entanglement points between chains

reduce and relaxation by SS bond interchanges between protein chains cannot take place quickly enough to prevent local extension of the chains and molecular SS scission.

Work input and mixing intensity speed are two critical factors for optimal dough development. High mixing speed lead to a large disorientation and destruction of dough structure hence reduced viscosity [MacRitchie, (1985)]. On the other hand, water is responsible in hydrating the protein fibrils and interactions between the proteins cross-links with the disulphide bonds during dough mixing and an optimum level is required to develop dough with optimum gluten strength. The addition of too much water to the flour will result in slurry, whereas too little water results in a slightly cohesive powder [Faubion and Hosenev, (1989)].

Hence, an optimum water level is essential to develop cohesive, viscoelastic dough with optimum gluten strength. Strong semolina requires higher water level than weak semolina largely due to the higher protein content and dense particles in the strong semolina [Sliwinski et al. (2004c)].

Optimal value of work over time is the function of semolina quality too. In fact, protein content is known to be an important factor in determining the water uptake of semolina [Sliwinski et al. (2004)]. Ablett et al. (1985) explained the effect of water content on gluten networks in terms of a rubbery network such that its elongation reduced as water content increased.

During mixing, the energy flow and the hydration processes are accompanied with a temperature increase. Temperature is another factor that influence elastic properties of dough. The temperature growth is dependent on the speed of mixing [Wilson et al. (2001)], but it is assumed that the type of the semolina used influences the dough heating. Specifically speaking, the resistance of elastin increase with increasing temperature in the same way as that of rubber [Dorrington and McCrum, (1977)].

The literature considers 28-30°C the optimum temperature range for dough mixing [Hui Y. H., (2006)].

When the temperature is relatively high, the dough becomes soft and viscous but shows less elastic properties. Elasticity and firmness are changed because

fermentative activity is growing. If the temperature is relatively low, the dough is hard to push and difficult to extend. The plasticity of dough is decreases and that affect the quality of the finite products.

The temperature of the dough will rise due to:

- heat generated by the frictional forces;
- heat of hydration of the semolina.

The frictional heat results from the mechanical energy gives to dough during mixing. The amount of friction developed is related to the water added and absorbed and then to the gluten development. As mixing time is changed, the friction factor changes as well.

The heat of hydration is the energy with gets liberated when a substance absorbs water [Zhou W., (2014)]. The amount of heat liberated varies with the degree to which water is absorbed. The temperature of the dough is also induced by other factors such as: temperature of ingredients; size and type of mixing equipment; batch size; mixing procedures and room temperature.

Finally, another factor influencing the strength of the gluten during mixing of dough is the sodium chloride [Niman, (1981)]. Salt must be added early in the dough mixing to give maximum dissolution time and accelerate gluten formation. Usage level is normally between 1.8%-2.2%. Legislation may vary from country to country because the intake of too much salt is considered as a health risk. In Belgium for instance the maximum allowed is 1.8%, while in France 2.0% is allowed. Salt is used to overcome the low pH of dough since the effect of pH will alter the mixing time; a low pH gives a shorter time and a high pH gives a longer time [Hoseney, (1987)]. Roach et al. (1992) suggested that influences of salt on the protein solubility affect the final dough properties.

Salt decreases the solubility of protein in the wheat flour dough as its concentration increases. Salvador et al. (2006) found that the elastic modulus falls marginally in the presence of salt.

This reduction is probably due to decrease in inter-protein hydrophobic interactions, which reduce the tendency of the proteins to aggregate and thus reduce the elasticity.

Salt toughens the gluten and the reason must be sought in the fact that gluten is made of negatively charged proteins. Negatively charged molecules will repel and not attract each other. .

5. Dough making process

Starch and proteins undergo successive structural changes during the pasta making process. The transformation of semolina into pasta involves dosing, premixing, mixing and extrusion stages.

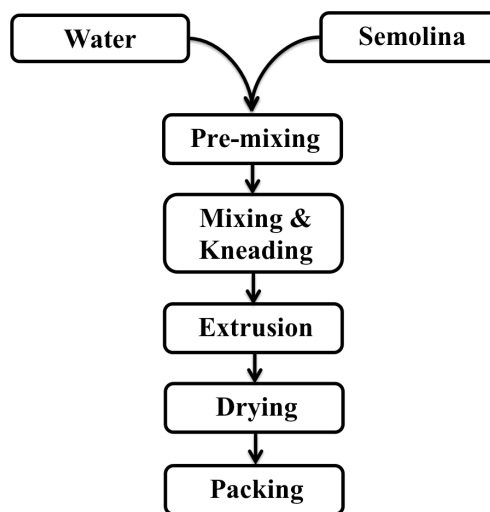


Figure 5. Dry pasta production line.

The Figure 5 shown phases those take place in an automatic pasta production line. This sequence of operations was developed on an industrial automated scale beginning in the early 1930s with the introduction of the continuous press, then with the use of automatic dryers, and finally, in the mid-to-late 1940s, with the manufacture of continuous, automatic production lines.

The resultant wet pasta has a network of protein that encapsulates the starch granules, to produce a structure that has the minimum of cracks and voids.

The process of disulphide-bond formation continues during the ripening of the grain, and it even continues into storage [Wrigley and Békés (1999)].

In the Figure 6, disulphide-bond formation again accelerates during the heat treatment of processing.

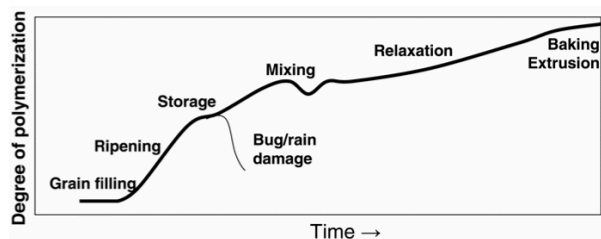


Figure 6. Pasta processing: degree of polymerization versus time.

These processes make significant contributions to the degree of polymerization of the glutenin proteins and thus to the molecular weight distribution of the overall gluten-protein complex.

The initial step, raw material dosing, is of primary importance for the subsequent steps dough formation and pasta manufacture.

The water-semolina ratio determines the rheological behaviour of the semolina dough and the mechanical energy input for each product.

Semolina dosers can be volumetric or gravimetric, while water dosing can be achieved using either a mechanically or a volumetrically based system that is synchronized with the semolina doser.

Water temperature is controlled by a simple thermostatic system and usually ranges between 20 and 50°C [Dawe (2001)]. All the components of solid and fluid dosers are built of stainless steel and food-grade materials.

In the next stage, the weighed semolina, which particles have variable diameter (10-500 μm), and a defined percentage of water pass through a mixing-kneading process designed to produce homogeneously hydrated dough.

During phase of mixing, the water is distributed among the dry semolina, to produce an even moisture distribution and to produce dough with moisture content of approximately 33%.

As mixing continues, glutenin interacts with gliadin to form gluten, the viscoelastic matrix of the dough and increases the protein mobility through a plastifying effect [Hoseney et al. (1986)], allowing the formation of a protein network. Dough formation and development requires a critical balance of constituents, ingredients, and energy input by mixing.

The interaction among these three factors is complex. The mixture moves to a laminator where it is pressed into sheets by large cylinders.

To obtain the most homogeneous hydrated mass possible, semolina and water first undergo high-speed premixing (using a single or double shaft, vertical or horizontal) to ensure intimate contact between semolina particles and water droplets. Further mixing then takes place in the main mixing unit, generally under vacuum, before the mass passes into the extrusion section. Vacuum chamber is used to remove air bubbles from the pasta before extruding to reach the optimum water content of 12%. If the air is not removed prior to extruding, pasta formed small bubbles that reduce the mechanical strength and contribute the finished product a whit.

In the mixer-kneaders, as well as vacuum mixers, residence times range from 10 to 15 min, according to the semolina's particle size distribution granulation.

Once the first mixing phase commences, the gluten proteins are stretched, and, as the temperature rises, an interlinked protein framework is established [Dawe (2001)].

After hydration and mixing, the wetted semolina particles enter the extrusion stage, where pasta dough development largely occurs.

Extrusion involves the operation of a suitably designed screw inside a cylinder that transports the pasta dough along the screw concomitant with increasing compression or pressure to stimulate dough development.

The extrusion auger not only forces the dough through the die, but it also kneads the dough into a homogeneous mass, controls the rate of production, and influences the overall quality of the finished product.

Friction must remain at low levels to prevent increased dough temperature over 40°C, the cylinder and head are cooled so that their maximum temperature does not exceed 45°C.

During this stage, a transition occurs from hydrated granular semolina to a homogeneous fluid, with an associated increase in specific weight along the screw from 750 to 1350 kg/m³.

The extrusion system is composed of a screw-barrel subsystem, which pushes the

product and a die that restricts the flow-out of the dough.

As a consequence, the die creates increasing backpressure along the screw, which results in dough development. Further energy input is transferred to the forming dough to push it through the die hole and shape the product.

Grooves along the sides of the barrel also are important, as they increase the shear effect and make the dough adhere to the barrel, which generates a kneading action.

This process leads to development of the gluten network but also to starch damage and heat generation. A cooling system is necessary to keep the heat generated by the extrusion process from causing negative effects on gluten network quality. The material used to make dies is bronze with inserts made of Teflon or bronze, the design and construction of which are arts in themselves and influence pasta shape and smoothness [Dawe (2001)].

As the wet mix passes into the vacuum screw and to extruder, it is formed into dough and the application of mechanical work causes the protein to fuse and form the gluten network. Pasta shaping comprises dough compression and extrusion phases, which take place as the dough is forced under high pressure through small holes in a die, followed by cutting.

The die holes are designed to give the desired pasta shape and size.

If the temperature rises above 55°C, the gluten becomes increasingly tough and stiff and irreversibly forms a gel [Blanshard (1995)].

This process is undesirable in the extruder and any gluten in this condition will appear in the pasta as fragments of broken gel and these make the pasta strands weaker.

The crumbly dough obtained is fed to an extrusion screw or a sheeter and formed into the desired shape. To give the pasta some resistance to overcooking, the protein network must not be adversely damaged. To avoid this, kneading of the dough in the screw must be gentle. It is shearing forces that can damage the protein network. Fresh pasta is then dried in order to reduce its moisture content to about 12% [Dalbon et al. (1996)], to remove excess moisture to a water activity at which microbial growth is impossible ($a_w < 0.65$).

Nowadays, the majority of pasta-drying processes adopt air temperatures that range from about 70 to 100°C, while keeping product temperatures between 60 and 90°C. The difference between product temperature and air temperature is mitigated by air moisture content and ongoing evaporation through the water-removal process.

Drying is the most difficult and critical step to control in the pasta production process. Drying temperature and relative humidity increments are important factors in drying. Since the outside surface of the pasta dries more rapidly than the inside, moisture gradients develop across the surface to the interior of the pasta.

If dried too quickly, the pasta will crack, giving the product a poor appearance and very low mechanical strength. Cracking can occur during the drying process or as long as several weeks after the product has left the drier.

If the pasta is dried too slowly, it tends to spoil or become moldy during the drying process. Therefore, it is essential to have a good pasta that the drying cycle has been successful; in this way the pasta will be firm but also flexible enough so that it can bend to a considerable degree before breaking.

The drying process is subdivided into the following phase:

- high temperature;
- humidification;
- cooling.

During the drying process, in the first phase, the pasta is preheated before it is fed into the predryer and heating ventilation units' controls automatically throughout heat and humidity.

Predryers usually are classified into different areas with independent temperature and humidity control along with overheated-water heat exchangers and air extraction groups. The structure in processing areas is entirely made of stainless steel.

The drying phase takes place as the sticks and pasta travel along following tiers of chains that usually are separated from each other. This separation allows the pasta to pass through zones of different temperature and humidity and provides higher flexibility in the setting of drying diagrams. Each tier of stainless steel chains,

which transport the sticks, is driven by an independent gear and is equipped with specially shaped hooks that enable the sticks to move in a vertical direction when they reach the end of a tier. Probes monitor temperature and humidity, and the resulting feedback is used to maintain drying conditions as programmed.

Thermal energy is transferred to the pasta by an airflow coming from ventilation units and the product passes through successive drying and stabilization phases.

The phase humidification included adding back some moisture by steam injection and thus eliminating residual tensions and enhancing product stabilization.

This module has a steam injection unit complete with filter, condensate discharge, and passage indicator, controlled by appropriate probes and valves.

A system installed on the discharge side and synchronized with the rest of the line transfers the sticks with the dried product to the cooler by means of a stainless steel lowering device.

The last phase of the pasta drying process is cooling phase.

In this phase, the pasta is acclimatization to a condition that is in balance with the ambient outer environment, making it ready for immediate packaging.

Outer panels made of material with high insulation power cover drying system modules.

They may be covered with stainless steel sheeting with watertight portholes at the dryer end for inspecting the dryer interior. The bottom sections of the dryers are equipped with a condensation collection and removal system.

The storage section has an air circulation system to maintain homogeneous temperature and humidity conditions during storage.

In the phase of packaging, the product has to be free from contamination. Packaging protects the pasta from damage during shipment and storage.

The principal packaging material for pasta is the cellophane bag, which provides, moisture-proof protection for the product and is used easily on automatic packaging machines, but is difficult to stack on grocery shelves.

The package itself is a necessary means of providing among other things important nutritional information to the consumer.

Dried pasta can be load manually or by machine into stainless steel buckets,

which move along a conveyor belt to the appropriate packaging station.

The pasta is measured by machine into pre-printed boxes, which also list the type of noodle, ingredients, preparation, and expiration date.

The boxes are then sealed by machine. Conveying system can be constructed in "S," "C," or "Z" configurations, or as horizontal conveyor belts.

These systems move the pasta up and down and across the plant at heights up to 3 m. Workers at the floor-level stations monitor the packaging process. The mechanism allows for workers to package the pasta manually if necessary.

6. Phase transition

In semolina the gluten is glassy but upon the addition of some water it becomes rubbery and elastic, acquiring the ability to form strands and sheets via inter molecular bonds. This matrix helps to trap the starch granules in pasta and hold its shape during cooking. When the hydrated gluten is heated, irreversible protein-protein cross-link is formed. Upon heating, starch loses its rigid structure, becomes rubbery passing its glass transition, and allows changes in its physical and chemical nature. Moisture diffusion within the pasta generates a moisture gradient that can cause thermoviscoelastic stresses that result in superficial and subsurface cracks. Indeed, the rheological properties of the pasta change with the local moisture content and the temperature of the matrix. This causes an increase in viscosity as the granules swell and release soluble material from the granule. These properties are fundamental to its role as the continuous matrix, which traps and encapsulates starch in pasta and holds the product shape during manufacture and cooking. The concept of glass-rubber transitions is particularly helpful in understanding the physical control of pasta manufacture [Slade et al. (1991) and Blanshard (1995)].

Figure 7 shows two phases during high-temperature (HT) drying (80°C):

- Plastic: in this phase extends from the beginning of drying 30% moisture (w.b.) to 16-18% moisture. During this phase, pasta may support deformations without generation of any cracks;
- Elastic: in this phase extends from 16-18% to the final product moisture

12.5%. At this stage, stresses generated by the drying process must be prudently controlled. If the stresses become higher than the mechanical resistance of the pasta matrix, cracks are generated within the product.

The transition point between the plastic and elastic phases is of critical importance to final-product stability. During drying, pasta is subjected to internal tensions because the product volume is decreasing with loss of water.

Pasta in the plastic phase is more able to relax and redistribute such stresses, but in the elastic state it is unable to do so, which contributes to the creation of possible points of fracture.

At room temperatures and low moisture, less than 12% w.b.), both the gluten and starch in the semolina behave as a glassy material. At slightly higher moisture, the gluten will behave as a rubbery material as it undergoes glass transition and as more water is added to around 33%, the gluten will flow under applied stress.

During this phase the water is distributed among the dry semolina to produce an even moisture distribution. As the wet dough passes into the vacuum screw and to the extruder, the pasta is formed and the application of mechanical work causes the fusion of protein which form the gluten network.

If the temperature rises above 55°C, the gluten becomes stiff and forms an irreversibly gel [Blanshard (1995)].

This process is undesirable in the extruder and the gluten in this condition will appear in the pasta as fragments of broken gel and these make the pasta strands weaker. Thus, maximum dough temperatures are held below 55°C.

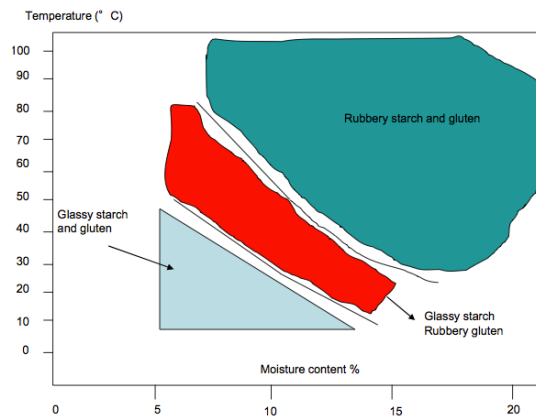


Figure 7. Starch and gluten: glass transition [Sissons, (2008)].

Finally, to have a resistance to overcooking to the pasta, the protein network must not be adversely damaged. To avoid this, kneading of the dough in the screw must be gentle, because the shear forces can damage the protein network.

REFERENCES

- 1) Ablett S., Attenburrow G. E. and Lillford P. J. (1985). The significance of water in the baking process, *Chemistry and physics of baking*, 30-41
- 2) Angioloni A. and Dalla Rosa M., (2005). Dough thermo-mechanical properties: influence of sodium chloride, mixing time and equipment, *Journal of Cereal Science*, (41), 327-331
- 3) Belton P.S., (1999). Mini review: on the elasticity of wheat gluten, *J Cereal Science*, (29), 103-107
- 4) Blanshard J. M. V., (1995). The glass transition, its nature and significance in food processing, *Physico-chemical Aspects of Food Processing*, 16-48
- 5) Buleon A., Colonna P., Planchot V. and Ball S. (1998), Starch granules: structure and biosynthesis, *Int. J. Biol. Macromol.*, (23), 85-112
- 6) Cornell, H. (2003). The chemistry and biochemistry of wheat. In Cauvain, S. P. (eds) *Bread making*, pp 28-68. Boca Raton (USA): CRC
- 7) Cuq B., Yildiz E. and Kokini J., (2002). Influence of mixing conditions and rest time on capillary flow behaviour of wheat flour dough, *Cereal Chemistry*, (79), 129-137
- 8) D'Appolonia B. L. and Gilles K. A. (1971), Effect of various starches in baking, *Cereal Chemistry* (48), 625-636
- 9) Dalbon C., Grivon D. and Pagani M., (1996). Continuous manufacturing process, *In pasta and noodle technology*, 13-58
- 10) Dawe P.R., (2001). Pasta mixing and extrusion, *Pasta and Semolina Technology*, (86), 118
- 11) Dobraszczyk B. J. and Morgenstern M.P., (2003). Rheology and the breadmaking process, *Journal of Cereal Science*, (38), 229-245
- 12) Dorrington K. L. and McCrum N. G., (2004). Elastin as a rubber, *Biopolymers*, (16), 1201-1222
- 13) Edwards N. M. (2003). Role of gluten and its components in determining durum semolina dough viscoelastic properties, *Cereal Chemistry*, (80), 755-763

- 14) Faubion J. M. and Hoseney R. C. (1990). The viscoelastic properties of wheat flour doughs, *Dough rheology and baked product texture*, 29-66
- 15) Feillet P. and Dexter J. E. (1996). Pasta and noodle technology, *AACC St. Paul MN*, 95-131
- 16) Greenwell P. and Schofield J. D. (1986), A starch granule protein associated with endosperm softness in wheat, *Cereal Chemistry*, (63), 379-380
- 17) Hoseney R. C., (1986). A note on the gelatinization of starch, *Starch* (38), 407-409
- 18) Hoseney R.C. (1985). The mixing phenomenon, *Cereal Foods World*, (30), 453-457
- 19) Hoseney R. C. and Rogers D. E. (1987). Test to determine the optimum water absorption for saltine cracker doughs, *Cereal Chemistry*, (64), 370-372
- 20) Hui Y. H., (2006). Handbook of food science, technology, and engineering (Vol. 149). CRC press
- 21) Kilborn R. H. and Tipples K. H. (1972). Factors affecting mechanical dough development. I. Effect of mixing intensity and work input, *Cereal Chemistry* (49), 34-47
- 22) Kuktaite R., Larsson H. and Johansson E., (2004). Variation in protein composition of wheat flour and its relationship to dough mixing behaviour, *Journal of cereal science*, (40), 31-39
- 23) Letang C., Piau M. and Verdier C., (1999). Characterization of wheat flour-water doughs. Part I: Rheometry and microstructure, *Journal of Food Engineering*, (41), 121-132
- 24) McLeish T. C. B. and Larson R. G., (1998). Molecular constitutive equations for a class of branched polymers: The pom-pom polymer, *Journal of Rheology*, (42), 81-110
- 25) MacRitchie F., (1985). Physicochemical process in mixing, *Chemistry and Physics of baking*, 132-146

- 26) Mani K., Eliasson A. C., Lindahl L. and Tragardh C., (1992). Rheological properties and breadmaking quality of wheat flour doughs made with different dough mixers, *Cereal Chemistry*, (69), 222-225
- 27) Marchylo B. A., Dexter J. E. and Malcomson L. M., (2004). Improving the texture of pasta, *Solid food*, (2), 475-500
- 28) Niman C. E., (1981). Salt in bakery products, *Cereal foods world*, (26), 116
- 29) Park S. H., Chung O. K. and Seib P. A., (2005). Effects of varying weight ratios of large and small wheat starch granules on experimental straight-dough bread, *Cereal Chemistry*, (82), 166-172.
- 30) Příhoda J., Skřivan P. and Hrušková M., (2003). Cerealni chemie a techmologie I.
- 31) Roach R. R., Lai C. S. and Hoseney R. C., (1992). Effect of certain salts on bread loaf volume and on soluble nitrogen of wheat flour and non fat dry milk slurries, *Cereal chemistry*, (69), 574-576
- 32) Salvador A., Sanz T. and Fiszman S. M., (2006). Dynamic rheological characteristics of wheat flour-water doughs. Effect of adding NaCl, sucrose and yeast, *Food Hydrocolloids*, (20), 780-786
- 33) Sebecic B (1995), Wheat flour starch granule-size distribution and rheological properties of dough. Part2 Extensographic measurements, *Die Nahrung* (39), 117-123
- 34) Shewry P. R., Popineau Y., Lafiandra D. and Belton P., (2001). Wheat glutenin subunits and dough elasticity: findings of the EUROWHEAT project, *Food science & technology*, (11), 433-441
- 35) Sissons M. J., (2004). Pasta, *Encyclopaedia of grain science*, 409-418
- 36) Sissons, M. J., (2008). Role of durum wheat composition on the quality of pasta and bread. *Food* (2), 75-90
- 37) Skeggs P.K., (1985). Mechanical dough development-dough water level and flour protein quality. *Cereal Chemistry*, (62), 458-462

- 38) Slade L., Levine H. and Reid D. S., (1991). Beyond water activity: Recent advances based on an alternative approach to the assessment of food quality and safety, *Food Science and Nutrition*, (30), 115-360
- 39) Sliwinski E.L., Kolster P., Prins A. and van Vilet T., (2004). On the relationship between gluten composition of wheat and large-deformation properties of their doughs, *Journal of Cereal Science*, (39), 247-264
- 40) Sliwinski E. L., Kolster P., Prins A. and Van Vilet T., (2004c). On the relationship between gluten protein composition of wheat flours and large-deformation properties of their doughs, *J. Cereal Science*, (39), 247-264
- 41) Soh H. N., Sissons M. J. and Turner M. A., (2006). Effect of starch granule size distribution and elevated amylose content on durum dough rheology and spaghetti cooking quality, *Cereal Chemistry* (83), 513-519
- 42) Stone BA (1996), Cereal grain carbohydrates, *Cereal grain quality*, 250-288
- 43) Tilley K. A., Benjamin R. E., Bagorogoza K. E., Okot-Kotber B. M., Prakash O. and Kwen H., (2001). Tyrosine cross-links: molecular basis of gluten structure and function, *J. Agric Food Chem*, (49), 2627-2632
- 44) Tkachuk R. and Hlynka I. (1968), Some properties of dough and gluten in D₂O, *Cereal Chemistry*, (45), 80-87
- 45) Troccoli, A., Borrelli, G. M., De Vita, P., Fares C. and Di Fonzo, N. (2000). Durum wheat quality: a multidisciplinary concept. *Journal of Cereal Science* (32), 99-113
- 46) Wall J. S., (1971). Disulfide bonds: determination, location and influence on molecular properties of proteins, *Agricultural and food chemistry*, (19), 619-625
- 47) Wieser H., (1996). Relation between gliadin structure and coeliac toxicity, *Acta Paediatr Supplement*, (412), 3-9
- 48) Wieser H. and Kieffer R. (2001), Correlations of the amount of gluten protein types to the technological properties of wheat flours determined on a microscale, *J. Cereal Science* (34), 19-27

- 49) Wieser H., Bushuk W. and MacRitchie F., (2006). The polymeric glutenins, *America association of cereal chemistry*, 213-240
- 50) Wilson A.J., Morgenstern M. P. and Kavale S., (2001). Mixing response of a variable speed 125 g laboratory scale mechanical dough development mixer, *Journal of Cereal Science*, (34), 151–158
- 51) Wrigley C. W., Békés F. and Bushuk W., (2006a). Gluten: A balance of gliadin and glutenin, *AACC. Press, St Paul, USA* 3-34
- 52) Wrigley C. W., Bekes F and Bushuk W., (2006b). Gluten: Manipulation of gluten structure and function, *AACC. Press, St Paul, USA* 447-453
- 53) Wrigley C. W. and Békés F., (1999). Glutenin-protein formation during the continuum from anthesis to processing, *Cereal Foods World*, (44), 56-2-565
- 54) Zaidel Abang D. N., Chin N. L. and Yusof Y. A., (2010). A review on rheological properties and measurements of dough and gluten, *Journal of Applied Sciences*, (20), 2478-2490
- 55) Zhou W., (2014). Bakery products science and technology. Second edition, *Willey Blackwell*

Chapter II

Small strain characterization of durum semolina dough

1. Introduction

Processing of dried durum semolina pasta involves conditioning and mixing of semolina with water, compacting and shaping by extrusion or sheeting and dehydration. Properties of durum wheat semolina dough and pasta quality are largely determined by gluten strength of the raw material.

Several chemical and instrumental methods have been developed to measure gluten strength, with attempts to relate these data to process characteristics and end-product quality [Cole (1991)].

The rheological techniques commonly used are farinograph, mixograph and alveograph tests, eventually adapted. [Irvine et al., (1961); Quick and Donnelly, (1980); Walle and Trentesauz, (1980)].

These tests are purely descriptive and dependent on the type of instruments, size and geometry of the sample and the specific conditions under which the test was performed, but they are still useful, especially for determination of relative strength and extensibility of cultivars.

Problems encountered with such non fundamental test are: complex instrumentation which is expensive, time consuming, difficult to maintain in an industrial environment and requires high levels of technical skills; moreover during test it is used inappropriate deformation conditions and difficulty in interpretation of results.

Rheological measurements are increasingly being used as rapid, sensitive indicators of changes in polymer molecular structure and the gluten can be viewed

as a polymer.

2. State of art

Rheology is the study of the flow and deformation materials. The general aims of rheological measurements are:

- to obtain a quantitative description of the materials' mechanical properties;
- to obtain information related to the molecular structure and composition of the material;
- to characterise and simulate the material's performance during processing and for quality control.

Rheology can be used as an aid in process control and design, and as a tool in the simulation and prediction of the materials response to the complex flows and deformation conditions. For the purpose, many rheological tests have been used to attempt to predict final product quality such as mixing behaviour, mouthfeel, texture and final quality of pasta.

Rheological tests attempt to measure the force or displacement required to produce a given controlled deformation or force.

The rheological measured properties are independent from the size, shape and how they are measured. Usually, small deformation dynamic oscillatory measurements are performed to characterize dough and, more generally, wheat flour-water mixtures and several techniques have been employed for investigating the fundamental mechanical properties of wheat flour doughs including stress relaxation [Launay and Buré, (1974), Fu et al., (2008)], creep and creep recovery [Hibberd and Parker, (1979); Campos et al., (1996)], and dynamic oscillatory measurements [Abdelrahman and Spies, (1986); Faubion and Hoskeny, (1990); Amemiya and Menjivar, (1992)].

Small deformation dynamic oscillatory measurements are used to characterize wheat-flour water mixtures. These measurements, performed under mild conditions, are known to preserve the structure of the sample tested, and thus permit to obtain information on the volume properties of the dough.

From dynamic oscillation tests result that the elastic modulus (G') is higher than

viscous modulus (G'') for dough and this is in agreement with the behaviour of cross-linked polymers. Other works, which have utilized this test method on dough, include studies on effect of protein content, water level, mixing time on rheological properties on the rheological properties of dough and gluten.

Many authors have published results concerning the rheometrical properties of the wheat our doughs. It has been discussed the problem of linearity, finding that when this region exist, it is situated at strain levels smaller than 1%. Beyond this limit, both the elastic modulus G' and the loss modulus G'' decrease. In the linear region the frequency sweep tests have shown that the modulus follow a power law behaviour. Campos and coworkers (1997) have used dynamic oscillatory and creep measurements on undeveloped doughs and doughs prepared by mixing in a farinograph bowl in an attempt to decouple the effects of hydration and energy input and they reported that undeveloped doughs exhibited lower complex modulus (G^*) values than developed doughs. Generally, the water level and the protein/starch ratio influence the modulus, and the dough strength could be established by measurement of G' . Particularly, G' decreases increasing the water and by strain sweep tests large changes in the rheological properties has been detected, with the storage modulus increasing in magnitude as the proportion of starch in the dough has been increased. Moreover, the phase angle reveals that gluten-starch mixtures behaved as elastic solids and the linear viscoelastic region changes with starch concentration: the linearity strain limit decreases exponentially as the starch content increases. These results were obtained on gluten-starch mixtures mixed with constant water level.

These results were compared with mixtures mixed with their optimal water levels. It has been found that the storage modulus decreases with increasing protein and gluten concentration, whilst the opposite was seen when constant water levels were used, with the storage modulus increasing with increasing protein and gluten concentration. Edwards N. M. et al. (2003) established the gluten contributes to the viscoelastic properties of dough to varying degrees depending on its source differing with both gliadin/glutenin ratio and LMW-GS. Gliadin enhances viscous flow of dough. An addition of 2% gliadin results in increased dough extensibility

and $\tan(\delta)$ as compared to gluten and glutenin additions. Glutenin addition, on other hand, results in more elastic dough in comparison with gluten and gliadin additions. Addition of glutenins at constant protein basis contributes to the dough strength with marked differences among donor cultivar. Increasing the glutenin/gliadin ratio improves maximum shear viscosity and dough strength [(Uthayakumaran et al., (2000)]. Both low molecular weight glutenin subunits (LMW-GS) and high molecular weight glutenin subunits (HMW-GS) contribute to overall dough strength but LMW-GS enrichment improves the elasticity by introducing greater number of physical crosslinks. The source of LMW-GS influences the viscoelastic characteristics of doughs while source of HMW-GS does not show such an effect. Studies about the influence of mixing time do not provide general conclusions and most work has either concentrated on empirical measurement of mixer motor torque, voltage or power consumption during mixing as a qualitative indication of changing rheology, or measurement of rheological changes at some time after mixing. Problems associated with these approaches are: failure to take into account motor and drive losses, frictional and surface effects between the dough and the mixer, varying signal damping and data acquisition rates, effects of aeration on rheology, and rheological relaxation effects.

From the literature it is possible obtain information about mixing speed and energy (work input) on optimum mixing time for bread dough [Kilborn and Tipples, (1972)], but not for pasta in dynamic control mode.

3. Materials and methods

Durum semolina, with different protein and gluten content, was mixed with a water to obtain the final pasta dough. Durum semolina was supplied by Rummo S.p.A. (Benevento, Italy) at different protein levels. For all the durum flours the company supplied a technical sheet for the right water addition level, which is in the range of 30-35% w/w. In Table 1 is shown the composition of the durum semolina analyzed in terms of protein, gluten content and water required.

| Durum semolina type | $y_{\text{protein}}(\%)$ | $y_{\text{gluten}}(\%)$ | m_{water} for 100g of durum semolina [g] | u_{final} of dough(w.b.) [-] |
|---------------------|--------------------------|-------------------------|---|---------------------------------------|
| S1 | 14.53 | 12.74 | 34 | 34.15 |
| S2 | 14.27 | 12.49 | 36 | 34.21 |
| S3 | 14.08 | 12.36 | 36 | 34.06 |
| S4 | 13.94 | 12.04 | 38 | 33.87 |
| S5 | 12.83 | 11.33 | 36 | 34.95 |
| S6 | 12.11 | 11.33 | 36 | 34.21 |

Table 1. Durum semolina type: gluten, protein fraction and quantity of water necessary to obtain the optimal dough.

All the ingredients were measured by an analytical balance (Mettler Toledo PG403-S (Italy)).

The quality of durum semolina was characterized by rheological point of view through rheometric measures in oscillatory and dynamic-mechanical analysis.

3.1 Dough preparations and mixing

Water and semolina were conveyed to a mixer. Samples were obtained using the Farinograph of Brabender. Once in the mixer, the semolina mixture was hydrated with water and it was used the content of water reported in Table 1.

The engine body, which can operate at different speeds, was connected to the rotating blades, the shape of which is defined to “zeda”. This allows the ingredients to blend completely. The shape of the mixer is as basket, to allow loading of the ingredients above, and is jacketed and connected to a thermal bath which allows control of the temperature in the phase of mixing.

The bath temperature is measured by a thermocouple and can be set through the control thermostat. The stirring speed is fixed to 63 rpm and the durum semolina quantity was fixed at 200g.

The total time of mixing phase is 35 minutes and samples are taken every 5 minutes.

3.2 Samples preparation

After the mixing phase, the dough was laminated through the use of a sheeting

machine for pasta with a level regulator, which allows the obtaining of sheets with an appropriate size, then the sheet was formed in circular geometry, having a thickness of about 2.3mm and the diameter of 25mm. This shape was used for the rheometric tests. The samples were left to rest for twenty minutes to relax the stress induced by the mixing and sheeting processes, wrapping all the samples, one for each, in parchment paper and aluminum at the purpose to reduce the water loses and, finally, closing in a plastic box.

The rheological behaviour of the dough was studied for different mixing time: 5-10-15-20-25-30 and 35 minutes [Zaidel et al.,(2008)] to control the dough behaviour evolution.

In order to assess how the temperature of the mixing influences the mixing time [Kieffer et al., (1998)], the rheological properties were studied for three different temperatures of mixing: 20, 30 and 40°C.

All samples prepared and analyzed are reported in Table 2. Each sample is defined with an identifying name that will be used in following chapters.

| Durum semolina type | t_{mix} [min] | | | | | | | | T_{mix}[°C] |
|----------------------------|------------------------------|----|----|----|----|----|----|----|----------------------------|
| S1-20 | 5 | 10 | 15 | 20 | 25 | 30 | 35 | 20 | |
| S1-30 | 5 | 10 | 15 | 20 | 25 | 30 | 35 | 30 | |
| S1-40 | 5 | 10 | 15 | 20 | 25 | 30 | 35 | 40 | |
| S2-20 | 5 | 10 | 15 | 20 | 25 | 30 | 35 | 20 | |
| S2-30 | 5 | 10 | 15 | 20 | 25 | 30 | 35 | 30 | |
| S2-40 | 5 | 10 | 15 | 20 | 25 | 30 | 35 | 40 | |
| S3-20 | 5 | 10 | 15 | 20 | 25 | 30 | 35 | 20 | |
| S3-30 | 5 | 10 | 15 | 20 | 25 | 30 | 35 | 30 | |
| S3-40 | 5 | 10 | 15 | 20 | 25 | 30 | 35 | 40 | |
| S4-20 | 5 | 10 | 15 | 20 | 25 | 30 | 35 | 20 | |
| S4-30 | 5 | 10 | 15 | 20 | 25 | 30 | 35 | 30 | |
| S4-40 | 5 | 10 | 15 | 20 | 25 | 30 | 35 | 40 | |
| S5-20 | 5 | 10 | 15 | 20 | 25 | 30 | 35 | 20 | |
| S5-30 | 5 | 10 | 15 | 20 | 25 | 30 | 35 | 30 | |
| S5-40 | 5 | 10 | 15 | 20 | 25 | 30 | 35 | 40 | |
| S6-20 | 5 | 10 | 15 | 20 | 25 | 30 | 35 | 20 | |
| S6-30 | 5 | 10 | 15 | 20 | 25 | 30 | 35 | 30 | |
| S6-40 | 5 | 10 | 15 | 20 | 25 | 30 | 35 | 40 | |

Table 2. Samples analyzed.

In order to avoid water evaporation during test, the samples were suitably lubricated with silicone oil ($\mu=1000 \text{ Pa}\cdot\text{s}$) [Sliwinski et al.(2004a-b-c)].

4. Rheological characterization: oscillatory tests

The rheological tests was carried out by using a controlled strain rheometer ARES-RFS (TA Instrument, USA). The temperature control is guaranteed by a Peltier¹ system, acting under the lower plate.

The rheometer is equipped with a parallel plate geometry ($\Phi = 25\text{mm}$) using a gap of $2.1\pm 0.1\text{mm}$.

On the material were performed the following oscillatory tests:

- ✓ Dynamic Strain Sweep Tests: carried out at three different temperatures: 30, 50 and 70°C at 1Hz. This type of test is used to determine the region of linear viscoelasticity exhibited by the material (the area in which the two modules, G' and G'' , are maintained roughly constant). When materials are tested in the linear range, material functions do not depend on the magnitude of the stress, the magnitude of the deforming strain, or the rate of application of the strain [Steffe, (1996)]. Before the test, for each temperature, is imposed a waiting time (400, 500 and 600 s) in order to relax the stresses imposed during loading the sample and allow to reach the temperature set to the heart of the sample;
- ✓ Dynamic Time Sweep Tests: the G' and G'' moduli are determined as a function of time. With this test, it is possible to follow the change of structure of the material over time; the test is executed at fixed temperature, strain and frequency and observing the moduli evolution between 0 and 1000 s;
- ✓ Dynamic frequency Sweep Test: G' and G'' are determined as a function of frequency. During the test is imposed a range of frequency, from 0.01 Hz to 10 Hz. Strain, temperature and waiting time are fixed;

¹ The system uses the semiconductor Peltier, exploiting a potential difference applied across the semiconductor generates a flow of current proportional to a flow of heat. Applying a current flow in a certain direction ensures a flow of heat in that direction and vice versa, in this way it is possible to cool and heat the upper surface almost the same way by simply reversing the flow [Herring, (1954)].

- ✓ Dynamic Temperature Ramp Test; performed by varying the sample temperature to the desired value with a heating rate of 1°C/min, in the linear region and at 1 Hz. The temperature variations involve structural variations of the sample and, consequently, also variations in the response of the material to the imposed deformations.

For all the samples, the tests were performed at three temperatures: 30°C, 50°C, 70°C. For each time of mixing, samples were analysed in duplicate and each test was carried out in triplicate.

5. Weak gel model

The data obtained were reported in terms of complex modulus (G^*) and according to Gabriele et al. (2001), rheological properties of the material can be obtained by considering the dough as a weakly structured three-dimensional network.

The model of the weak-gel is valid for systems weakly structured as foods, cosmetics and pharmaceutical products. The typical behaviour of the modules G' and G'' as a function of frequency, which is often found for this type of systems, is the following in a log-log, shown in Figure 1.

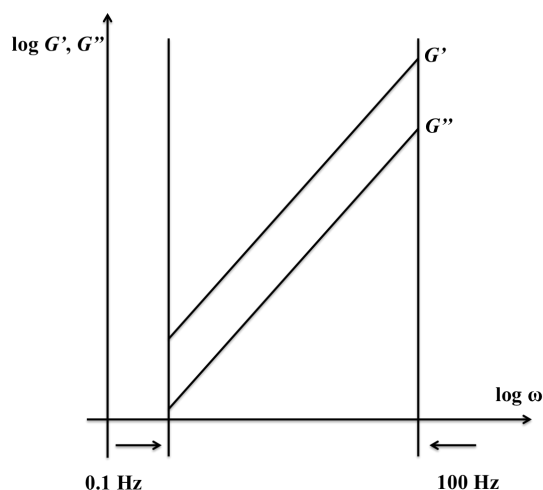


Figure 1. A weak-gel model

The two modules have a linear trend and are almost parallel if analysed between 0.1 and 100 Hz..

Mechanical characteristics of this network are determined by considering the number of the interacting units inside the structure and the strength of the connections among them. At any temperature T, if the complex modulus G^* is considered as a combination of the elastic modulus G' and the dissipative one G'' , data can be fitted using a two parameter power law reported:

$$G^*(\omega) = \sqrt{(G'^2 + G''^2)} = A \cdot \omega^{\frac{1}{z}} \quad (1)$$

where the parameter z is related to the number of interacting rheological units within the three-dimensional network and A is the strength of these interactions [Gabriele et al., (2001)].

When A increases the interaction forces within network are increasing whilst a high z value indicates a large number of interacting units cooperating and increasing the network connectivity. All data fitting is performed through Table Curve 2D Software (Jandel Scientific, USA).

6. Results and discussions

From the rheological test performed at several temperatures within the linear region, it was found that the measured values of G' is major than G'' , showing a quasi-linear behaviour in a log-log plot over a wide range of frequency. A typical example of frequency sweep is shown in Figure 2 for S1-30 sample.

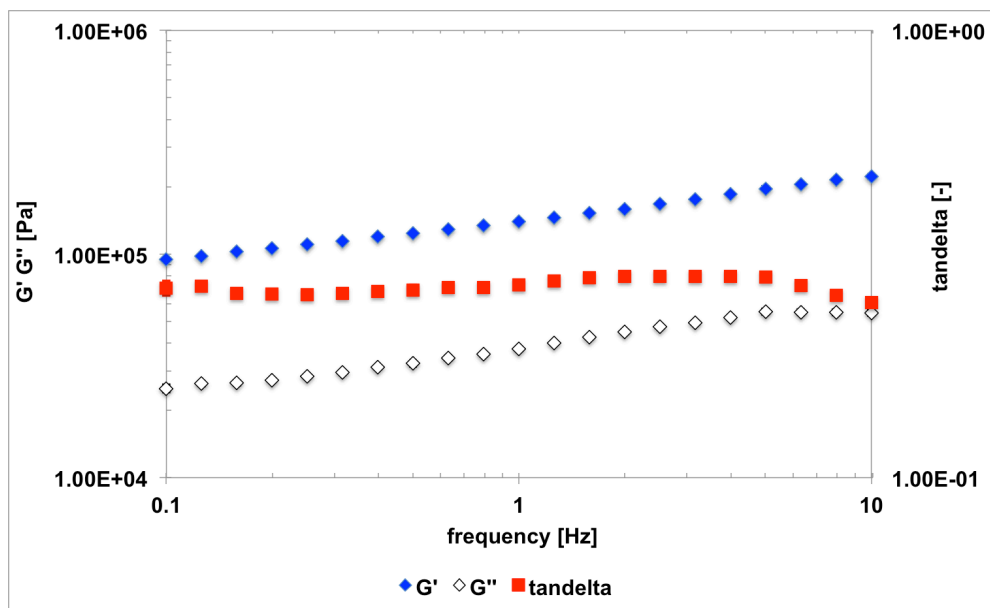


Figure 2. Sample S1-30. Trends of dynamic moduli G' , G'' and $\tan \delta$ for $t_{\text{mixing}} = 20$ min and $T_{\text{mixing}} = 30^\circ\text{C}$.

The samples were tested for different mixing conditions, time and temperature, and the results will be discussed below.

6.1 Effect of time mixing

In Figure 3 and 4 are showed the results obtained by fitting the experimental data with Eq. (1) for the sample S5-30. The analysis shown below refers to the tests carried out for the mixing temperature of 30°C . Experimental data are shown only to the temperature of measure 30°C .

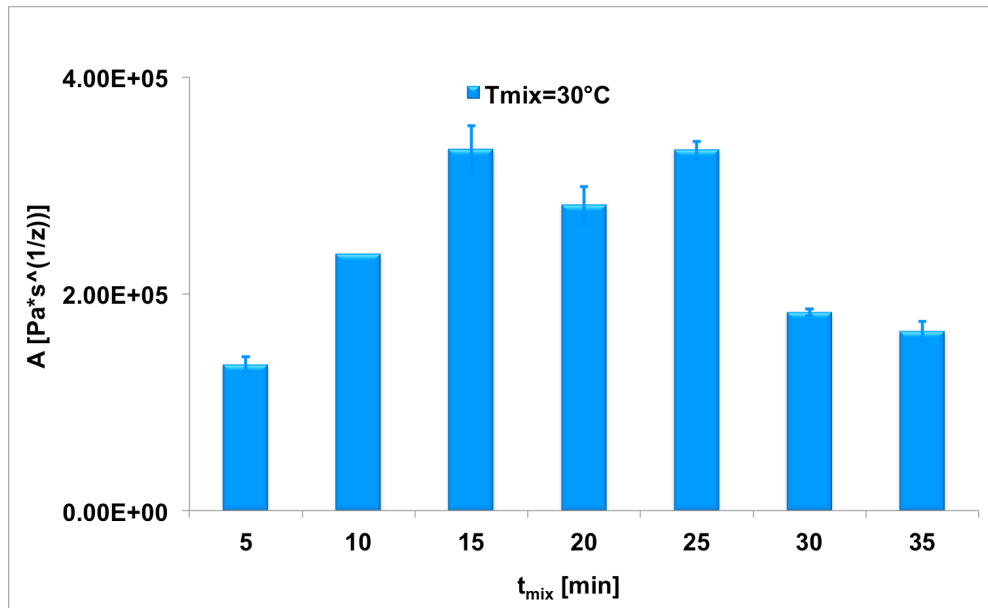


Figure 3. Trends of parameter A vs time of mixing for the sample S5-30.

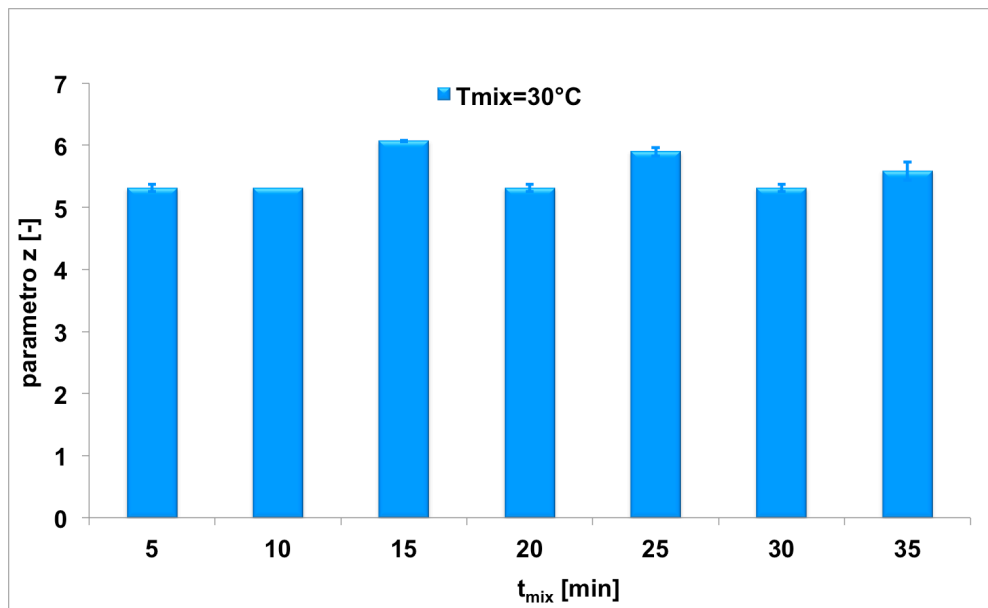


Figure 4. Trends of parameter z vs time of mixing for the sample S5-30.

A parity of the temperature of mixing can be seen as the parameter A has a slight increase with the time of mixing, with a maximum point at around 15 minutes, while the extension z is constant. The Figure 3 shows that increasing the temperature of mixing, the optimal mixing time of dough decreases, the development of the dough begins before.

The results shown for the sample S5 seem to show a good time, in fact the analysis conducted on other durum semolina showed no significant variations with the rheological parameters, in fact the values of the parameters A and z are nearly constant under varying operating conditions.

For the sample S3 has not been possible to complete the trend of evidence for the little semolina provided by the company. While for the sample S6, for the little semolina provided by the company, were analyzed only the times of 10, 15, 20 and 25 minutes.

In Figure 5, 6, 7, 8, 9, 10, 11 and 12 are illustrated the results under the same conditions obtained for samples S1, S2, S4 and S6.

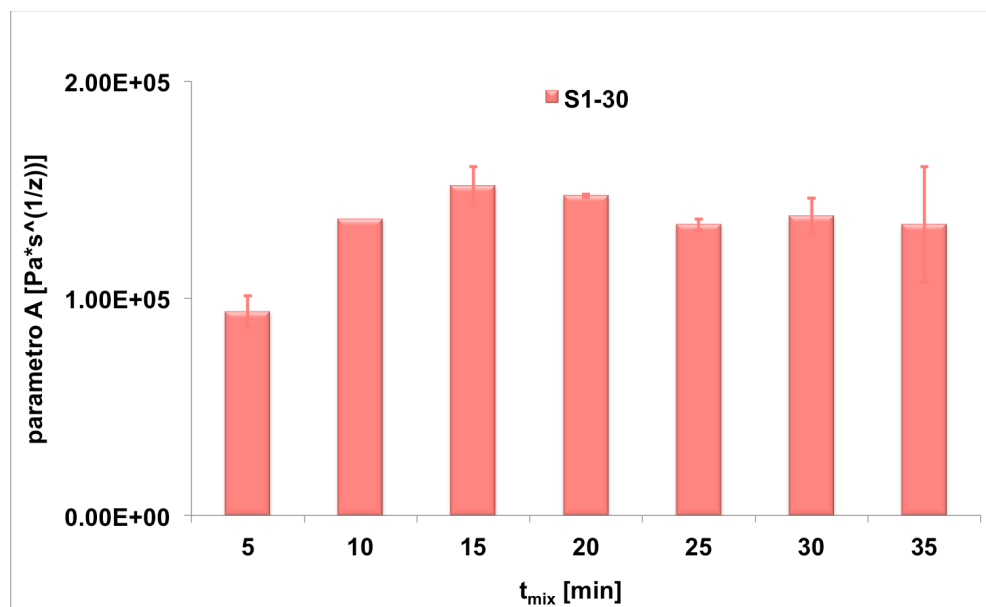


Figure 5. Trends of parameter A vs time of mixing for the sample S1-30.

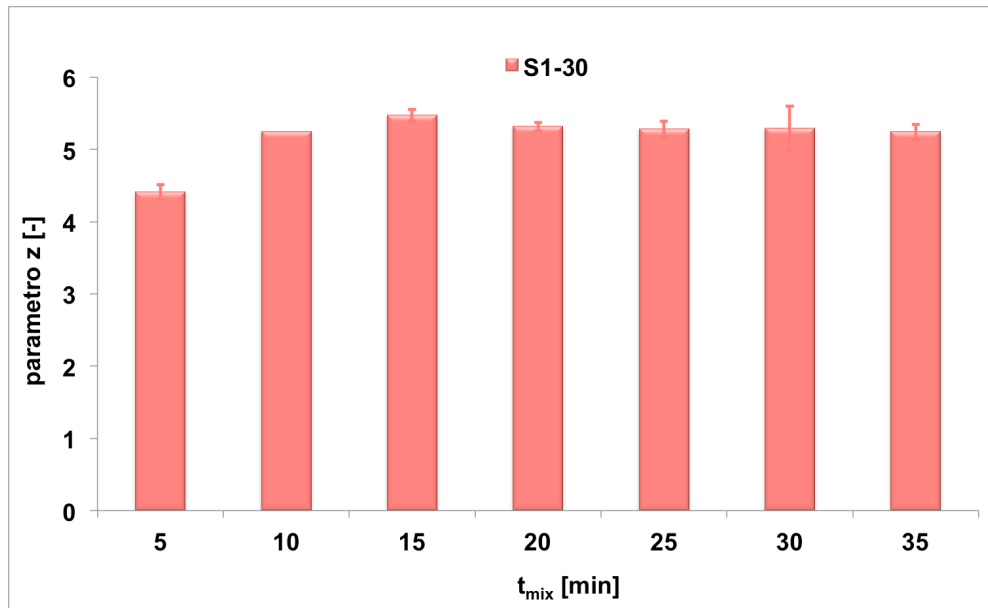


Figure 6. Trends of parameter z vs time of mixing for the sample S1-30.

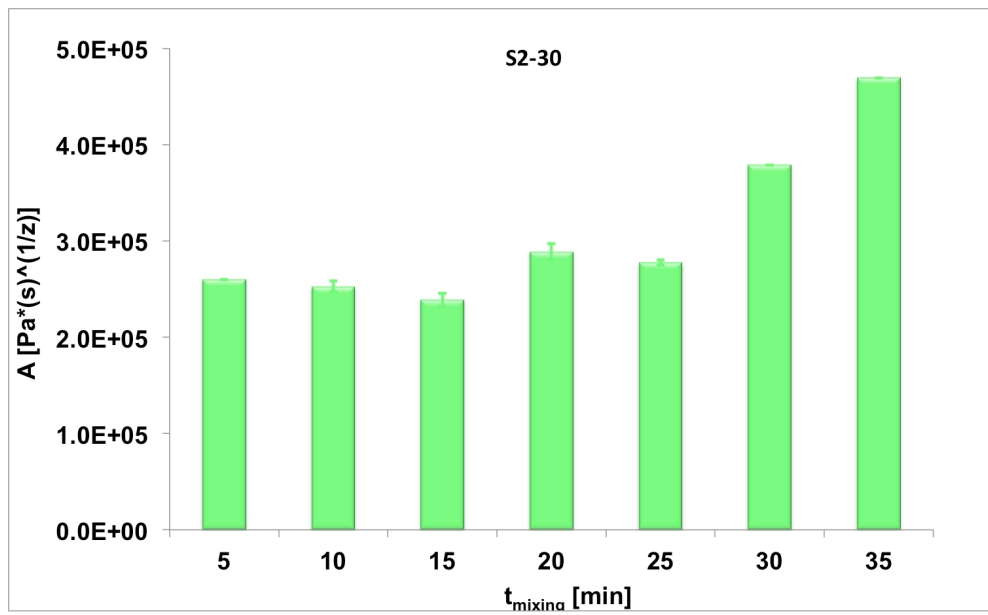


Figure 7. Trends of parameter A vs time of mixing for the sample S1-30.

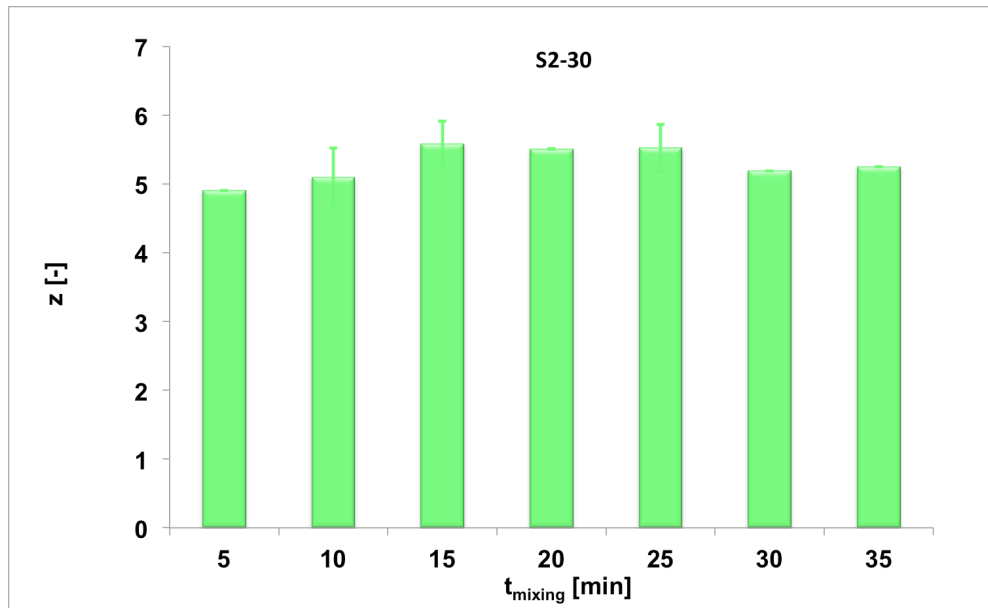


Figure 8. Trends of parameter z vs time of mixing for the sample S2-30.

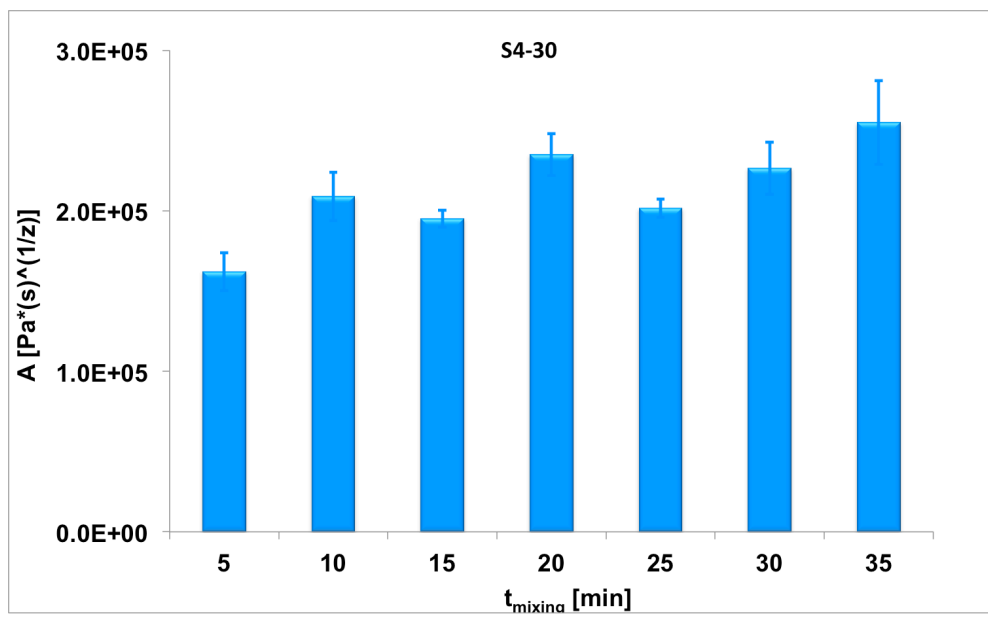


Figure 9. Trends of parameter A vs time of mixing for the sample S4-30.

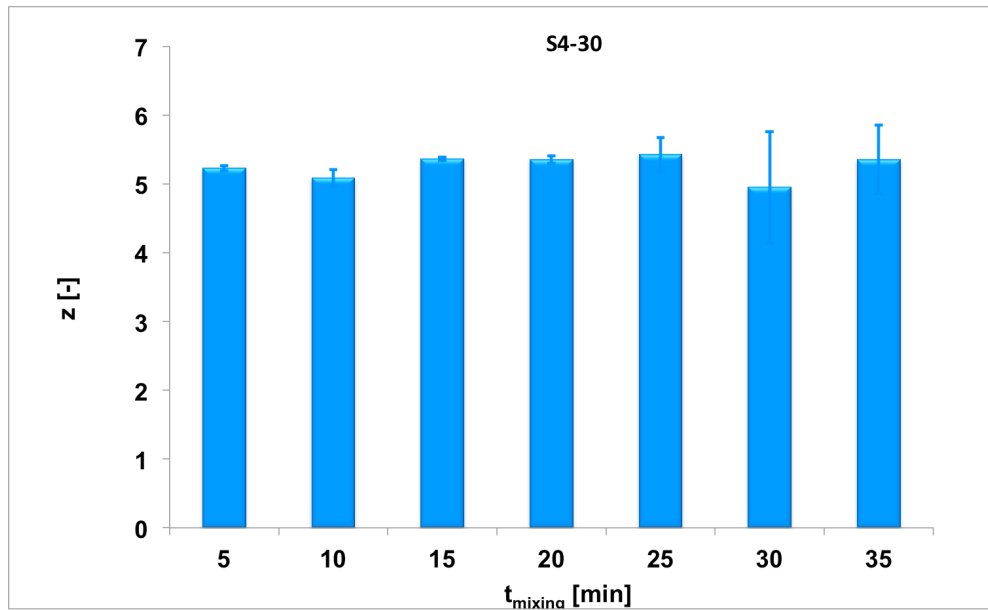


Figure 10. Trends of parameter z vs time of mixing for the sample S4-30.

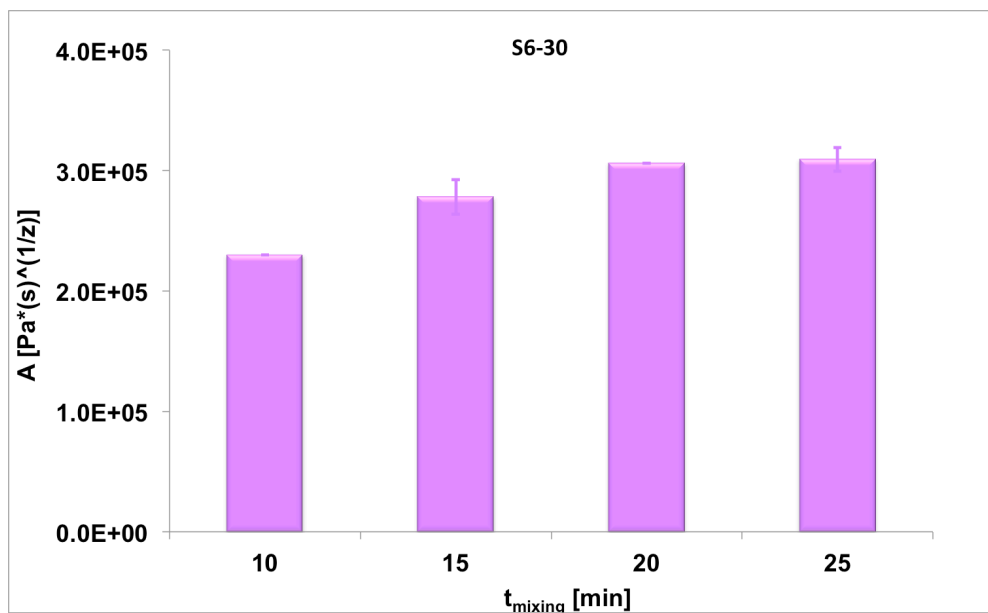


Figure 11. Trends of parameter A vs time of mixing for the sample S6-30.

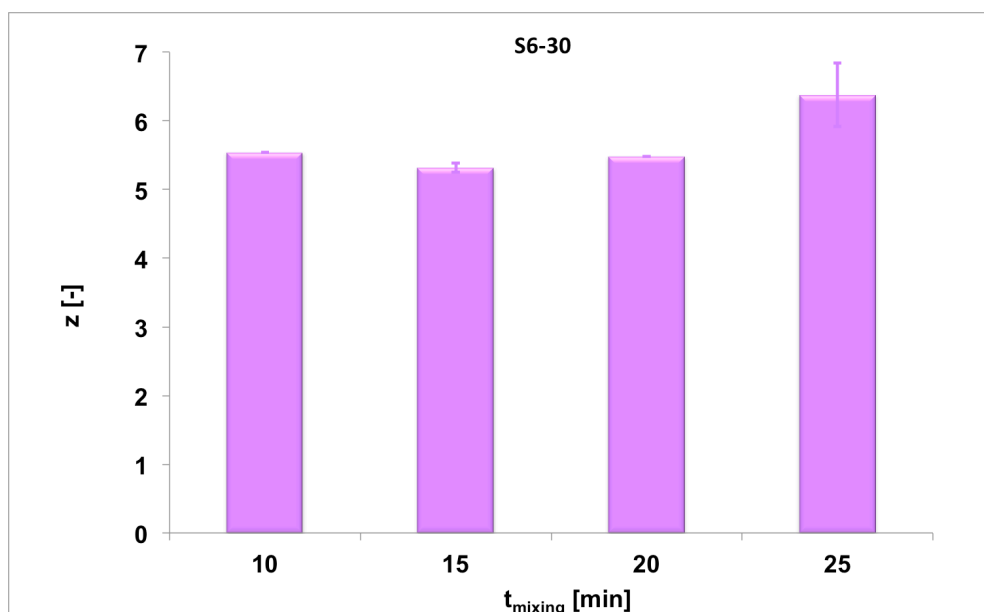


Figure 12. Trends of parameter z vs time of mixing for the sample S6-30.

Mixing at different times affects both the rheological and structural characteristics of dough. Excessively long mixing times lead to soft dough, less consistent and stickier than optimal mixed. However, as reported in the figures 5, 7, 9 and 11 above, it can be seen the effect of over-mixing is strongly related to the type of semolina.

The figures are reported as a function of the protein content and gluten content. However you can see that each has a different behaviour from the other semolina. The rheological characterization is therefore not able to show a direct effect with the optimum mixing time, but only allows effects under the conditions of overmixing [Gomez et al., (2011)].

Experimental data valuated at a temperature of mixing of 30°C have been reported in term of $\tan \delta$ at a frequency of 1 Hz with time of mixing, as shown in Figure 13.

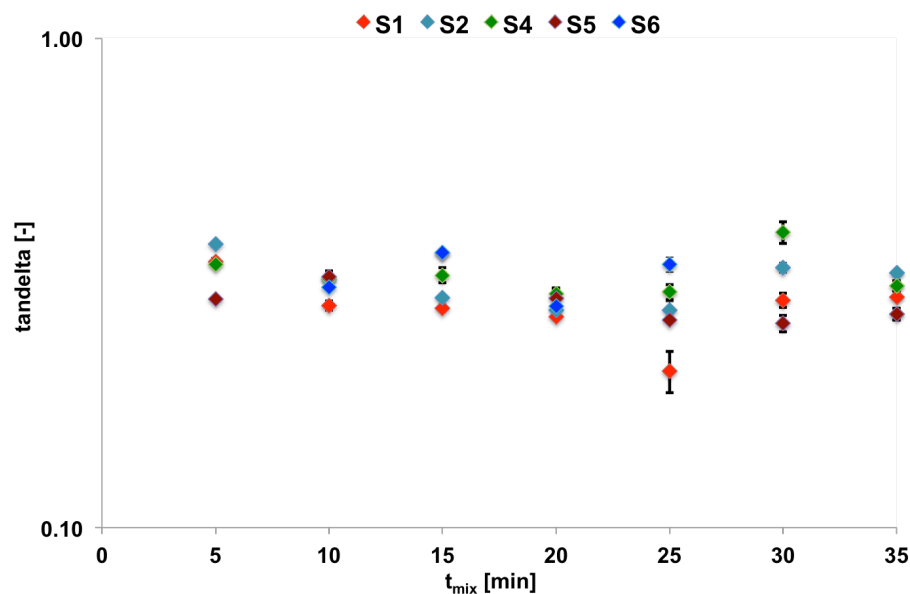


Figure 13. Curve of $\tan \delta$ at a frequency of 1 Hz with the time of mixing for each sample of durum semolina (S1-S2-S4-S5-S6).

For each sample of semolina dough, $\tan \delta$ does not change with the time of mixing. With respect to the $\tan \delta$ value ($\tan \delta < 0.5$), all the semolina doughs have higher elastic characteristics than viscous characteristics [González-Segura et al. (2013)].

Also, it is found that doughs of durum semolina made with high gluten content and protein quality (S1 sample), have lower value of $\tan \delta$ than doughs made with lower content of gluten and protein [Miller and Hosney, (1999); Samaan et al. (2006)].

To better highlight results are below also shows the values in table 3,4,5,6 and 7 are illustrated the results under the same conditions obtained for samples S1, S2, S4 and S6. The tables illustrate the trend of the parameters A, z and $\tan \delta$.

| S1_t _{mix} [min] | A _{T_{mix}=30°C} | z _{T_{mix}=30°C} | $\tan \delta$ _{T_{mix}=30°C} |
|---------------------------|-----------------------------------|-----------------------------------|---|
| 5 | 93947±7345 | 4.409±0.106 | 0.3487±0.0062 |
| 10 | 136641±943 | 5.245±0.029 | 0.2844±0.0061 |
| 15 | 151866±8888 | 5.470±0.079 | 0.2809±0.0044 |
| 20 | 147337±780 | 5.315±0.061 | 0.2695±0.0034 |
| 25 | 140307±2532 | 5.278±0.110 | 0.2086±0.0201 |
| 30 | 137929±8333 | 5.287±0.311 | 0.2916±0.0097 |
| 35 | 134027±26629 | 5.242±0.104 | 0.2957±0.0039 |

Table 3. Trends of parameters A vs time of mixing, z and $\tan \delta$ for the samples S1-30.

| S2_t _{mix} [min] | A _{T_{mix}=30°C} | Z _{T_{mix}=30°C} | $\tan \delta$ _{T_{mix}=30°C} |
|---------------------------|-----------------------------------|-----------------------------------|---|
| 5 | 259539±4245 | 4.902±0.697 | 0.3801±0.0010 |
| 10 | 252485±14602 | 5.089±0.313 | 0.3214±0.0092 |
| 15 | 238775±10705 | 5.578±0.109 | 0.2951±0.0024 |
| 20 | 288565±8737 | 5.506±0.144 | 0.2783±0.0079 |
| 25 | 277281±11582 | 5.521±0.260 | 0.2779±0.0112 |
| 30 | 378551±18263 | 5.187±0.762 | 0.3398±0.0085 |
| 35 | 469195±4706 | 5.248±0.419 | 0.3313±0.0057 |

Table 4. Trends of parameters A vs time of mixing, z and $\tan \delta$ for the samples S2-30.

| S4_t _{mix} [min] | A _{T_{mix}=30°C} | Z _{T_{mix}=30°C} | $\tan \delta$ _{T_{mix}=30°C} |
|---------------------------|-----------------------------------|-----------------------------------|---|
| 5 | 162147±14386 | 5.227±0.042 | 0.3450±0.0025 |
| 10 | 208949±6369 | 5.083±0.033 | 0.3224±0.0067 |
| 15 | 195064±7783 | 5.364±0.022 | 0.3276±0.0116 |
| 20 | 235012±15873 | 5.351±0.177 | 0.3006±0.0078 |
| 25 | 201529±14848 | 5.422±0.343 | 0.3029±0.0107 |
| 30 | 226467±7238 | 4.951±0.486 | 0.4011±0.0209 |
| 35 | 254924±51932 | 5.351±0.0179 | 0.3120±0.0076 |

Table 5. Trends of parameters A vs time of mixing, z and $\tan \delta$ for the samples S4-30.

| S5_t _{mix} [min] | A _{T_{mix}=30°C} | Z _{T_{mix}=30°C} | $\tan \delta$ _{T_{mix}=30°C} |
|---------------------------|-----------------------------------|-----------------------------------|---|
| 5 | 134885±7072 | 5.309±0.057 | 0.2932±0.0025 |
| 10 | 236739±2847 | 5.021±0.106 | 0.3256±0.0094 |
| 15 | 333676±21389 | 6.060±0.014 | 0.3640±0.0044 |
| 20 | 281838±17310 | 5.403±0.057 | 0.2940±0.0122 |
| 25 | 332820±7905 | 5.894±0.072 | 0.2657±0.0038 |
| 30 | 182752±3177 | 6.152±0.336 | 0.2611±0.0.103 |
| 35 | 165627±8920 | 5.586±0.1463 | 0.2728±0.0076 |

Table 6. Trends of parameters A vs time of mixing, z and $\tan \delta$ for the samples S5-30.

| S6_t _{mix} [min] | A _{T_{mix}=30°C} | Z _{T_{mix}=30°C} | $\tan \delta$ _{T_{mix}=30°C} |
|---------------------------|-----------------------------------|-----------------------------------|---|
| 10 | 230013±5292 | 5.542±0.089 | 0.3099±0.0013 |
| 15 | 278115±2429 | 5.316±0.245 | 0.3644±0.0057 |
| 20 | 306159±15591 | 5.482±0.175 | 0.2832±0.0161 |
| 25 | 309527±8238 | 6.378±0.205 | 0.3447±0.0121 |

Table 7. Trends of parameters A vs time of mixing, z and $\tan \delta$ for the samples S6-30.

6. 2 Effect of temperature mixing

In Figure 14 and 15 are showed the results obtained by fitting the experimental data with Eq. (1) for the sample S4-20, S4-30 and S4-40. For a mixing temperature of 20 ° C the mixture is found to be rougher and incoherent in the first minutes of mixing. For this reason the samples were carried out at this temperature suffering from a mixing time of 15 minutes. The analysis shown below refers to the tests carried out for two mixing times, the center of the range

analyzed, 15 and 25 minutes e for three temperatures of measure (30, 50 and 70 °C).

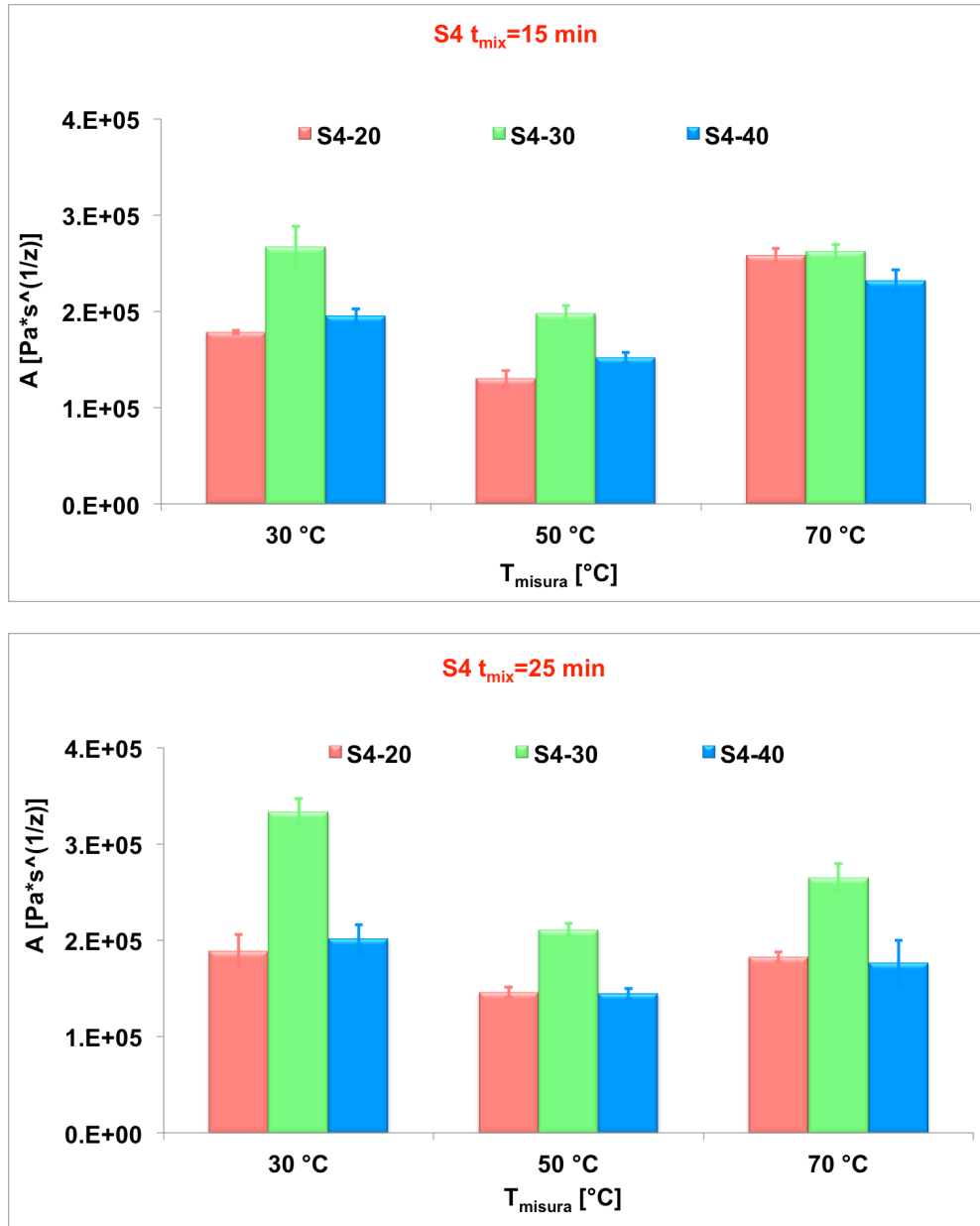


Figure 14. Trends of parameter A for the samples S4-20, S4-30 and S4-40 for time of mixing: 15 and 25 minutes.

Observing the parameter A can be seen that, for a mixing temperature of 20°C and 40 ° C, the value is low and is equal for both. Apparently the dough seems to be

underdeveloped.

Observing the z parameter only small differences can be seen at the same temperature of analysis, but at different mixing conditions. This trend suggest no change in the structure development of dough, or small differences changing the mixing temperature, moreover seems to be similar for samples mixed at 20 and 40°C.

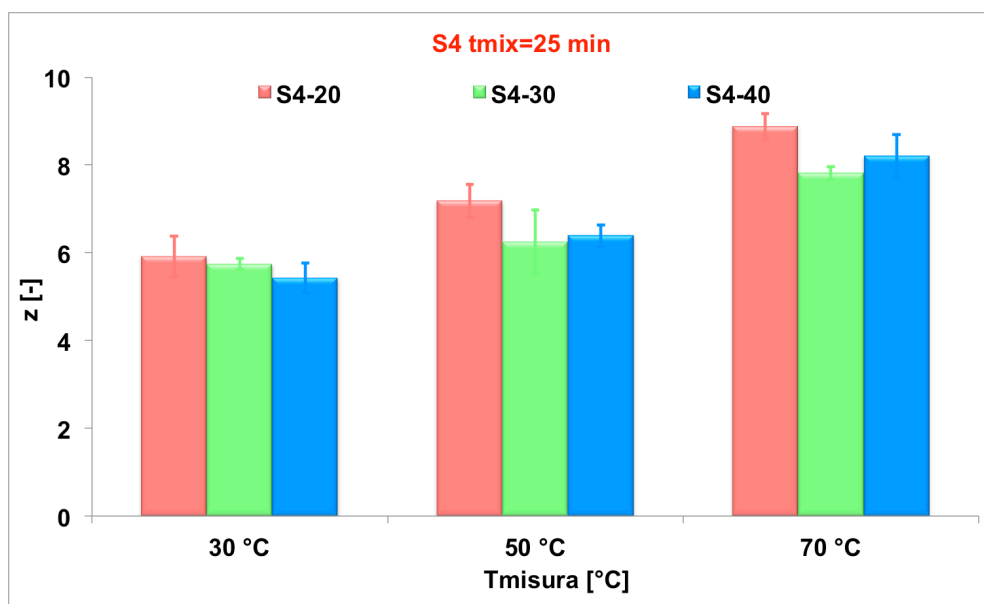
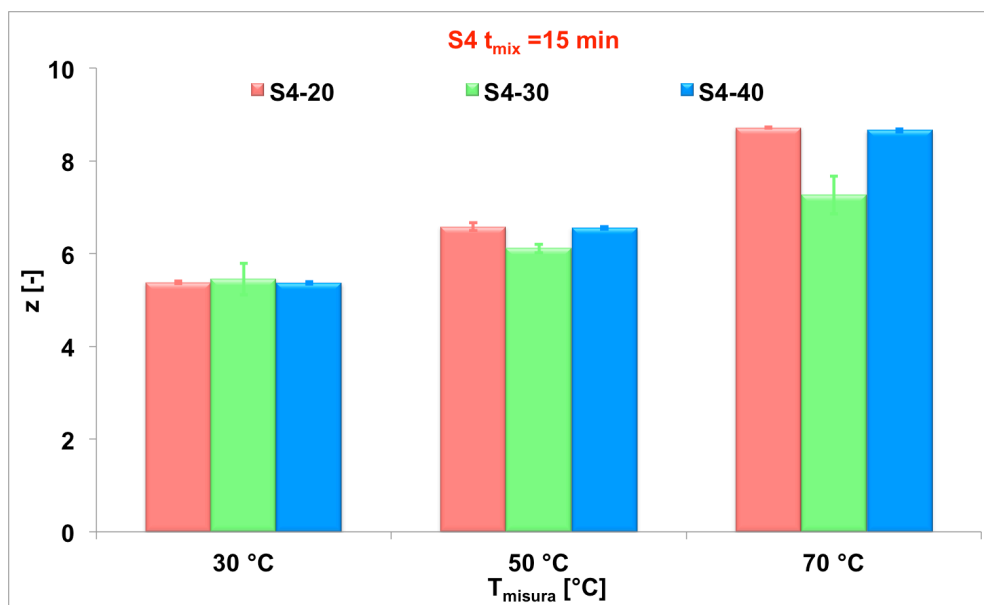


Figure 15. Trends of parameter z for the samples S4-20, S4-30 and S4-40 for time of mixing: 15 and 25 minutes.

Looking at the A parameter, for a given time of measure, a maximum is observed for dough mixed at 30°C, a temperature that is similar to those commonly used in the industrial process (about 33°C), while the number of cross-linking, z, is maintained almost constant with the mixing temperature, as seen before.

Similar results are obtained for the other samples. In Figure 16, 17, 18 and 19 are illustrated the results under the same conditions obtained for samples S1 and S5.

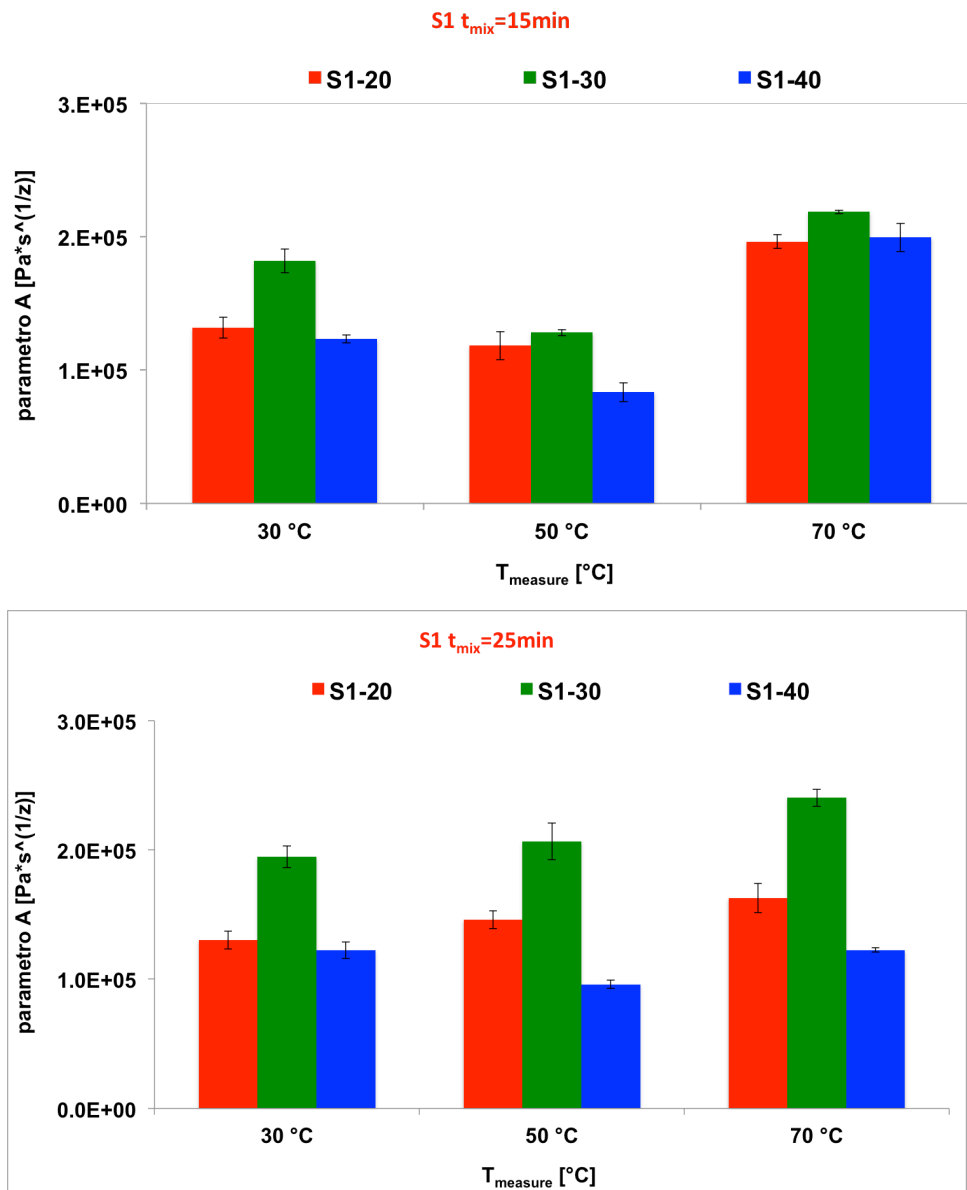


Figure 16. Trends of parameter A for the samples S1-20, S1-30 and S1-40 for time of mixing: 15 and 25 minutes.

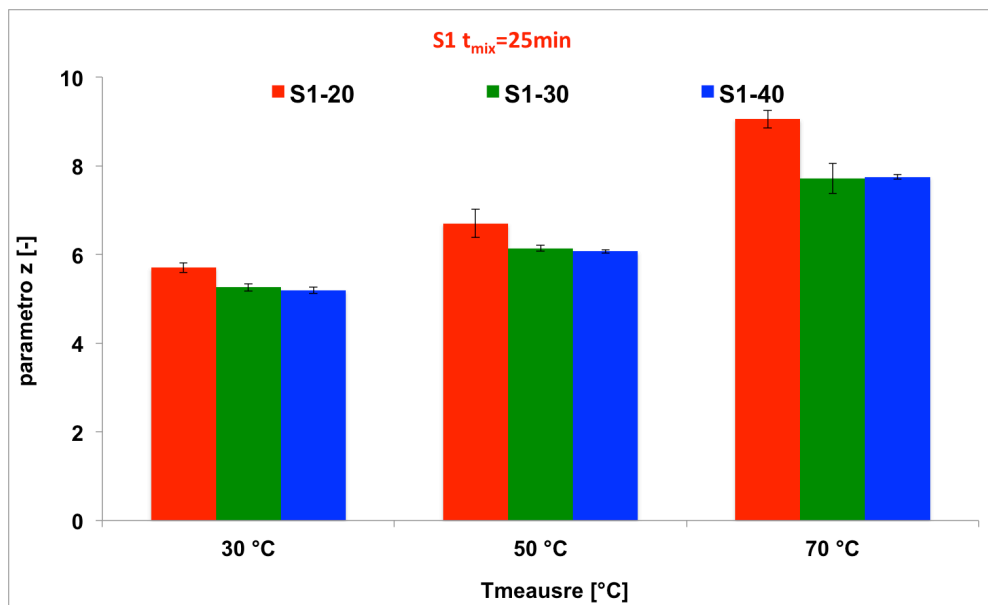
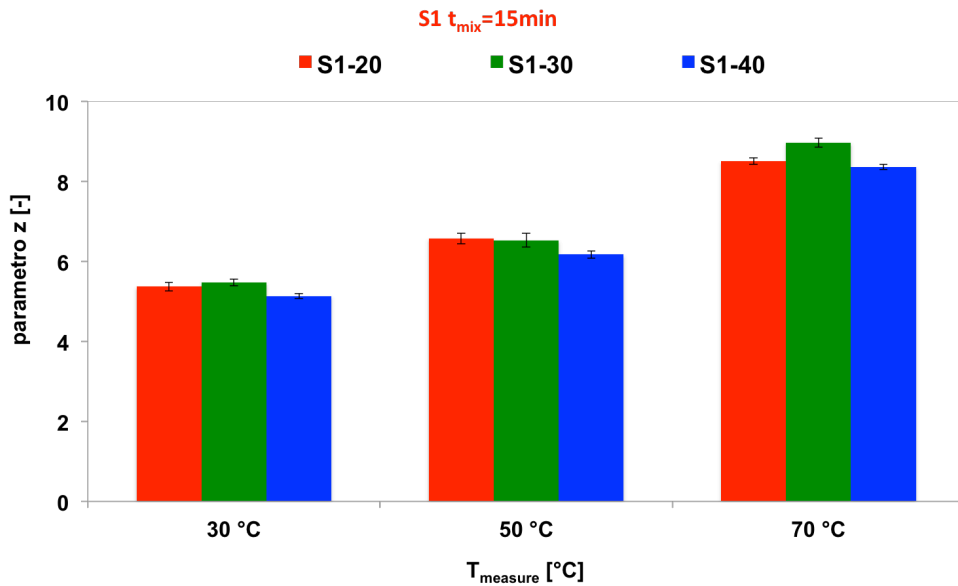


Figure 17. Trends of parameter z for the samples S1-20, S1-30 and S1-40 for time of mixing: 15 and 25 minutes.

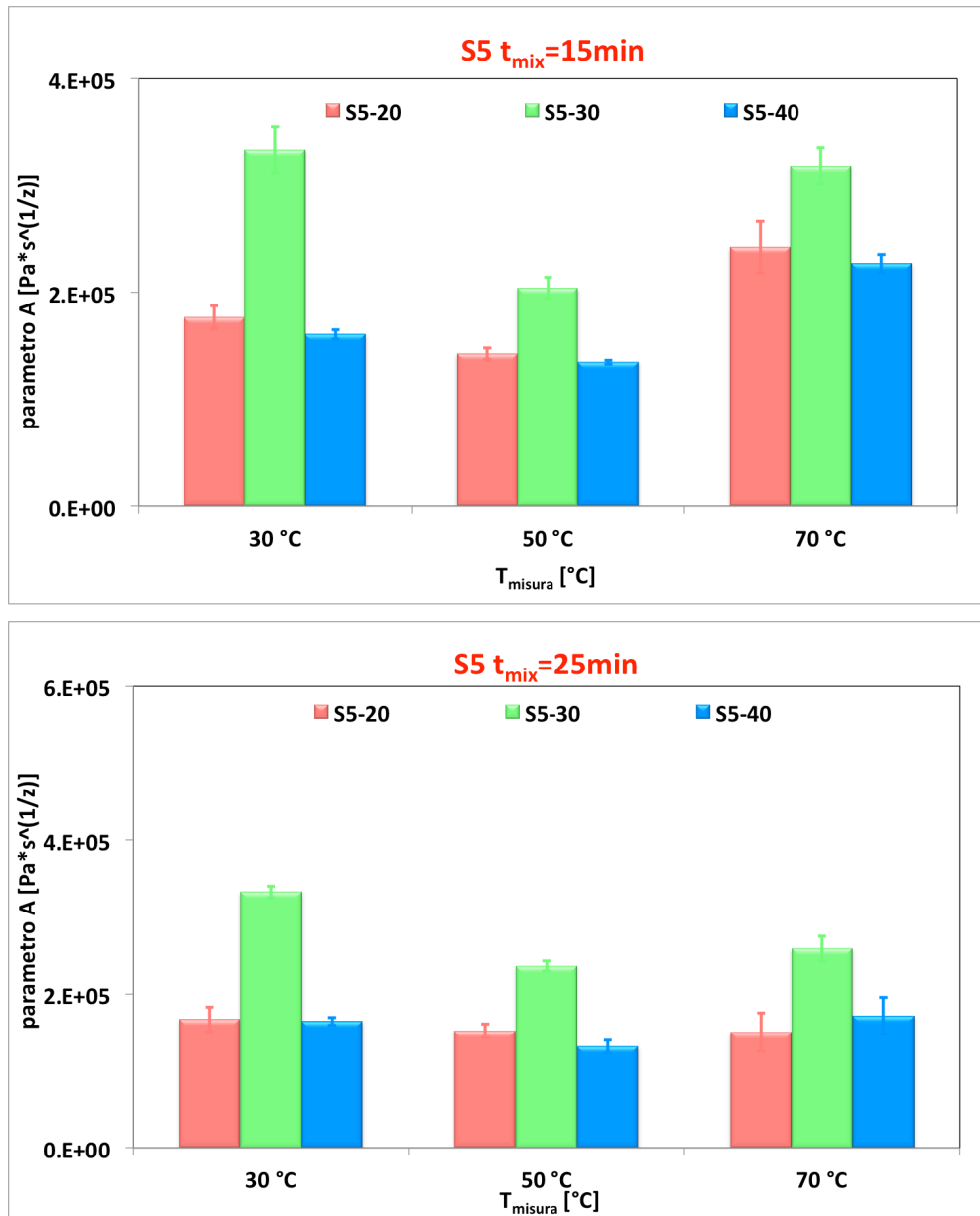


Figure 18. Trends of parameter A for the samples S5-20, S5-30 and S5-40 for time of mixing: 15 and 25 minutes.

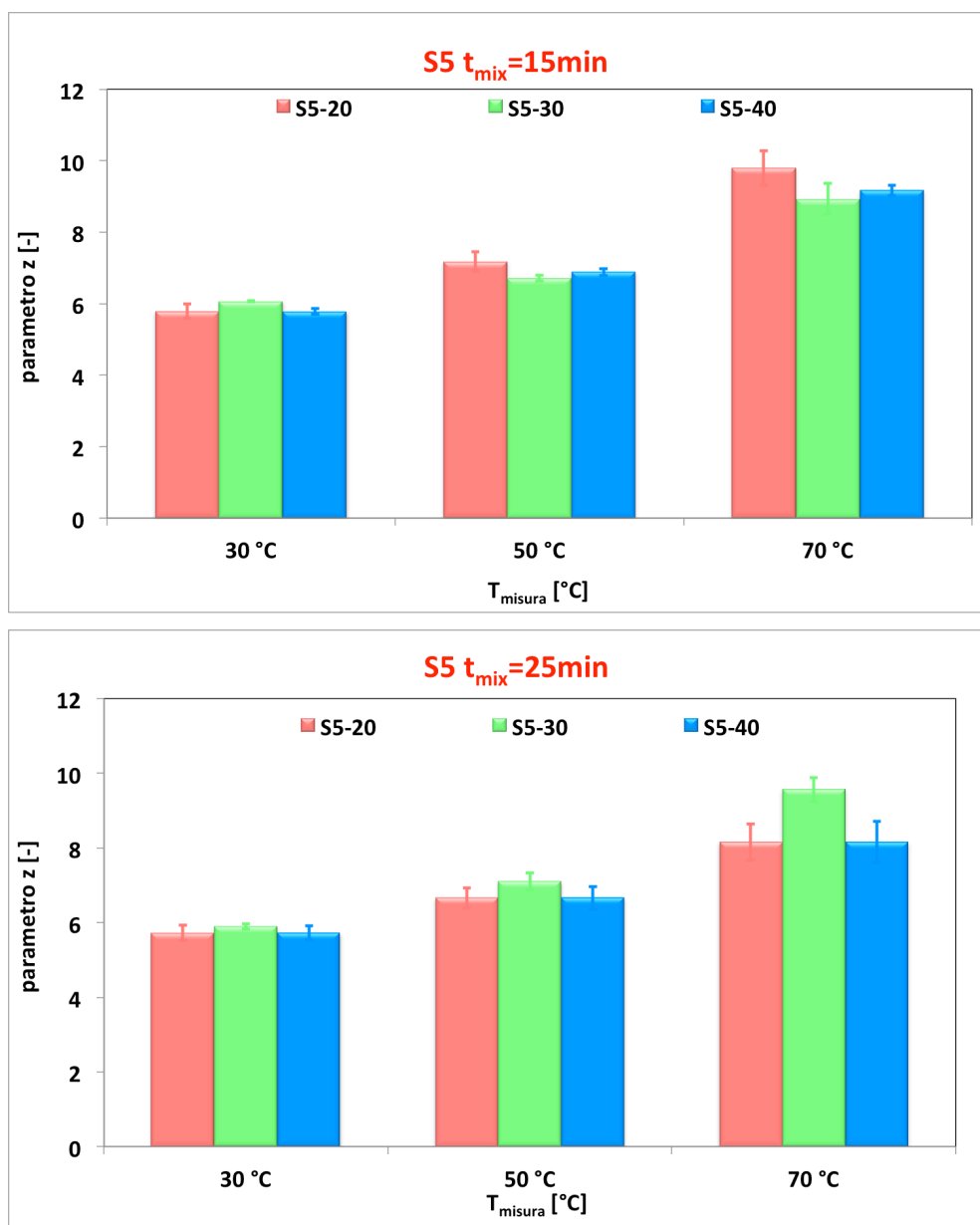


Figure 19. Trends of parameter z for the samples S5-20, S5-30 and S5-40 for time of mixing: 15 and 25 minutes.

For samples S2, S3 and S6 has not been possible to complete the trend of evidence for the little semolina provided by the company.

To better highlight results are below also shows the values in Tables 8 and 9 for the temperature of measure 30°C.

| $T_{\text{mixing}} [^{\circ}\text{C}]$ | Parameters of weak gel model | S1_tmix=15min | S1_tmix=25min |
|--|------------------------------|---------------|---------------|
| 20 | A | 131778±7788 | 130250±6952 |
| | z | 5.37±0.108 | 5701±0.108 |
| 30 | A | 181865±8888 | 194575±8430 |
| | z | 5.47±0.079 | 5.259±0.084 |
| 40 | A | 123222±2992 | 122395±6341 |
| | z | 5.135±0.063 | 5.192±0.069 |

Table 8. Trends of parameters A and z for the samples S1-20, S1-30 and S1-40. Time of mixing of 15 and 25 minutes and $T_{\text{measure}} = 30^{\circ}\text{C}$.

| $T_{\text{mixing}} [^{\circ}\text{C}]$ | Parameters of weak gel model | S5_tmix=15min | S5_tmix=25min |
|--|------------------------------|---------------|---------------|
| 20 | A | 176645±11004 | 166804±15845 |
| | z | 5.78±0.09 | 5.74±0.20 |
| 30 | A | 499909±20057 | 332820±7905 |
| | z | 6.07±0.01 | 5.89±0.07 |
| 40 | A | 160571±4523 | 164592±5148 |
| | z | 5.78±0.07 | 5.72±0.18 |

Table 9. Trends of parameters A and z for the samples S5-20, S5-30 and S5-40. Time of mixing of 15 and 25 minutes and $T_{\text{measure}} = 30^{\circ}\text{C}$.

6.3 Effect of temperature measure

In Figure 20 are shown the results obtained by fitting the experimental data with Eq. (1) conducted at three temperatures (30°C, 50°C, 70°C) for the S1-30 sample for a mixing time of 15 minutes.

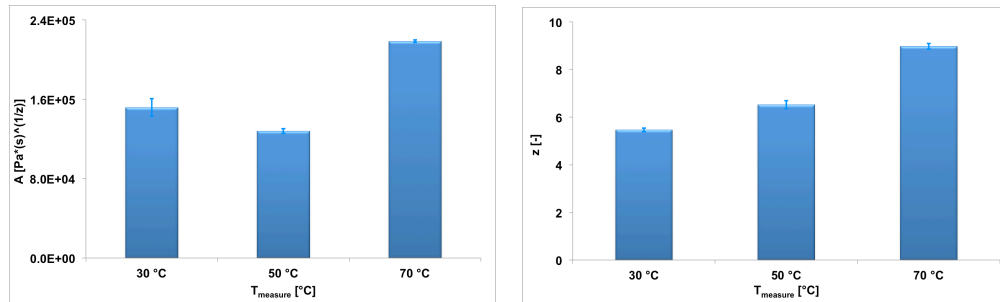


Figure 20. Trends of parameter A and z for the samples S1-30. Time of mixing of 15 minutes.

Figure 20 shown that the coordination number increases increasing the temperature, due to the fact that with increasing temperature the mixture tends to be structured with temperature. This trend occurs for all samples.

The parameter A decreases with the measurement temperature, reaching a minimum value in correspondence of 50°C and then grow again. This is the

classic behaviour of the dough in which initially there is a reduction of the strength of the network and then increase again as a result of starch gelatinisation [Peressini et al. (1999)].

This result can be confirmed by a time cure test at 1 Hz shown in Figure 21.

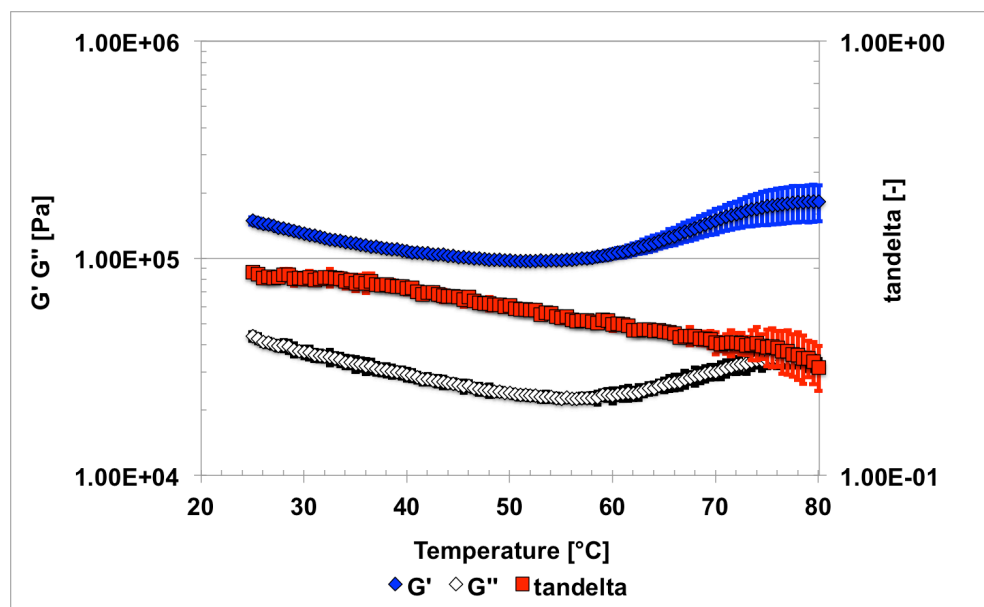


Figure 21. Sample S1-30. Time cure test for $t_{\text{mixing}}=20$ min and $T_{\text{mixing}}=30$ ° C.

This evidence may be explained by noting that, with increasing temperature, the temporary network becomes weaker due to a kinetic effect, after the occurrence of the gelatinisation the network became stronger and therefore both dynamic moduli increase.

The ratio between them, the loss tangent, remains about the same. This means that temperature has no effects on the extension of network as evidenced by almost constant value of z . On the contrary a reduction of the network strength is observed by the decrease of G' and G'' .

In Table 10, 11, 12, 13, 14 and 15 lists the parameters obtained by fitting the experimental result to Eq. (1) conducted under the same conditions obtained for the S1-30 for all mixing time.

Small strain characterization of durum semolina dough

| $T_{\text{measure}} [^{\circ}\text{C}]$ | A_{average} | A_{error} | Z_{average} | Z_{error} |
|---|----------------------|--------------------|----------------------|--------------------|
| 30 | 93947±7345 | 8% | 4.409±0.106 | 2% |
| 50 | 60117±4845 | 8% | 4.712±0.069 | 1% |
| 70 | 175847±18748 | 11% | 7.178±0.265 | 4% |

Table 10. Sample S1-30. Trends of parameter A e z for $t_{\text{mixing}} = 5$ min and $T_{\text{mixing}} = 30^{\circ}\text{C}$.

| $T_{\text{measure}} [^{\circ}\text{C}]$ | A_{average} | A_{error} | Z_{average} | Z_{error} |
|---|----------------------|--------------------|----------------------|--------------------|
| 30 | 136641±944 | 1% | 5.245±0.029 | 1% |
| 50 | 92778±4934 | 5% | 6.214±0.059 | 1% |
| 70 | 211005±7343 | 3% | 8.366±0.086 | 1% |

Table 11. Sample S1-30. Trends of parameter A e z for $t_{\text{mixing}} = 10$ min and $T_{\text{mixing}} = 30^{\circ}\text{C}$.

| $T_{\text{measure}} [^{\circ}\text{C}]$ | A_{average} | A_{error} | Z_{average} | Z_{error} |
|---|----------------------|--------------------|----------------------|--------------------|
| 30 | 147337±781 | 1% | 5.315±0.061 | 1% |
| 50 | 98493±3148 | 3% | 6.822±0.065 | 1% |
| 70 | 191759±7625 | 4% | 9.573±0.062 | 1% |

Table 12. Sample S1-30. Trends of parameter A e z for $t_{\text{mixing}} = 20$ min and $T_{\text{mixing}} = 30^{\circ}\text{C}$.

| $T_{\text{measure}} [^{\circ}\text{C}]$ | A_{average} | A_{error} | Z_{average} | Z_{error} |
|---|----------------------|--------------------|----------------------|--------------------|
| 30 | 140307±2532 | 1% | 5.278±0.110 | 2% |
| 50 | 114915±1327 | 1% | 6.154±0.08 | 1% |
| 70 | 137627±6458 | 3% | 7.525±0.104 | 1% |

Table 13. Sample S1-30. Trends of parameter A e z for $t_{\text{mixing}} = 25$ min and $T_{\text{mixing}} = 30^{\circ}\text{C}$.

| $T_{\text{measure}} [^{\circ}\text{C}]$ | A_{average} | A_{error} | Z_{average} | Z_{error} |
|---|----------------------|--------------------|----------------------|--------------------|
| 30 | 137929±8333 | 6% | 5.287±0.311 | 6% |
| 50 | 101916±11841 | 12% | 6.508±0.121 | 2% |
| 70 | 155922±18003 | 12% | 8.937±0.328 | 4% |

Table 14. Sample S1-30. Trends of parameter A e z for $t_{\text{mixing}} = 30$ min and $T_{\text{mixing}} = 30^{\circ}\text{C}$.

Chapter II

| $T_{\text{measure}} [^{\circ}\text{C}]$ | A_{average} | A_{error} | Z_{average} | Z_{error} |
|---|----------------------|--------------------|----------------------|--------------------|
| 30 | 134027±26629 | 8% | 5.242±0.104 | 2% |
| 50 | 142553±10619 | 4% | 6.524±0.198 | 3% |
| 70 | 155361±7360 | 3% | 8.22±0.396 | 5% |

Table 15. Sample S1-30. Trends of parameter A e z for $t_{\text{mixing}} = 35$ min and $T_{\text{mixing}} = 30^{\circ}\text{C}$.

REFERENCES

- 1) Abdelrahman A. and Spies R., (1986). Dynamic rheological studies of dough systems, *Fundamental of dough rheology*, 87-103
- 2) Amemiya J. I. and Menjivar J. A., (1992). Comparison of small and large deformation measurements to characterize the rheology of wheat flour doughs, *Journal of food engineering*, (16), 91-108
- 3) Campos D. T., Steffe J. F. Ng P. K. W. (1996). Mixing wheat flour and ice to form undeveloped dough, *Cereal Chemistry*, (73), 105-107
- 4) Cole M. E., (1991). Prediction and measurement of pasta quality, *International Journal of Food science & Technology*, (26), 133-151
- 5) Edwards N. M., Mulvaney S. J., Scanlon M. G. and Dexter J. E., (2003). Role of gluten and its components in determining durum semolina dough viscoelastic properties, *Cereal Chemistry*, (80), 755-763
- 6) Faubion j. M. and Hosoney R. C., (1989). The viscoelastic properties of wheat flour doughs, *Dough Rheology and baked product texture*, van Nostrand teinhold, New York, USA, 29-66
- 7) Fu L., Tian J., Sun C. and Li C., (2008). RVA and farinograph properties study on blends of resistant starch and wheat flour, *Agricultural sciences in China*, (7), 812-822
- 8) Gabriele D., de Cindio B. and D'Antona P., (2001). A weak gel model, *Rheol Acta*, (40), 120-127
- 9) Gomez A., Ferrero C., Calvelo A., Anon M. C., Puppo M.C., (2011). Effect of mixing time on structural and rheological properties of wheat flour dough for breadmaking, *International Journal of food Properties*, (14), 583-598
- 10) Gonzàlez-segura E., Magana-Barajas E., Torres-Chavez P. I., Manthey F. and Ramirez-Wong B., (2013). Characterization of the dynamic viscoelastic behaviour of semolina dough obtained from Mexican durum wheat cultivars, *Advanced chemical engineering research*, (3), 58-63
- 11) Herring C., (1954). Theory of the thermoelectric power of semiconductors, *Physical Review*, (96), 1163-1187

- 12) Hibberd G. E. and Parker N. S., (1979). Nonlinear creep and creep recovery of wheat flour doughs, *Cereal Chemistry*, (56), 232
- 13) Hoseney R. C., Zeleznak K. and lai C. S., (1986). Wheat gluten as a glassy polymer, *Cereal Chemistry*, (63), 285-286
- 14) Irvine G. N., Bradley J. W. And Martin G. C., (1961). A farinograph technique for macaroni doughs, *Cereal Chemistry*, (38), 153
- 15) Kieffer R., Wieser H., Henderson M. H. and Graveland A., (1998). Correlations of breadmaking performance of wheat flour with rheological measurements on a micro-scale, *J. Cereal Science*, (27), 53-60
- 16) Kilborn R. H. and Tipples K. H., (1972). Factors affecting mechanical dough development I. Effect of mixing intensity and work input, *Cereal Chemistry*, (49), 4-47
- 17) Launay B. and Buré J., (1974). Application of a viscometric method to the study of wheat flour doughs, *J. Texture Stud.*, (4), 82
- 18) Miller, K. A. and Hoseney R. C., (1999). Dynamic Rheological Properties of Wheat Starch-Gluten Doughs 1, *Cereal Chemistry*, (76), 105-109
- 19) Peressini D., Sensidoni A., Pollini C.M., de Cinido B., (1999). Improvement of wheat fresh pasta making influence of sodium chloride on dough rheological properties, *Ital food beverage technol.*; (17), 20-23
- 20) Quick J. S. and Donnelly B. J., (1980). A rapid test for estimating durum wheat gluten quality. *Crop Science*, (20), 816-818
- 21) Samaan J., El-Khayat G. H., Manthey F. A., Fuller M. P. and Brennan C. S., (2006). Durum wheat quality: II. The relationship of kernel physicochemical composition to semolina quality end product utilisation, *International journal of food science and technology*, (41), 47-55
- 22) Sliwinski E. L., Kolste P., Prins A. van Vilet T., (2004a). On the relationship between gluten protein composition of wheat flours and large deformation properties of their dooughs, *Journal of cereal Science*, (39), 247-264

- 23) Sliwinski E. L. Kolste P., van Vilet T., (2004b). Large deformation properties of wheat flour in uni-and biaxial extension. Part I. Flour dough, *Rheologica Acta*, (43), 306-320
- 24) Sliwinski E. L. Kolste P., van Vilet T., (2004c). On the relationship between large-deformation properties of wheat flour dough and baking quality, *Journal of cereal Science*, (39), 231-245
- 25) Uthayakumaran S., Newberry M., Phan-Thien N. and Tanner R., (2002). Small and large strain rheology of wheat gluten, *Rheologica Acta*, (41), 162-172.
- 26) Walle M. and Trentesauz E., (1980). Contribution to the study of a practical method of evaluating the aptitude of hard wheats and hard wheat farina in pasta manufacture, by using the Chopin Alveograph, *Tecnica Molitaria*, (12), 917-922
- 27) Zaidel A. D. N., Chin N. L., Rahman A. R. and Karim R., (2008). Rheological characterisation of gluten from extensibility measurement, *Journal of food engineering*, (86), 549-556

Chapter III

Large-deformation properties and microstructure of durum wheat dough

1. Introduction

The main problem in the process of pasta is represented by the process conditions which cause structural changes, which give rise to marked shrinkage with consequent fractures more or less evident and organoleptic characteristics altered. The drying conditions, such as temperature, humidity and airflow, strongly influence the quality of pasta.

If the pasta is dried too quickly, will be obvious fracture lines or billing on the product, with a consequent weakening of the structure and a deterioration of the final quality of the pasta itself.

The final quality of products as pasta, bread and simil products is also heavily dependent on the rheological and mechanical properties of the dough before processing [Charalambides et al. (2006)].

The rheology of the material and the structural changes with time and temperature is necessary for simulation and optimization of processes, such as extrusion, rolling and calendaring [Charalambides et al. (2006)].

These processes involve large strain and strain rates in strong shear and extensional flows [Dealy and Wissbrun (1990)] then the oscillatory tests are not able to explain properly the behaviour of dough during processing.

On the contrary the large deformations technique offers the opportunity of studying the material structural properties under process condition. In fact during

mixing large deformation are imposed on the dough.

Large deformation tests more clearly showed differences among optimal, under and overmixed dough. At the beginning of the mixing stage, the resistance to deformation of the dough is low. With time, this resistance increases until a peak known as the peak dough development value. This value depended on the type of flour or semolina. When mixing continues, the dough consistency reduces again. This phenomenon can be described with depolymerisation of the gluten network and characterised by a partial solubilisation of the insoluble gluten proteins.

In the work of Zheng et al. (2000), it is shown that dough extensional properties increased with mixing until peak dough development in large deformation.

The dough is developed primarily by extensional flow. Dough can be treated in a non-linear region at any strain. In the study of Khatkar et al. (2002), suggesting that both moduli decrease with increasing strain and that this non-linearity exists over all strains. Also they are studying the influence of starch and gluten fractions on the non-linearity of wheat flour dough.

2. State of art

It is well known that dough is an elasticoviscous material and a wide range of test methods is employed for systematically characterizing the extensional rheology of dough [Padmanabhan M. (1995)], in an attempt to study protein quality/content, molecular extensibility and macroscopic strain hardening.

In extensional flow the molecules are strongly oriented in the direction of the flow field since there are no forces to cause rotation. The behaviour of long chain high molecular weight polymer melts is influenced by extensional flow.

Extensional flow causes maximum stretching of molecules, producing a chain tension that may result in a large resistance to deformation [Sahin and Sumnu, (2006)]. The molecular orientations caused by extensional flow leads to the development of final products with unique textures [Padmanabhan et al. (1995)].

Dough processing is an important food process in which extensional flow is significant. Examples of extensional flow are extrusion, which involves a combination of shear and extensional flow and carbon dioxide gas during

fermentation of bread dough involves extensional deformation.

Common extensional tests can be separated in three categories, uniaxial, planar and biaxial extension tests.

During uniaxial extension, material is stretched in one direction with a size reduction in the other two directions. In planar extension, a material is stretched in the one direction with a corresponding decrease in the second direction, while width in the third direction remains unchanged. In biaxial extension the flow produce a radial tensile stress. There are many test methods that measure the uniaxial extensional properties of dough such as the Brabender Extensograph and the Stable Microsystems Kieffer dough and gluten extensibility rig [Dobraszczyk and Morgenstern (2003)].

These test include extensigraphs and mechanical testing systems [Uthayakumaran et al., (2000); Sliwinski et al., (2004); Tschoegl et al., (1970)].

In the biaxial tests, properties of food are measure with an inflation method and compression between flat plate using lubricated surfaces [Chatraei et al. (1981); Dobraszczyk and Vincent, (1999)]. Examples of biaxial extensional devices include alveographs and squeeze flows tests (uniaxial compression tests) [Dobraszczyk et al., (1994); Dobraszczyk et al., (2003); Huang et al., (1993)].

All the uniaxial extension tests can provide measurements of the maximum force required to extend the dough and the distance the dough can be extended before rupture.

Although much work has been done on bread dough rheology, little is published on pastry dough rheology. Some for assessing pastry flour quality has used methods that are used for determining bread flour quality.

Pastry dough is quite different, not only in composition, but also in the strains and strain rates that are applied during pastry making [Morgenstern et al. (1996)].

Tschoegl et al. (1970a) determined the large deformation and fracture properties of flour dough in uniaxial extension using a method whereby dough rings are submerged in a liquid matching density and are stretched at constant rates of extension until fracture occurred. They found that at a constant strain rate the true stress increased continuously with the strain, indicating that the elastic retractive

force increases throughout the test and no trend towards steady-state flow develops.

Schweizer and Conde-Petit (1997) have studied the large deformation and fracture properties of flour dough in uniaxial extension using the elongational rheometer RME based on the rotary clamp technique, it appeared that with dough careful preparation of samples (mixing, sheeting and resting) is extremely important. They found that the stress depend on the sheeting direction: the stress is higher if the sample is elongated parallel to the sheeting direction than perpendicular to it.

They also noticed that after a steady increase of the deformation the force suddenly decreased at a certain strain. At this elongation the sample started to neck or even showed fracture.

Kieffer et al. (1998) have developed a micro-method for extension tests with flour dough, extensibility rig that can be used in combination with most types of mechanical testing machines. A hook that moves upwards extends sample uniaxially.

Ng et al. (2007) proposed an experimental measurement of the transient elongation rheology obtained with two techniques, the Filament Stretching Rheometer (FISER) and the SER universal testing platform.

In both of these devices, the sample approaches uniform uniaxial extension flow at a constant strain rate over a large portion of its length.

The large dynamic range of these rheometers allows probing the viscoelastic nature of the dough at high rates.

The most significant property is elongation strain hardening, which is highly sensitive to the degree of entanglement.

Strain hardening has been shown to be an important characteristic for dough characterization and it is proposed as an indicator for its quality.

Strain hardening is first observed with amorphous glassy materials and polymer melts due to unstable necking when they are stretched uniaxially. Its importance is first recognized for metals and later for polymeric systems [Vincent et al. (1960)].

Strain hardening is defined as the phenomenon that the stress required to deform a material increases more than proportional strain, at constant strain rate and

increasing strain. The presence of chain branches is important in giving rise to strain hardening, which is a necessary property for stability of polymers undergoing large deformation [Dobraszczyk, (2003)].

During large extension of materials, plastic strain is uniform throughout the sample up to the point of maximum force. Beyond this point, force begins to decrease and it is at this point that localised and non-uniform plastic deformation begins to occur. The cross-sectional area begins to change in a non-uniform way, and a neck or localised constriction forms, which can either stabilise or propagate in an unstable manner to failure.

If the cross-section at any point is slightly less than elsewhere or there are any irregularities in the sample when the force is increasing in plastic flow, the stress will increase locally. While force is increasing the deformation is stable, any local constrictions are self-arresting. Under a decreasing force the deformation is no longer stable, leading to the formation and cumulative increase of necking and eventual failure. The occurrence of strain hardening in a material stabilises any regions of incipient localised thinning that could lead to unstable necking and eventual fracture during high extension, and can allow much larger extensions before rupture than would otherwise be possible [Dobraszczyk et al. (2003)].

Under extensional flow, entangled polymers exhibit strain hardening which is enhanced for polymers with a broad MW distribution, particularly a bimodal distribution [Osaki et al., (1999)], and branching [(McLeish and Larson, (1998)].

Dobraszczyk et al. (2003), Sliwinski et al (2004a), Tronsmo et al. (2003) and Zghal et al. (2002) have published many articles in which they described as strain hardening influenced dough properties.

Sliwinski et al. (2004) reported that strong flour dough possesses higher strain hardening than weak flour dough and thus prevents premature fracture of dough and gluten.

Uthayakumaran et al. (2000) performed the uniaxial extension of gluten dough by first compressing the dough sample in between two parallel plates before pulling the dough apart by the moving upper plates at a constant strain rate.

Their results showed that gluten dough possessed larger elongation viscosities than flour dough.

Strain hardening parameter is also using to describe dough with biaxial extension [Janssen et al. (1996)]. Material is stretched at equal rates in two perpendicular directions in one plane [Dobraszczyk and Morgenstern (2003)].

The extension of gas bubble is studying by van Vliet et al. (1992). Experiments in which this type of deformation is applied have been performed on wheat flour doughs by several researchers [Morgenstern et al. (1996) and Dobraszczyk (1997)].

The criterion is different in biaxial than in uniaxial extension and the stress at a certain strain is higher in uniaxial than in biaxial extension and the difference in stress-level became larger with increasing strain. The stress is maximum in the direction of extension and minimum in the direction perpendicular to the direction of extension [Levien and Slade (1990)].

In uniaxial extension, the stress increases more than proportionally with the strain. It indicates, that dough becomes stronger in the direction in which it is stretched. Schweizer and Conde-Petit (1997) support this conclusion, that studying dough in uniaxial elongation flow using the equipment of Meissner found that stress-levels are higher if dough after mixing has been reshaped in the direction of flow than if dough has been reshaped perpendicularly to the direction of flow. This phenomenon is attributed to the orientation of structure elements that plays an important role during extension of flour dough.

3. Data interpretation

In a tensile test mode, a specimen is clamped from both ends, the load cell measures the force applied to the specimen throughout the stroke. From this test a graph of load vs elongation is obtained.

To interpret the result of the test, the load-elongation data must be converted to engineering stress and engineering strains, using the following equations:

$$\sigma_{en} = \frac{F}{A_0} \quad (1)$$

$$\epsilon_{en} = \frac{\Delta L}{L_0} \quad (2)$$

where F is the tensile force, A_0 is the initial cross-sectional area of the specimen section, L_0 is the initial length and ΔL is the change in gage length ($L-L_0$).

In this way, the stress-strain curve is independent of initial specimen dimensions, because the free length between the clamps can change changing specimen.

When the specimen is elongated, the volume is constant, but the area decreases and incremental change in length acts over the entire length of the specimen, which becomes progressively longer as the test continues. Engineering stress value is converted to the true stress value according to the following equation [Davis J. R., (2004)]:

$$\sigma = \sigma_e(1 + e) \quad (3)$$

where A is the cross-sectional area at the time that the applied force is F and e is the engineering strain.

Then, it is possible write:

$$\epsilon = \ln(1 + e) \quad (4)$$

For some materials, such as dough, in order to obtain a certain deformation stress increases in a more than linear.

The true stress-strain diagram can be represent with the Hollomon equation [Van Vliet, (2008)]:

$$\sigma = K\epsilon^n \quad (5)$$

where n is the strain hardening exponent, and K is the strength coefficient.

The parameter n determines the rate at which the material hardens. The greater the exponent, the greater the effect of strain on material strength and hardness.

4. Extensional rheological theory

From numerous studies reported in the literature [Van Vilet et al., (2007)], it is possible to notice the non-linear behaviour of pasta dough subjected to uniaxial deformation. Specifically speaking, it is possible to consider a fluid element of initial length l_0 , subjected to a constant load, F , as shown in Figure 1.

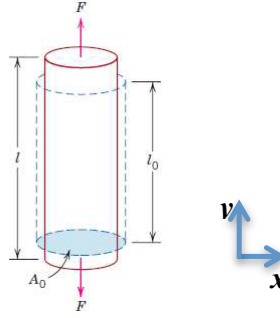


Figure 1. Fluid element of initial length l_0 subjected to a constant stress F

The test material is fixed to one end and pulled from the other one, producing an elongation in the direction of motion and a corresponding contraction in the transverse direction, which can be reasonably neglected when compared to the variation along the axial direction [Davis, (2004)].

Denoting by x the sliding direction and by y the normal to the sliding surface, the flow in elongation is characterized in that the deformation takes place exclusively along the main axes.

The effort can be derived in general form starting from the unique dependence of the Cauchy tensor.

This kinematics allows studying the solids within the limits of small deformations, for which the following applies for constitutive expression simplified equation:

$$\underline{T}_E = f(\underline{C}) = G \cdot \underline{C} \quad (6)$$

where G is the dynamic modulus and \underline{C} is the Cauchy tensor, defined as:

$$\underline{C} = \begin{vmatrix} \alpha_1^2 & 0 & 0 \\ 0 & \alpha_1^{-1} & 0 \\ 0 & 0 & \alpha_1^{-1} \end{vmatrix} \quad (7)$$

where α_1 is elongation ratio λ_1 .

Therefore in the case of uniaxial deformation will have the following results:

$$\begin{cases} T_{11} + p = \tau_1 = G\alpha_1^2 \\ T_{22} + p = \tau_2 = \frac{G}{\alpha_1} \\ T_{33} + p = \tau_3 = \frac{G}{\alpha_1} \end{cases} \quad (8)$$

Whereas the concept of extensional flow and in particular a flow with velocity gradient $\underline{\underline{L}}$ constant, we get:

$$\frac{d}{dt'}(\underline{\underline{F}}_t(t')) = \underline{\underline{L}} \cdot \underline{\underline{F}}_t(t') \quad (9)$$

that can be integrated between the initial condition taken as the current state at time t , that is where $\underline{\underline{F}}_t(t) = \underline{\underline{1}}$ and the current condition t' in the case of $\underline{\underline{L}} = \text{const}$ constant:

$$\underline{\underline{F}}_t(t') = \underline{\underline{1}} \cdot \exp[(t' - t)\underline{\underline{L}}] \quad (10)$$

if one considers the velocity gradient tensor symmetrical, that is $\underline{\underline{D}} = \underline{\underline{L}}$, you can make explicit $\underline{\underline{D}}$ and $\underline{\underline{F}}$ with respect to the principal axes of deformation, obtaining:

$$\underline{\underline{D}} = \begin{vmatrix} \dot{\varepsilon}_{xx}^2 & 0 & 0 \\ 0 & \dot{\varepsilon}_{yy}^2 & 0 \\ 0 & 0 & \dot{\varepsilon}_{zz}^2 \end{vmatrix} \quad (11)$$

$$\underline{\underline{F}}_t(t') = \begin{vmatrix} \exp(t' - t)\dot{\varepsilon}_1 & 0 & 0 \\ 0 & \exp(t' - t)\dot{\varepsilon}_2 & 0 \\ 0 & 0 & \exp(t' - t)\dot{\varepsilon}_3 \end{vmatrix} \quad (12)$$

where D is the tensor of strain rate and $\dot{\varepsilon}_i$ are the speed of extension.

The ratio of uniaxial elongation λ is defined as the ratio between the lengths before and after the deformation, and is generally expressed in terms of deformation Cauchy (or engineering):

$$\varepsilon = \frac{l_0 - l}{l_0} = \lambda - 1 \quad (13)$$

In reality, the more rigorous definition of elongation deformation is the following:

$$\varepsilon = \ln\left(\frac{l}{l_0}\right) = \ln(\lambda) = \ln(1 + e) \quad (14)$$

where ε is the Hencky strain (Hencky strain) and is equal to the natural logarithm of the elongation ratio and is the kinematic parameter of the relevant extension. The deformation of Cauchy represents the limit of the Hencky strain in the case of small deformations [Mohos, (2010)].

During the measurement is plotted automatically a diagram of the force as a function of distance. The data obtained from the test are restated in terms of stress

versus strain, dividing the strength and extent suffered from the material to the original size of the sample.

At the beginning of the test is known a rapid increase of the strength in the face of a small movement. During this stage the product is deformed under the load, there is no perforation of the tissues. This phase ends abruptly when the sample is broken and this is evident from the sudden change of the slope of the graph; This point is called the yield point or yield point.

The yield point marks the instant at which the mixture begins to rupture, causing a variation irreversible.

5. Material and methods

The uniaxial tensile tests are performed using a dynamic mechanical machine, the Instron Universal Testing Machine 4464 (Instron, UK) and Zwick/Roell Z005, shown in Figure 2 and 3.

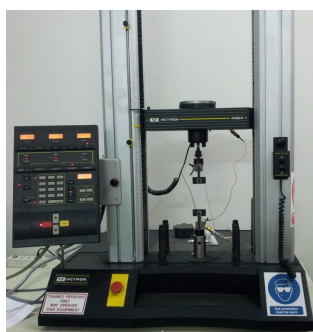


Figure 2. Instron Machine (INSTRON 4464-H1884, UK)



Figure 3. Zwick/Roell Z005

The test is performed by closing the sample in the clamps and applying a constant elongational rate over time until failure of the sample. The pneumatic clamps have a minimum value of pressure to the clamps at 4 bar.

The tool consists of two parts, a movable upper and one fixed lower. At the mobile part is connected, through a spindle, the upper clamp, while in the fixed part is connected the lower clamp. A typical example of how the test has been conducted, is reported in Figure 4.

The speed was set at three different values 3-12-120 mm/min [Sliwinski et al., (2004)]. The load cell used is of 1kN and 10 N.



Figure 4. A typical example of a uniaxial tension test

The samples were cutted in a rectangular shape (20x50x2 mm). In order to avoid the water evaporation and then a variation in the structure of the system, the samples were appropriately lubricated with silicone oil (viscosity 1000 Pa*s) [Sliwinski et al., (2004)].

The tests were carried out for the same samples described in chapter II, identifying them with the follow “sample identification” shown in Table 1.

| Durum semolina type | t_{mix} [min] | | | | | | | | T_{mix} [°C] | $v_{elongation}$ [mm/min] |
|--------------------------------|-----------------|----|----|----|----|----|----|----------|----------------|---------------------------|
| $S1^3$ _{20/30/40} | 5 | 10 | 15 | 20 | 25 | 30 | 35 | 20-30-40 | 3 | |
| $S1^{12}$ _{20/30/40} | 5 | 10 | 15 | 20 | 25 | 30 | 35 | 20-30-40 | 12 | |
| $S1^{120}$ _{20/30/40} | 5 | 10 | 15 | 20 | 25 | 30 | 35 | 20-30-40 | 120 | |
| $S2^3$ _{20/30/40} | 5 | 10 | 15 | 20 | 25 | 30 | 35 | 20-30-40 | 3 | |
| $S2^{12}$ _{20/30/40} | 5 | 10 | 15 | 20 | 25 | 30 | 35 | 20-30-40 | 12 | |
| $S2^{120}$ _{20/30/40} | 5 | 10 | 15 | 20 | 25 | 30 | 35 | 20-30-40 | 120 | |
| $S3^3$ _{20/30/40} | 5 | 10 | 15 | 20 | 25 | 30 | 35 | 20-30-40 | 3 | |
| $S3^{12}$ _{20/30/40} | 5 | 10 | 15 | 20 | 25 | 30 | 35 | 20-30-40 | 12 | |
| $S3^{120}$ _{20/30/40} | 5 | 10 | 15 | 20 | 25 | 30 | 35 | 20-30-40 | 120 | |

| | | | | | | | | | |
|---------------------------------------|---|----|----|----|----|----|----|----------|-----|
| S4 ³ _{20/30/40} | 5 | 10 | 15 | 20 | 25 | 30 | 35 | 20-30-40 | 3 |
| S4 ¹² _{20/30/40} | 5 | 10 | 15 | 20 | 25 | 30 | 35 | 20-30-40 | 12 |
| S4 ¹²⁰ _{20/30/40} | 5 | 10 | 15 | 20 | 25 | 30 | 35 | 20-30-40 | 120 |
| S5 ³ _{20/30/40} | 5 | 10 | 15 | 20 | 25 | 30 | 35 | 20-30-40 | 3 |
| S5 ¹² _{20/30/40} | 5 | 10 | 15 | 20 | 25 | 30 | 35 | 20-30-40 | 12 |
| S5 ¹²⁰ _{20/30/40} | 5 | 10 | 15 | 20 | 25 | 30 | 35 | 20-30-40 | 120 |
| S6 ³ _{20/30/40} | 5 | 10 | 15 | 20 | 25 | 30 | 35 | 20-30-40 | 3 |
| S6 ¹² _{20/30/40} | 5 | 10 | 15 | 20 | 25 | 30 | 35 | 20-30-40 | 12 |
| S6 ¹²⁰ _{20/30/40} | 5 | 10 | 15 | 20 | 25 | 30 | 35 | 20-30-40 | 120 |

Table 1. Samples analyzed

6. SEM Analysis

To study the structure formed when the durum wheat is mixed with water in different condition, it was carried out the tests of scanning electron microscopy, SEM with JEOL JSM-t = 330 operating a 20 kV, shown in Figure 5.



Figure 5. SEM, Scanning electron Microscopy

Scanning electron microscopy (SEM) permits observation of 3D structures. SEM evaluation of wheat-flour doughs showed that the protein matrix formed a smooth, enveloping, veil-like network stretched over the starch granules [Khoo et al. (1975)]; Evans et al. (1977)].

Immediately after mixing, the developed dough was thinly sheeted and cut (size 20x20 mm) without damaging the structure. The dough sample pieces were dried. For conventional imaging in the SEM, specimens must be electrically conductive, at least at the surface, and electrically grounded to prevent the accumulation of electrostatic charge at the surface.

They are therefore usually coated with an ultrathin coating of electrically conducting material, deposited on the sample either by low-vacuum sputter

coating or by high-vacuum evaporation. Finally, each sample was transferred to the microscope where it was observed at 20 kV.

7. Results and discussions

The results coming from extensional tests are reported in this section. In order to understand the behaviour of the different samples of durum semolina, the samples are studying in the different operative condition (time of mixing, temperature of mixing and rate of elongation). The comparisons of results obtained in the different conditions are shown subsequently.

7.1 Uniaxial elongation test

In Figure 7 and 8 are shown the results obtained by fitting the experimental data for the sample S1-30 and S1-40. The analysis shown below refers to the tests carried for three temperatures of mixing (20, 30 e 40 °C) and analyzed for three different rate of elongation (3, 12 and 120 mm/min).

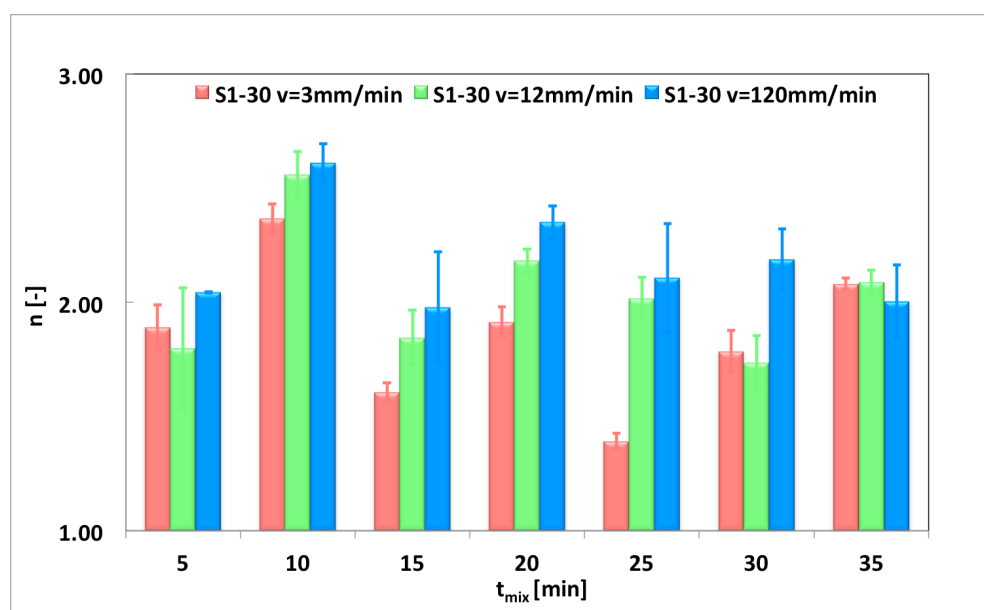


Figure 6. Trends of henky strain vs time of mixing for the samples S1-30. Experimental data are been evaluated for three rate of elongation (3-12 and 120 mm/min).

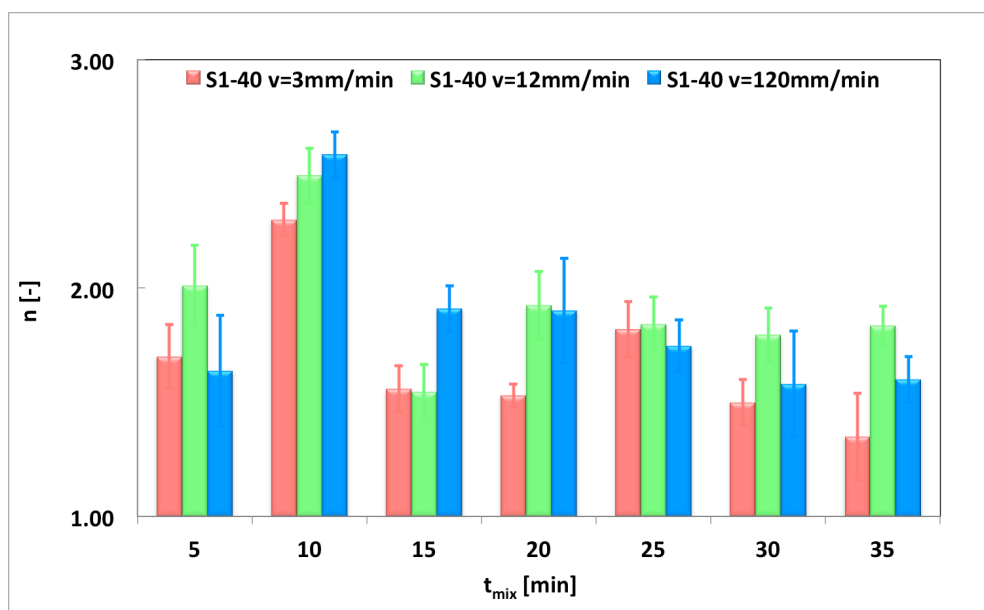


Figure 7. Trends of henky strain vs time of mixing for the samples S1-40. Experimental data are been evaluated for three rate of elongation (3-12 and 120 mm/min).

The index of strain-hardening, for a mixing temperature of 20°C, does not show a significant trend with the time of mixing, due to the fact that low temperatures do not favour hydration of starch and consequently entail a delay in the development of gluten chain. The mixture obtained at the mixing temperature of 20°C is found to be inconsistent and poorly developed. Comparing the value of Henky strain at the same time mixing, it can be noted that the Henky strain is greater at the mixing temperature of 20°C. In fact, the elongation test conducted under these conditions, has returned instead of values is not reliable, very probably due to the fact that the samples for the semolina S1 obtained in these operating conditions and analysed by the test elongation did not break in the central part of the sample. For mixing temperature of 30 and 40°C, Figure 6 and 7, the index of strain hardening increases reaching a maximum value, then slightly decreases and a major standard deviation is obtained too. It was hypothesized that the maximum in the curve corresponds to the optimum mixing time. Moreover at the maximum value it is evident the normal trend of strain hardening for which the value increase increasing the elongational velocity. Then, for the durum wheat S1, at 30 and 40°C, the optimum value is obtained after a mixing time of 10 minutes. The

higher standard deviation value after the optimum probably is due to the fact that the network formed in the first minutes is break, as a result of a overmixing, but not simultaneously in all the samples, then we obtain samples with different structure integrity and high variability (heterogeneity).

Similar results were obtained for the sample S2, S3, S4, S5 and S6. In the Figure 8, 9, 10, 11, 12, 13, 14 e 15 are reported the results only for the mixing temperatures of 30 and 40°C. The durum semolina S2, S3, S4, S5 and S6 have been mixed also to the mixing temperature of 20°C. Also in this case, the mixtures were obtained inconsistent and poorly developed. The tests carried out on these samples elongation did not return satisfactory results. The results are been shown to rate of elongation of 3, 12 and 120 mm/min. Below shows the tests performed for all samples.

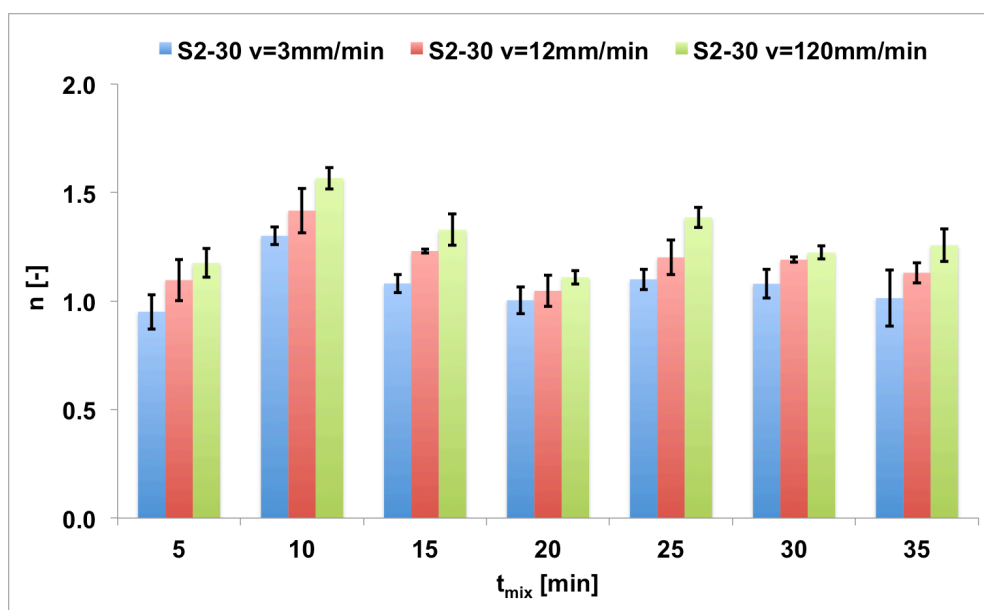


Figure 8. Trends of henky strain vs time of mixing for the samples S2-30. Experimental data are been evaluated for three rate of elongation (3-12 and 120 mm/min).

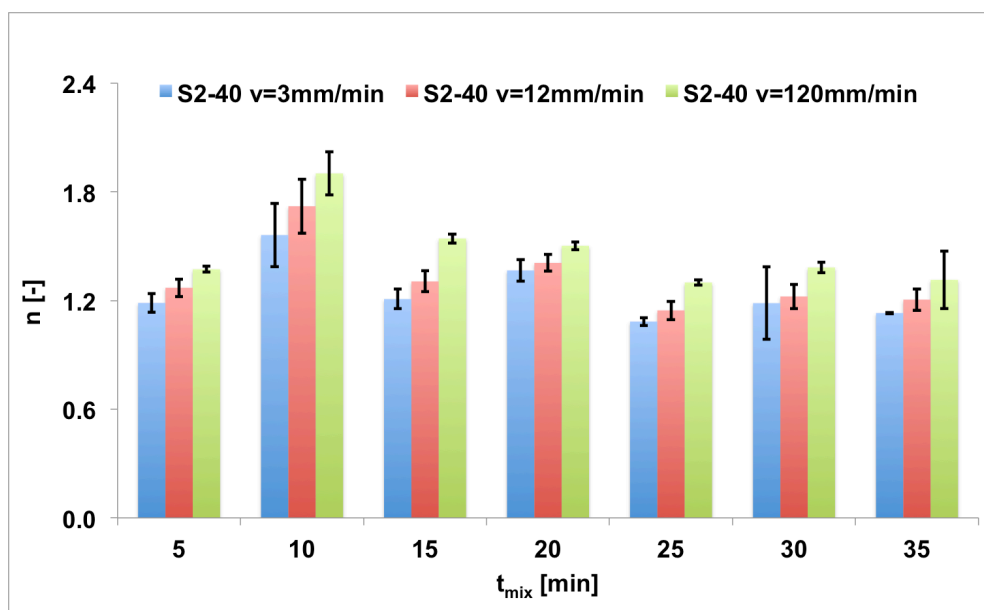


Figure 9. Trends of henky strain vs time of mixing for the samples S2-40. Experimental data are been evaluated for three rate of elongation (3-12 and 120 mm/min).

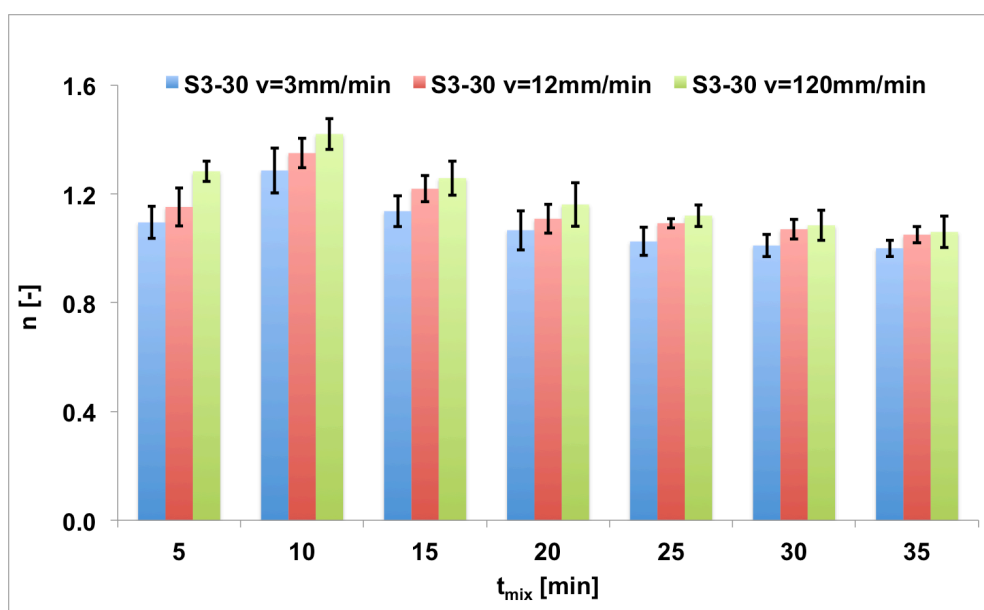


Figure 10. Trends of henky strain vs time of mixing for the samples S3-30. Experimental data are been evaluated for three rate of elongation (3-12 and 120 mm/min).

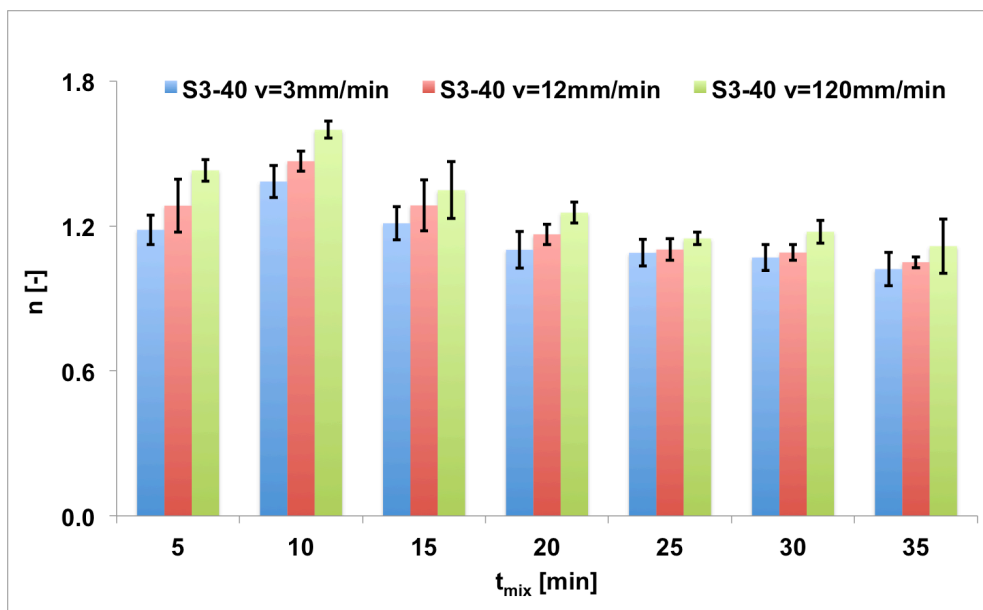


Figure 11. Trends of henky strain vs time of mixing for the samples S3-40. Experimental data are been evaluated for three rate of elongation (3-12 and 120 mm/min).

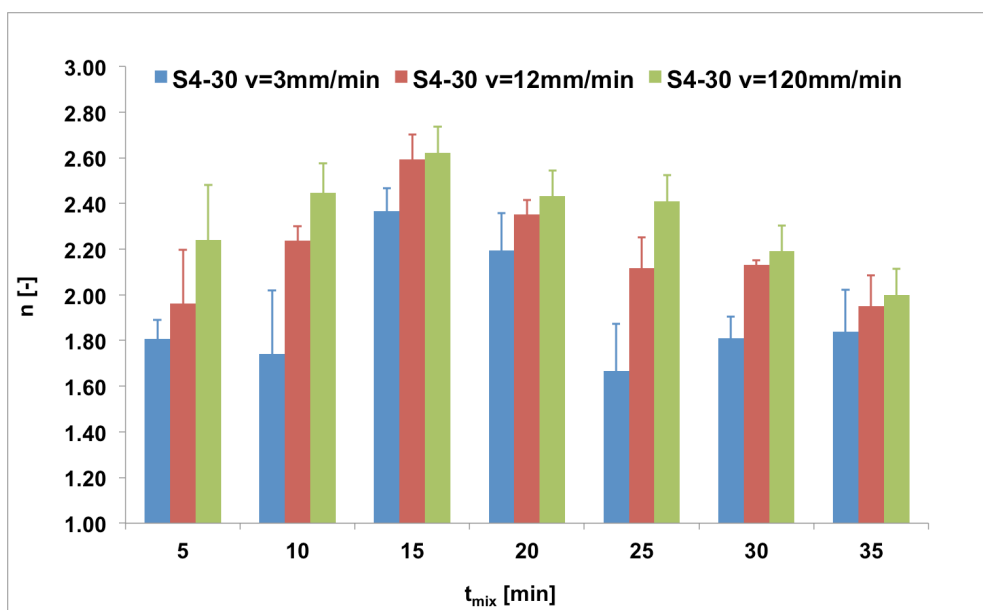


Figure 12. Trends of henky strain vs time of mixing for the samples S4-30. Experimental data are been evaluated for three rate of elongation (3-12 and 120 mm/min).

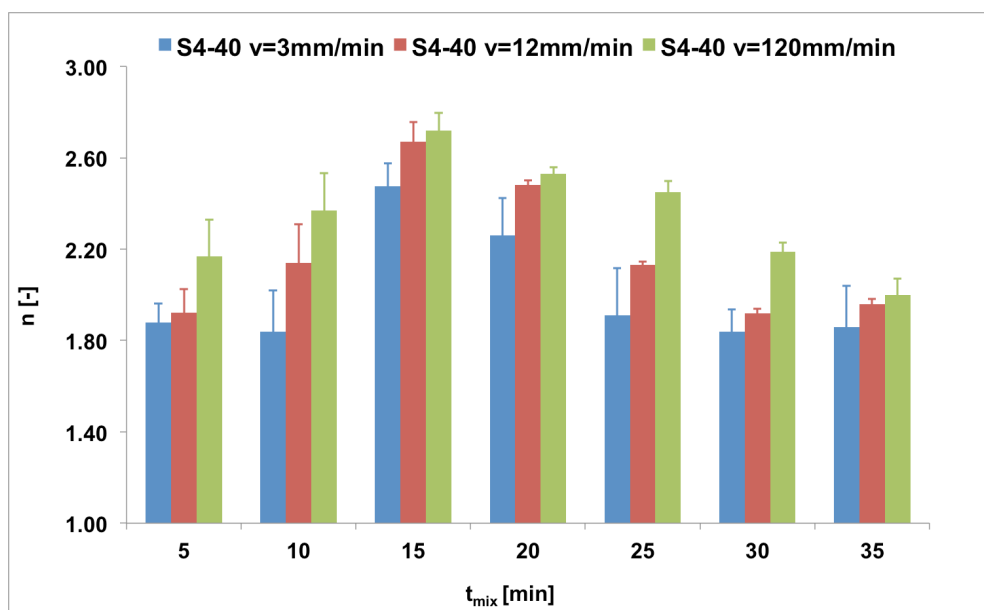


Figure 13. Trends of henky strain vs time of mixing for the samples S4-40. Experimental data are been evaluated for three rate of elongation (3-12 and 120 mm/min).

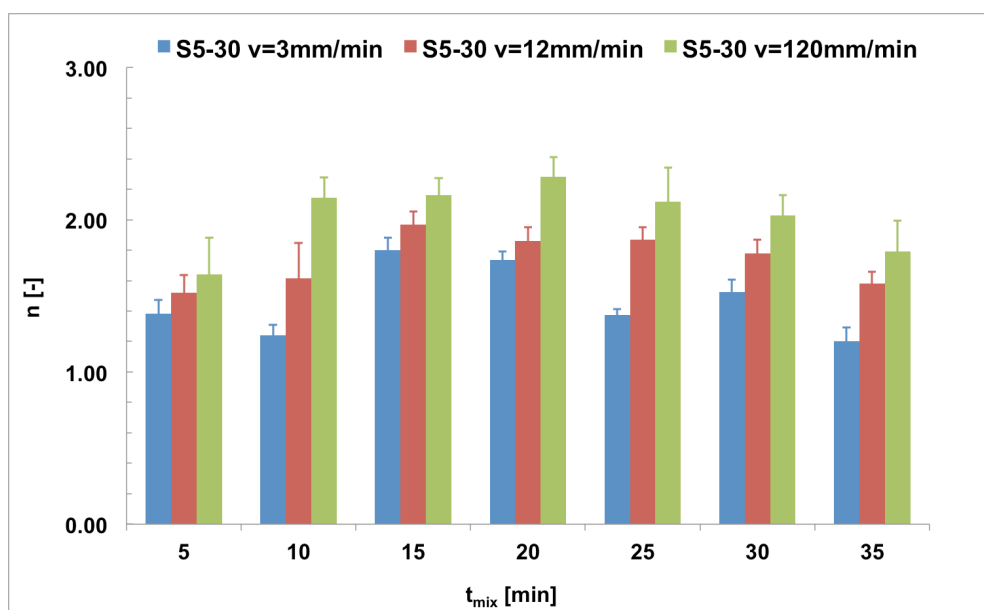


Figure 14. Trends of henky strain vs time of mixing for the samples S5-30. Experimental data are been evaluated for three rate of elongation (3-12 and 120 mm/min).

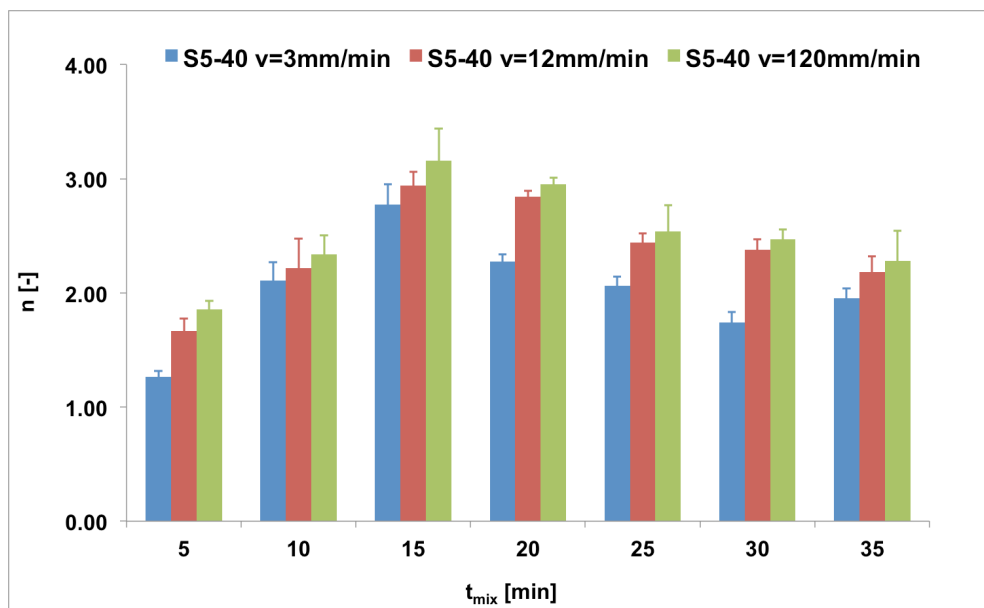


Figure 15. Trends of henky strain vs time of mixing for the samples S5-40. Experimental data are been evaluated for three rate of elongation (3-12 and 120 mm/min).

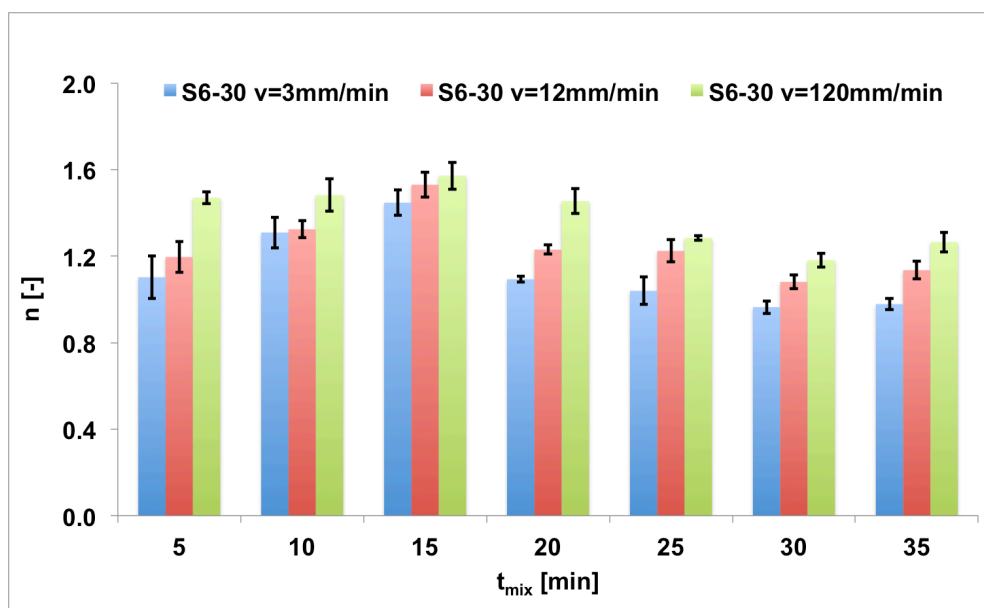


Figure 16. Trends of henky strain vs time of mixing for the samples S5-40. Experimental data are been evaluated for three rate of elongation (3-12 and 120 mm/min).

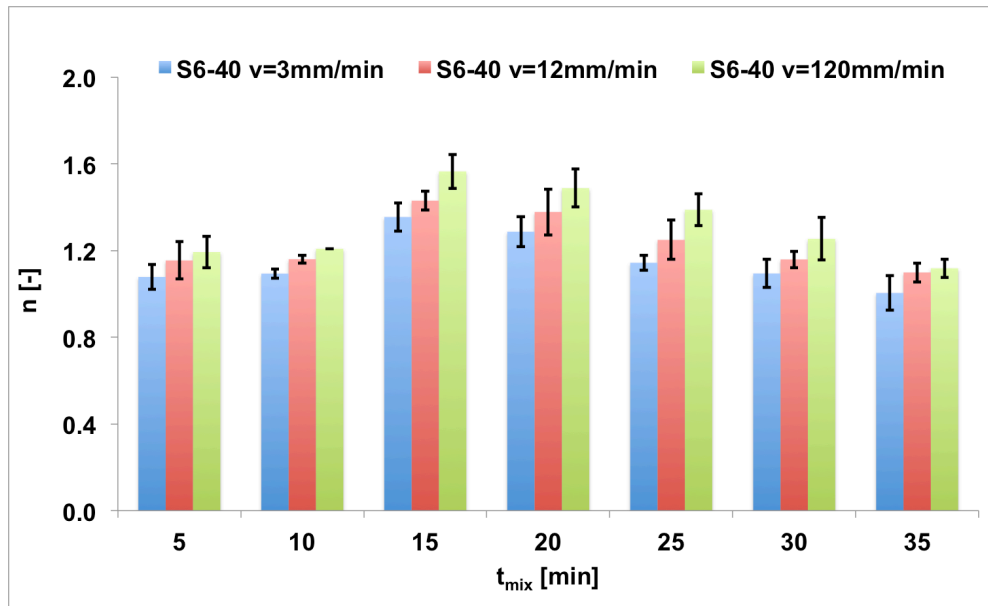


Figure 17. Trends of hencky strain vs time of mixing for the samples S5-40. Experimental data are been evaluated for three rate of elongation (3-12 and 120 mm/min).

In Figures 10 – 17 is shown the trend of the hencky strain index as a function of mixing time for the samples S2, S3, S4, S5 and S6 at both temperatures mixing 30°C and 40°C. For the samples obtained from durum semolina S2 and S3 the optimum time of mixing occurs at 10 minutes, while for the samples S4 and S6 at 15 minutes, while for S5 at 20 minutes. For the samples S2, S3, S4, S5 and S6, it can be seen that as the elongational rate increases, increases the strain hardening index and the material shows behaviour more solid-like.

To see the differences between the same durum semolina at different mixing temperatures (see Figures 18-22) it is reported the strain hardening index as a function of the time at 3 mm/min.

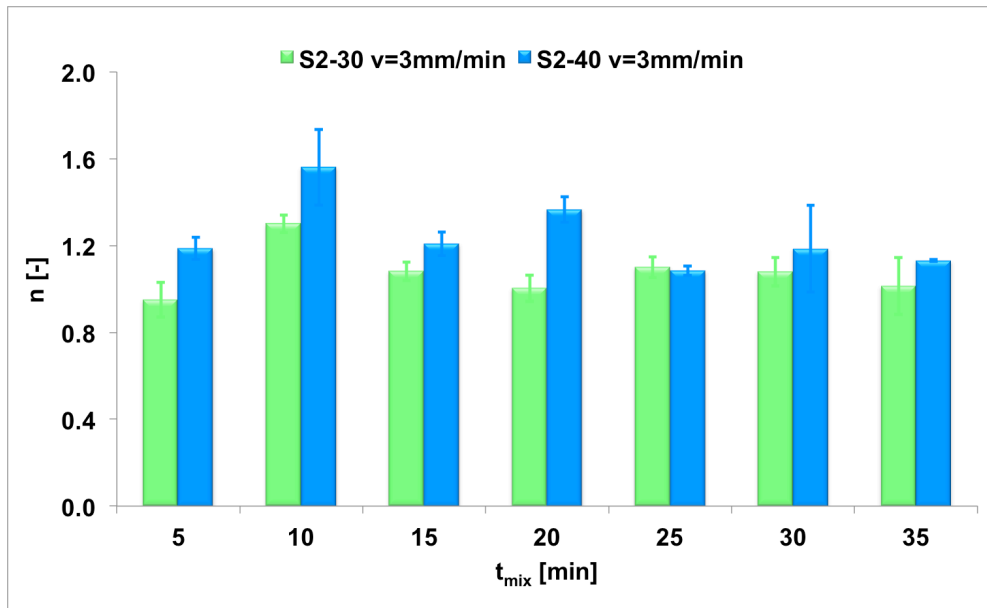


Figure 18. Trends of strain hardening vs time of mixing for the samples S2-30 and S2-40. Experimental data are been shown for rate of elongation of 3 mm/min.

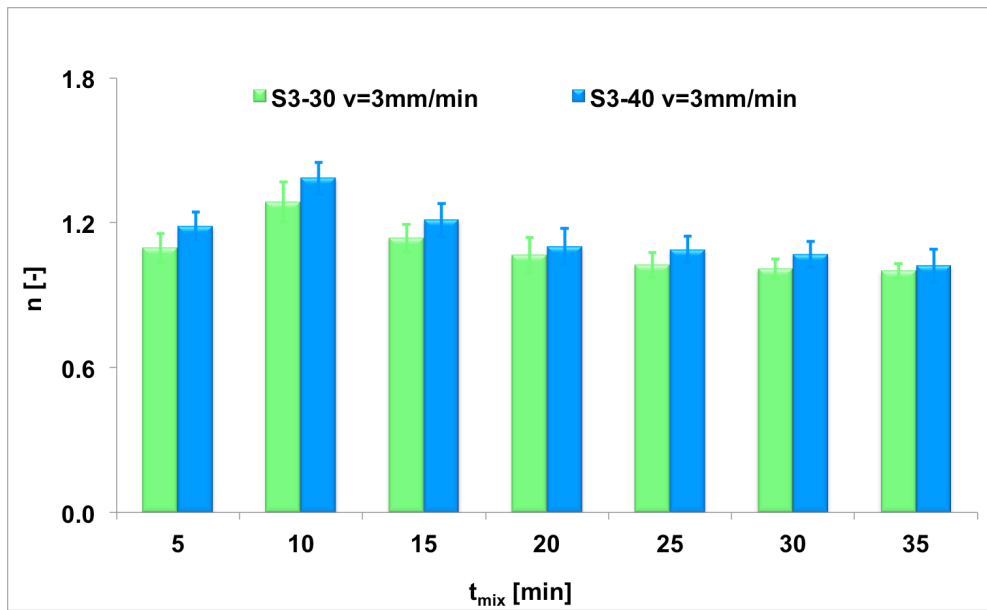


Figure 19. Trends of strain hardening vs time of mixing for the samples S3-30 and S3-40. Experimental data are been shown for rate of elongation of 3 mm/min.

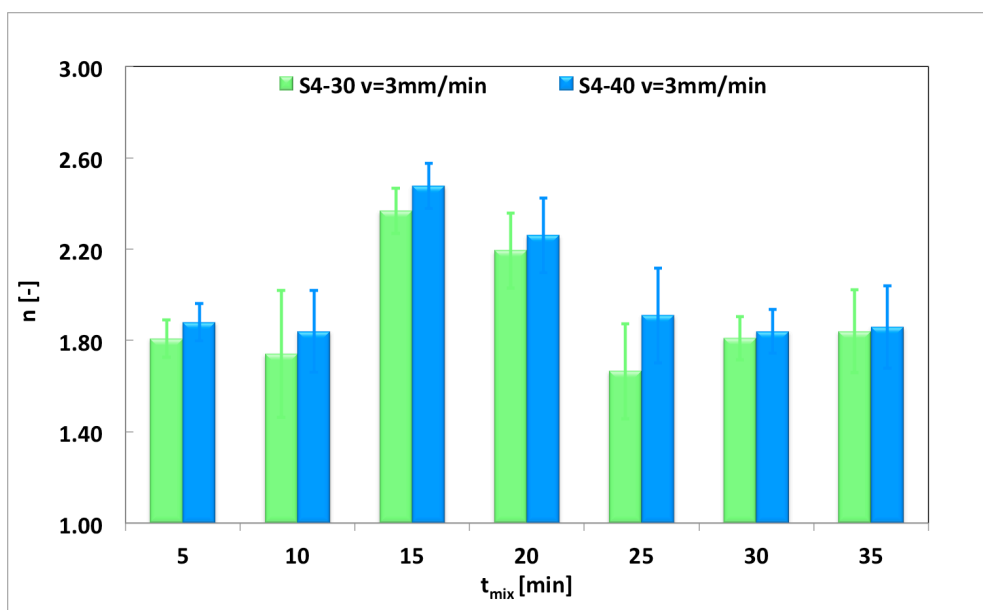


Figure 20. Trends of strain hardening vs time of mixing for the samples S4-30 and S4-40. Experimental data are been shown for rate of elongation of 3 mm/min.

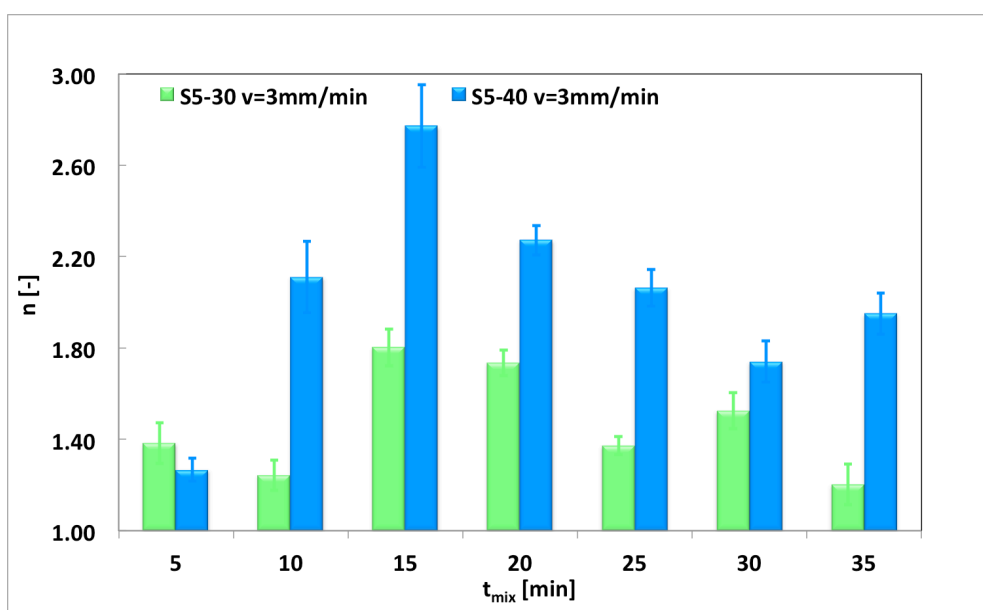


Figure 21. Trends of strain hardening vs time of mixing for the samples S5-30 and S5-40. Experimental data are been shown for rate of elongation of 3 mm/min.

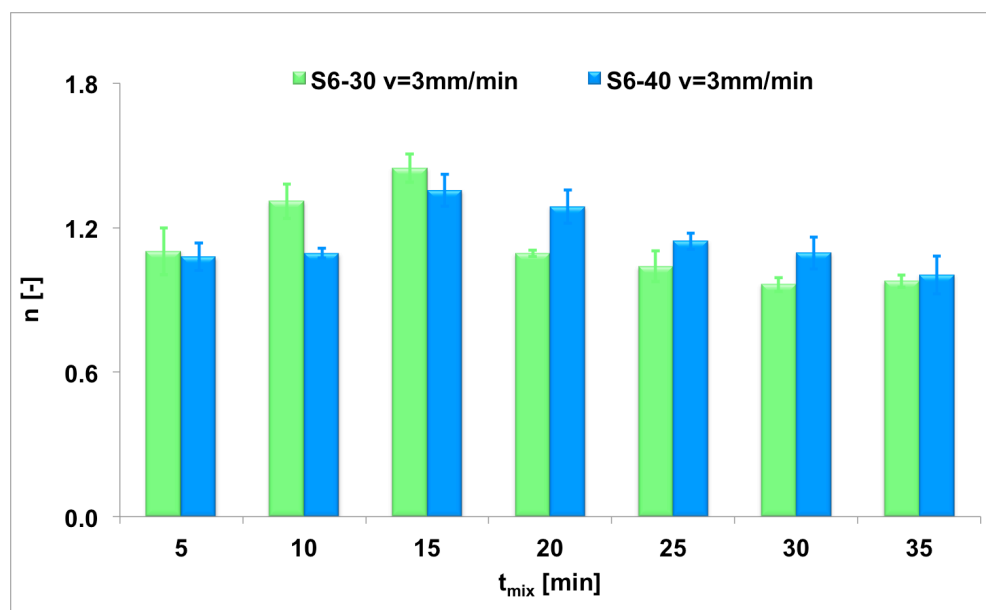


Figure 22. Trends of strain hardening vs time of mixing for the samples S6-30 and S6-40. Experimental data are been shown for rate of elongation of 3 mm/min

For both the mixing temperatures, 30°C and 40°C, the semolina S2 and S3 have the same optimum mixing time of 10 minutes, durum semolina S4 and S6 have the optimum at 15 minutes, while durum semolina S5 has an optimum mixing time at 20 minutes.

For the sample S5 at the mixing temperature of 30° C, it is observed from Figure 21 that, the index of strain hardening has a maximum value at 15 minutes and 20 minutes, but at 15 minutes with a high standard deviation, while in correspondence of 20 minutes the standard deviation is lower, then the optimal time of mixing would to oscillate between 15 and 20 minutes; for the same sample but at 40°C the index of strain hardening assumes the maximum value for a mixing time of 15 minutes.

The samples obtained from the different durum semolina have different behaviour with the mixing temperature. For semolina samples S2, S3, S4, S5 and S6 (Figures 18,19, 20, 21, and 22), the increase of the mixing temperature, increases the value of the strain hardening index. As the temperature of mixing increase, the water diffusion increases, so water diffuses better within the particles of durum

semolina [Kieffer R. et al., (1998)]. Only for the sample S6, as shown in figure 22, it can be noted that in the first minutes of mixing, between 5 and 15 minutes, the index value of strain hardening seems to be constant with the temperature of mixing.

7.2 SEM Analysis results

In order to verify what has been obtained by the tests in uniaxial elongation, the tests are performed of scanning electron microscopy, using SEM analysis. In the Figure 23 are shown the SEM images for the sample S1 to the temperature of mixing of 30°C and for different times of mixing.

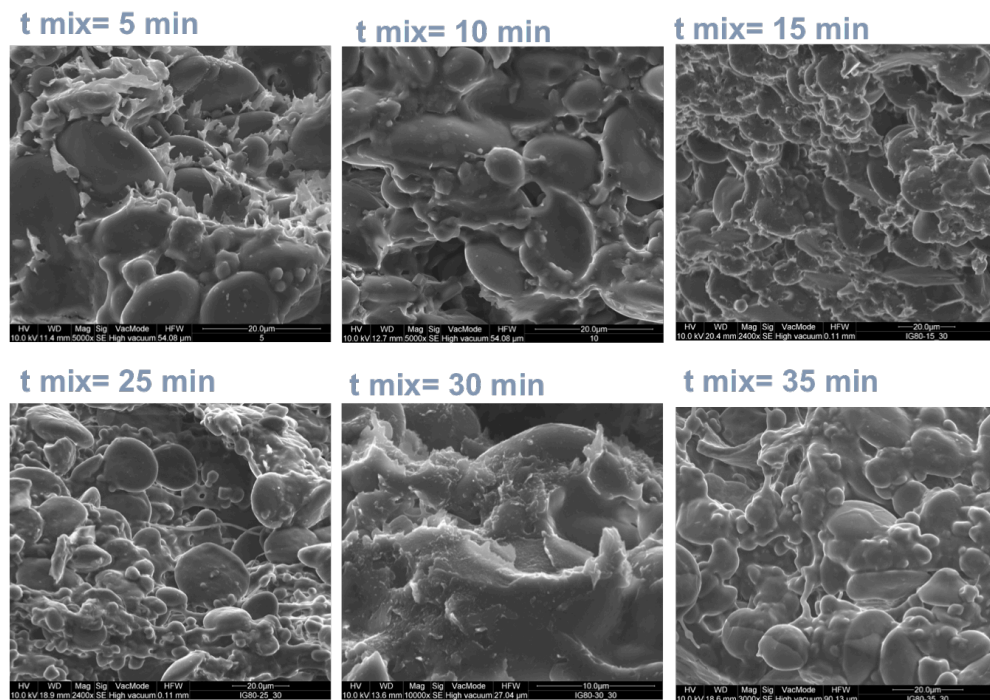


Figure 23. S1-30, SEM image for some time of mixing

By the first image, time mixing of 5 minutes, it is observable as a result the starch hydration and a beginning of gluten network formation. At the optimum time of mixing ($t_{\text{mixing}}=10$ min), the matrix has a smooth protein surface, which envelops and stretches on all the starch granules, covering them. In conditions of overmixing ($t_{\text{mixing}}>10$ min), that can be noted in the other pictures, we can see the

break of this gluten structure and a formation of an heterogeneous structure in which the starch granules and the fibrils of gliadin are well visible. This heterogeneity grows as a function of mixing time, confirming the hypothesis on the higher standard deviation after optimum mixing time.

Similar results are obtained for the sample S4 as shown in Figure 24.

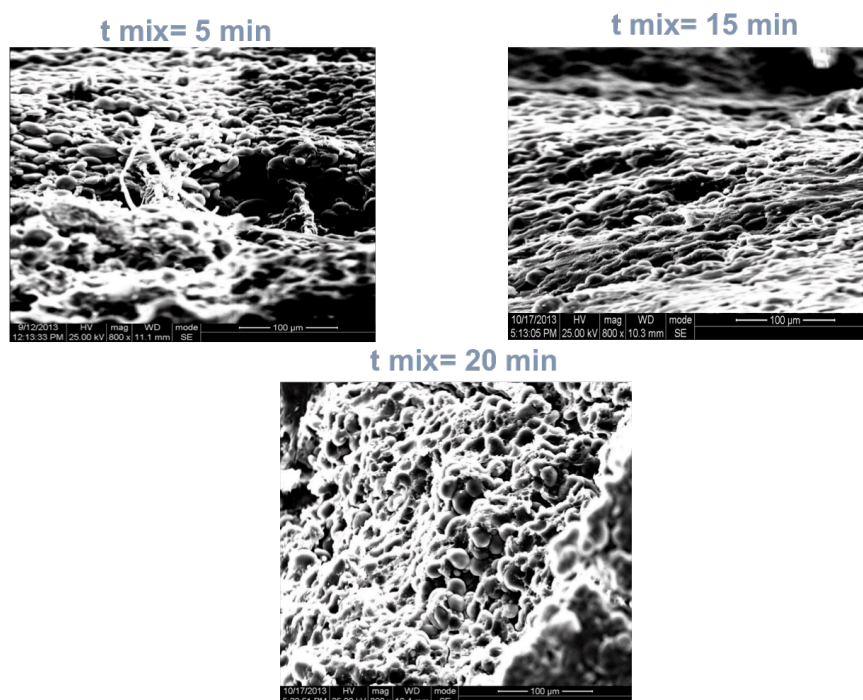


Figure 24. S4-30, SEM image for some time of mixing

The SEM images for sample S4 showed that the complete formation of the gluten network is in correspondence of the 15 minutes, thus demonstrating a correspondence with the value of great found in tests in uniaxial elongation.

For a mixing time greater than the optimum mixing time, which for the sample S4 is 15 minutes, you may notice a break in the network gluten, due to the fact that for mixing times of greater than 15 minutes we are in conditions of overmixing. The dough loses its elasticity and appears to be sticky and low mechanical properties. The SEM images for the sample S5, in the Figure 25, instead show more clearly, with respect to the tests of uniaxial elongation.

In fact for a mixing time of 15 minutes, the gluten network is not fully developed, in contrast to what is observed for a time of mixing of 20 minutes.

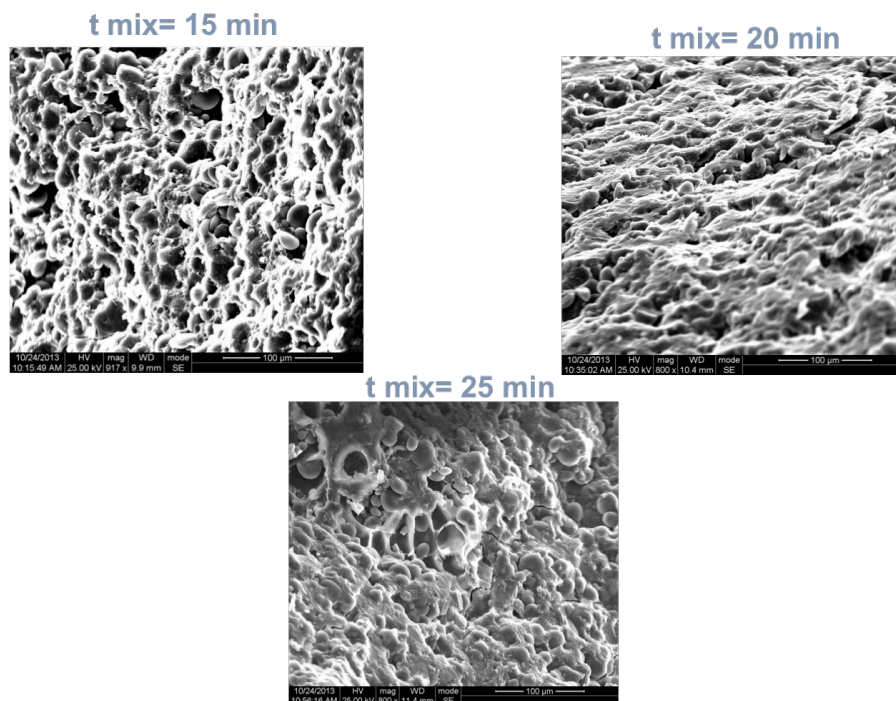


Figure 25. S5-30, SEM image for some time of mixing

In order to highlight the differences discussed so far, the maximum value of the index of Hencky strain has been reported in function of the fraction of gluten and protein content, as reported in literature for the wheat flour dough [Sliwinski et al., (2004)].

In figure 26 is shown the performance of the Hencky strain for each sample of semolina obtained in conditions of great. The data reported below are the values of the index Hencky strain obtained at mixing temperature of 30°C and analysed at a speed of elongation of 3 mm/min.

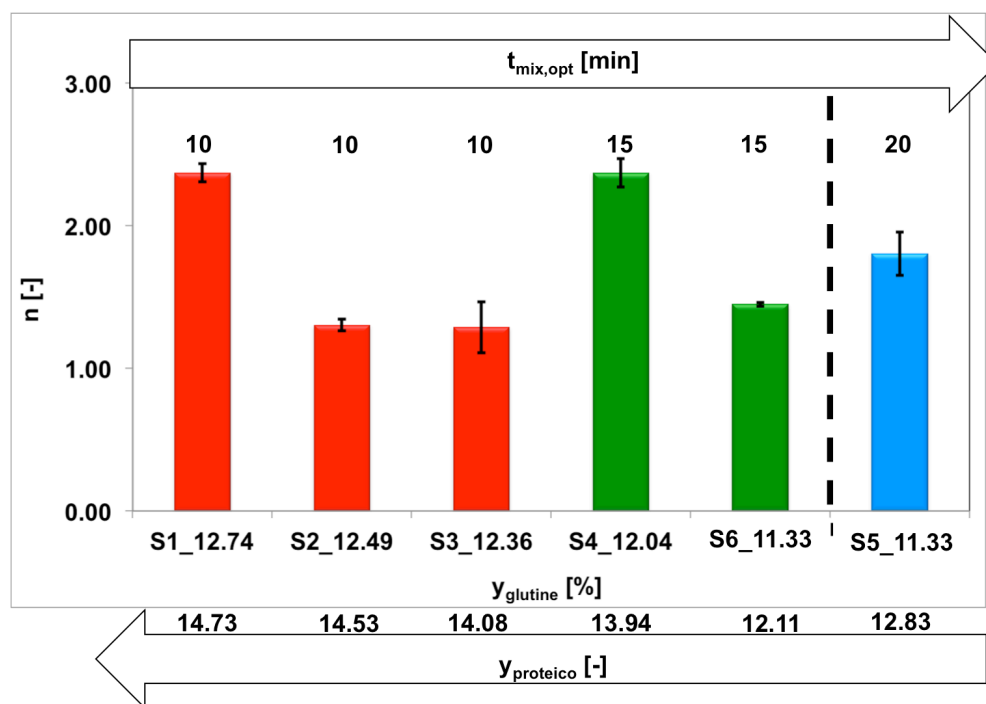


Figure 26. Trends of strain hardening vs to the protein and gluten content and also to the optimum time of mixing.

The index of strain hardening for mixtures of durum wheat with high protein content may be related to the protein and gluten content and also to the optimum time of mixing. In fact, analysis conducted have shown that with the increase of the protein and gluten content, there is a reduction of the optimum time of mixing and for higher gluten content, major of 12.30%, the optimum time of mixing is in correspondence of 10 minutes. For gluten content between 12.3 and 11.3 %, the optimum time of mixing is around 15 minutes. The only exception is for the sample S6 that despite having a higher protein content than the sample S5 has a great time mixing of 20 minutes, probably due to the gliadin to glutenin ratio or to other difference in the quality of the proteins

8. Conclusions

Through the measures carried out in uniaxial elongation, one can detect a dependency on the conditions of mixing by the protein content. The results, processed through the equation of Hollomon, and confirmed through SEM analysis, showed the evolution of the network gluten until reaching a maximum value, which determines the optimum time of mixing, and a subsequent disintegration of the same. The optimum time of mixing would appear to decrease with increasing temperature and increasing the protein content. The index of strain-hardening, for a mixing temperature of 20°C, does not show a significant trend with the time of mixing, due to the fact that low temperatures do not favour hydration of starch and consequently entail a delay in the development of gluten chain. The samples obtained from the different durum semolina have different behaviour with the mixing temperature. For the samples of semolina S2, S3, S4, S5 and S6, the increase of the mixing temperature, increases the value of the index of Hencky strain. As the temperature of mixing, the diffusion of the water increases, so water diffuses better within the particles of durum semolina [Kieffer R. et al., (1998)].

For each sample of durum semolina is evident the normal trend of the maximum value of the index of hencky strain for which the value increase increasing the elongational velocity.

REFERENCES

- 1) Charalambides, M. N., Wanigasooriya, L., Williams, J. G., Goh, S. M., & Chakrabarti, S., (2006). Large deformation extensional rheology of bread dough, *Rheol Acta*, (46), 239-248
- 2) Chatraei S. H., Macosko C. W., and Winter H. H., (1981). Lubricated squeezing flow: a new biaxial extensional rheometer, *Journal of Rheology*, (25), 433-443
- 3) Cumming D. B. and Tung M. A., (1975). The ultrastructure of commercial wheat gluten, *Can Inst Food Sci Tech*, (8), 67-70
- 4) Davis J. R., (2004). Tensile testing, second edition, *Asm International*, 1-283.
- 5) Dealy J. M. and Wissbrun k. F., (1990). Melt rheology and its role in plastics processing, *Van Nostrand-Reinhold*, New York
- 6) Dobraszczyk B. J. and Roberts C. A., (1994). Strain hardening and dough gas cell-wall failure in biaxial extension, *J, Cereal Sci.*, (20), 265-274
- 7) Dobraszczyk B. J., (1997). Development of a new dough inflation system to evaluate doughs, *Cereal Foods World*, (42), 516-519
- 8) Dobraszczyk B. J. and Vincent J.F.V., (1999). Measurement of mechanical properties of food materials in relation to texture: the materials approach, *Food texture: Measurement and perception*, 99-151.
- 9) Dobraszczyk B. J. and Morgenstern M. P., (2003). Rheology and the breadmaking process, *Journal of Cereal Science*, (38), 229-245
- 10) Evans L. G., (1977). Ultrastructure of bread dough with yeast single cell protein and/or emulsifier, *J. Food Sci.*, (42), 4-70
- 11) Huang H. and Kokini J. L., (1993). Measurement of biaxial extensional viscosity of wheat flour doughs, *J. Rheol*, (37), 879-891
- 12) Janssen A. M. Van Vliet T. and Vereijken J. M. (1996). Fundamental and empirical rheological behaviour of wheat flour doughs and comparison with bread making performance, *Journal of Cereal Science*, (23), 43-54

- 13) Kieffer R., Wieser H., Henderson M. H., and Graveland A., (1998). Correlations of the breadmaking performance of wheat flour with rheological measurements on a micro-scale, *Journal of Cereal Science*, (27), 53-60
- 14) Khatkar B. S., Fido R. J. Tatham, A. S. and Schofield, J. D., (2002). Functional properties of wheat gliadins. II. Effects on dynamic rheological properties of wheat gluten, *Journal of Cereal Science*, (35), 307-313
- 15) Khoo C. et al., (1975). Scanning and transmission microscopy of dough and bread, *Bakers Dig.*, (49), 6-24
- 16) Levine H. and Slade L. (1990). Influences of the glassy and rubbery states on the thermal, mechanical, and structural properties of doughs and baked products. In *Dough rheology and baked product texture*, Springer US, 157-330
- 17) McLeish T. C. B. and Larson R. G., (1998). Molecular constitutive equations for a class of branched polymers: The pom-pom polymer, *Journal of Rheology*, (42), 81-110
- 18) Mohos F., (2010). *Confectionery and Chocolate Engineering: Principles and Applications*, Wiley-Blackwell, 1-712
- 19) Morgenstern M. P., Newberry, M. P. and Holst S. E., (1996). Extensional properties of dough sheets, *Cereal chemistry*, (73), 478-482
- 20) Moss R., (1972). A study of the microstructure of bread doughs, *CSIRO Food Res Quart*, (32), 3-50
- 21) Ng, T. S. K., Gareth H. McK., and Mahesh P., (2007). "Linear to non-linear rheology of wheat flour dough, *Appl Rheol*, (16), 265-274
- 22) Osaki K., Watanabe, H., and Inoue T., (1999). Stress overshoot in shear flow of an entangled polymer with bimodal molecular weight distribution. *日本レオロジー学会誌*, (27), 63-64.
- 23) Padmanabhan M., (1995). Measurement of extensional viscosity of viscoelastic liquid foods, *Journal of Food Engineering*, (25), 311-327
- 24) Sahin S. and Sumnu G. S., (2006). Physical properties of foosds, *Food Science Text Serie*, 79-80

- 25) Sandstedt R. M. et al., (1954). The microscopic structure of bread and dough, *Cereal Chem.*, (31), 9-43
- 26) Schweizer T., and Conde-Petit B., (1997). Bread dough elongation, *In Proceedings of 1st International Symposium on Food Rheology and Structure*, 391-394
- 27) Sliwinski E. L. et al., (2004) Large deformation properties of wheat flour in uni-and biaxial extension. Part II. Gluten dough, *Rheologica Acta*, (43), 321-332
- 28) Sliwinski E. L. et al., (2004). On the relationship between large-deformation properties of wheat flour dough and baking quality, *Journal of Cereal Science*, (39), 231-245
- 29) Sliwinski E. L. et al., (2004a). On the relationship between gluten protein composition of wheat flours and large-deformation properties of their doughs, *Journal of Cereal Science*, (39), 247-264
- 30) Song Y. and Zheng Q., (2008). Network formation in glycerol plasticized wheat gluten as viewed by extensional deformation and stress relaxation. Final conclusions, *Food Hydrocolloids*, (22), 674-681
- 31) Tronsmo K. M. et al., (2003). Comparison of small and large deformation rheological properties of wheat dough and gluten, *Cereal Chemistry*, (80), 587-595
- 32) Tschoegl N. W. et al., (1970). Rheological properties of wheat flour doughs I, *J. Sci. Fd Agric*, (21), 65-70
- 33) Tschoegl N. W., Rinde J. A., and Smith T. L. (1970a), Rheological properties of wheat flour doughs I-Method for determining the large deformation and rupture properties in simple tension, *Journal of the Science of Food and Agriculture*, (21), 65-70
- 34) Uthayakumaran S. et al., (2000). Small and large strain rheology of wheat gluten, *Rheologica Acta*, (41), 162-172
- 35) Van Vilet T., (1992). Strain hardening of dough as a requirement for gas retention, *Journal of texture Studies*, (23), 439-460

- 36) Van Vilet T. and Hamer R. J., (2007). Fourteen years strain hardening as an indicator of bread-baking performance, questions still to be solved, *Gluten Proteins*, Am. Asso Cereal Chem., St. Paul, MN, 259-263
- 37) Van Vliet T., (2008). Strain hardening as an indicator of bread-making performance: A review with discussion *Journal of Cereal Science*, (48), 1-9
- 38) Vincent P. I., (1960). The necking and cold-drawing of rigid plastics, *Polymer*, (1), 7-19
- 39) Zghal M. C., Scanlon M. G. and Sapirstein H. D. (2002). Cellular structure of bread crumb and its influence on mechanical properties, *Journal of Cereal Science*, (36), 167-176.
- 40) Zheng H., Morgenstern M. P., Campanella O. H., and Larsen N. G., (2000). Rheological properties of dough during mechanical dough development. *Journal of Cereal Science*, (32), 293-306

Chapter IV

Drying process: mathematical modeling

1. Introduction

Drying is one of the most commonly used unit operations in industrial food process to improve the safeguarding and transport performance.

Drying process involves transient phenomena of heat and mass transfer with several changes, such as physical or chemical transformations, which cause changes in product quality.

It occurs by vaporization of liquid water, caused by heat. Heat may be supplied by convection (direct dryers), by conduction (contact or indirect dryers) and by radiation, or by a mix of these. Hot air is used both to supply the heat for evaporation and to carry away the evaporated moisture from the product.

The rate at which drying is accomplished is governed by the rate at which the two processes proceed.

The purpose of drying is to decrease the water content of fresh pasta from a value of 34% to 11.5% (d.b.) in order to reduce the risk of microbial growth, increase the product's shelf life and obtain pasta that is strong enough to be stored and transported easily [Owens, (2001)].

The quality of dried pasta such as texture and appearance depends by four factors that affect the drying process: humidity, temperature, time and air flow rate.

Airflow rate and time are the basic factors that can affect the two other factors.

In terms of airflow rate, drying occurs most efficiently when the air is at direct contact with the product, because of the increased product surface area exposed.

The humidity of the air needs to be controlled to meet the final moisture content requirement. Wet hot air is composed by 40-70% (w/w) of the humidity and is used to dry the pasta with direct content. This helps to prevent the product from cracking in the high temperature dryer. When the product is heated for a longer time, the temperature needs to be lower, for this reason exposure time influences the temperature. High temperature leads to an improvement in pasta colour and firmness, lower coking loss, higher cooked weight and less stickiness. Under high temperature drying conditions, in pasta occurs the Maillard reaction.

It is responsible for browning in food containing reducing sugars and free amino groups [(Hodge, (1953)]. This reaction influences flavour, functional and nutritional properties of processed foods.

But high temperatures can damage the product and destroy the nutrients and shows higher firmness and lower stickiness after cooking, this phenomenon is usually called “thermal damage”.

The complexity of the pasta production process lies in the fact that we need to simultaneously take into account the variables that will influence process.

Nowadays, the drying process of pasta is usually designed in an empirical way by trial-and-error runs and is rather based on practical knowledge of pasta producers than on engineering knowledge [Andrieu & Stamatopoulos, (1986); Migliori et al., (2005) and Veladat et al. (2011)].

When a new product is put on the market, many tests may be needed before satisfactory drying conditions are determined. For this reason, mathematical model have been developed to improve understanding of how the operating conditions impact the properties of dry pasta and also to minimize the number of tests required to determine optimal drying conditions and to develop efficient control strategies for the process [De Temmerman et al. (2007) and Veladat et al. (2011)].

The objective of this work is the study of a mathematical model of the transport phenomena that occur during the drying process in the production of dry pasta, solving a set of transient (time-dependent) heat and mass transfer equation to obtain a more accurate and predictive control of the process and therefore an

improvement in the quality of the product end.

2. State of art

The mathematical modeling of drying process of the dough is important to predict moisture content of pasta at any drying time. In literature are proposed many mathematical models, which describe the simultaneous transport of heat and mass transport as a function of the operating conditions that most influence the properties of the dried pasta.

Figure 1 shows a scheme of different mathematical models reported in the literature.

| Model | Geometry | Mass transfer | Heat transfer | Shrinkage | Calculated properties |
|--------------------------|-----------------|--|---|--|--|
| Litchfield et al. 1992 | Rectangular | $\frac{\partial M}{\partial t} = \frac{\partial}{\partial x} \left(D_{eff} \frac{\partial M}{\partial x} \right)$ | - | - | $D_{eff} = \left[A \exp \left(\frac{-E_a}{RT_0} \right) \right] \left[1 - \exp(-BM^c) + M^p \right] 10^{-12}$ |
| Migliori et al. 2005 | Hollow cilinder | $\frac{\partial U}{\partial t} = \frac{1}{r} \frac{\partial}{\partial r} \left(r D_d \frac{\partial U}{\partial r} \right)$ | $\rho_d C_d \frac{\partial T}{\partial t} = \frac{1}{r} \frac{\partial}{\partial r} \left(r k_d \frac{\partial T}{\partial r} \right)$ | $R = R_0 \left[1 + \alpha (U - U_0) \right]$ | $C_d(T, U), k_d(T, U), D_d(T, U), \rho_d(T, U)$ |
| De Temmerman et al. 2007 | Rectangular | $\frac{\partial M}{\partial t} = \frac{1}{\xi} \frac{\partial}{\partial \xi} \left[\left(\frac{D_{eff}}{(1 + \alpha_{vol} M)^2} \xi \right) \frac{\partial M}{\partial \xi} \right]$ | $\frac{\rho_{vs}}{\rho_s} \frac{\partial [(1 + X)h]}{\partial t} = \frac{1}{\xi} \frac{\partial}{\partial \xi} \left[\left(\frac{k}{(1 + \varepsilon X)} \right) \frac{\partial T}{\partial \xi} \right]$ | $\frac{\rho_{app}}{\rho_s} = \frac{1 + \bar{M}}{1 + \alpha_{vol} \bar{M}}$ | $D_{eff} = A \exp \left[-B \left(\frac{1}{T_{\infty}} - \frac{1}{T_{ref}} \right) \right] \exp(CM)$ |
| De Temmerman et al. 2008 | Cilindrycal | $\frac{\partial M}{\partial t} = \frac{\partial}{\partial \xi} \left[\left(\frac{D_{eff}}{(1 + \alpha_{vol} M)} \xi \right) \frac{\partial M}{\partial \xi} \right]$ | - | $\frac{\rho_{app}}{\rho_s} = \frac{1 + \bar{M}}{1 + \alpha_{vol} \bar{M}}$ | $D_{eff} = A \exp \left[-B \left(\frac{1}{T_{\infty}} - \frac{1}{T_{ref}} \right) \right] \exp(CM)$ |
| Mercier et al. 2011 | Cilindrycal | $\frac{\partial M}{\partial t} = D_{eff} \left(\frac{\partial^2 M}{\partial r^2} + \frac{1}{r} \frac{\partial M}{\partial r} \right)$ | - | $\lambda_r(t) = \frac{1 - \eta}{v(1 + M_0)} (M_0 - M_c)(1 - \alpha)$ | $\rho_{app}(t) = \frac{\rho_w (1 + \Delta M_d + M_c)}{\Delta M(\eta - 1)(1 - \alpha) + v(1 - M_0)}$ $\varepsilon_r(t) = \frac{1 - \eta}{v(1 + M_0)}$ $\frac{\rho_w (1 + \Delta M_d + M_c)}{\Delta M(\eta - 1)(1 - \alpha) + v(1 - M_0)} \left[\frac{1}{(1 + 1/r) \rho_{stem}} + \frac{1}{(1 + 1/r) \rho_{ppc}} + \frac{\Delta M_d + M_c}{\rho_w} \right]$ |

Figure 1. Scheme of mathematical models in the literature.

According to Ogawa et al. (2012), pasta drying can be divide in two drying rate period, where 20% of water is evaporated, followed by a falling rate period.

Generally, it is considered that the mass transfer mechanism involve the diffusion of the water in liquid form to the surface of the product, followed by evaporation of the water on the surface [Migliori et al. (2005) and De Temmerman et al. (2007)].

The internal resistance to the transport of water represents the limiting factor of the process. During drying, moisture diffusion is described using Fick-type laws [(Andrieu et al. (1986), Migliori et al. (2005) and De Temmerman et al. (2007)].

In fact, in most models, only the mass transfer in the smallest dimension of the pasta is considered [Litchfield et al. (1992); De Temmerman et al. (2007) and

Mercier et al. (2011)] and the Fick law is applied for two different shapes: rectangular [Litchfield et al. (1992)] and cylindrical [De Temmerman et al. (2008) and Mercier et al. (2011)].

The heat transfer mechanism is treated only in the model developed by Migliori et al. (2005) and De Temmerman et al. (2007), respectively for shapes tubular and cylindrical.

In the study of De Temmerman et al. (2007), the coefficient of mass transfer, h_m is calculated using the relationship of Lewis, in which, h , the coefficient of heat transfer by convection, is measured experimentally by means of a thermocouple, capable of measuring the flow of heat that is realized between the metal surface, in which lies the sample, and the air. Migliori et al. (2005) determine the heat and mass transfer using the Chilton-Colburn analogy.

In these models, the analysis is extended to mechanical, rheological and chemical properties of pasta, studying the dimension, porosity, density, rigidity, formation of cracks and furosine production [Andrieu et al., (1986); Ponsart et al., (2003); Migliori et al., (2005) and Mercier et al., (2011)].

The examining of these properties generates a more complete database that can be used to study the relationship between product quality and drying conditions.

In fact in the model proposed by Litchfield et al. (1992) and De Temmerman et al. (2007) are identifying the empirical correlation that exists between the effective diffusion coefficient, D_{eff} , and operational conditions.

The equation on the effective diffusion coefficient suggested by De Temmerman et al.(2007) is correlated to Arrhenius equation and is divided for an auxiliary factor that is in turn a function of humidity, the density of the dry solid and the density of water. Only in the work of Migliori et al. (2005), the properties of dough (heat capacity, density, coefficient of diffusion and coefficient of mass transfer) were reconsidered as function of temperature and moisture content, and the shrinkage, which influences the quality of the product, was considered too. In the work developed by Migliori et al. (2005), shrinkage it is considered to have a linear proportionality with the radial dimension and the loss of moisture. In the model proposed by De Temmerman et al. (2007) the volume reduction due to the

loss of water is considered writing the balance of material and energy in Lagrangian coordinates Mercier et al. (2011) observes shrinkage equivalent to 21% and 30% of initial pasta volume when drying at 40°C and 80°C respectively, they showed that a higher temperature has a greater influence on the physical properties of the dough. Shrinkage is considered using a dimensionless coefficient describing the fraction of water lost during drying that is replaced by air inside the gluten network.

Also they have found a direct influence the shrinkage phenomenon with the apparent density and porosity of the product obtained and studying the behaviour of these properties as a function of the drying time.

The models developed to date present varying degrees of complexity depending on the mass and heat transfer mechanisms considered and the hypotheses used. Depending on this degree of complexity, the models can lead to an analytical solution or have to be solved using numerical methods. The analytical solution models are generally preferred for their simplicity.

These models provide more direct information in terms of the impact of operating conditions on product properties, but, generally, the model solution requires the simplifying the phenomena involved, which can reduce the accuracy of the final results.

3. Physical phenomena

The modeling of drying process starts from the definition of the system to be analysed, which can be schematized in two phases: the pasta dough, constituted by water and semolina, and the fluid phase, composed by air at humidity and temperature controllable.

The simultaneous heat and mass transfer is sketched in the Figure 2 and shows the boundary contour between pasta and drying air.

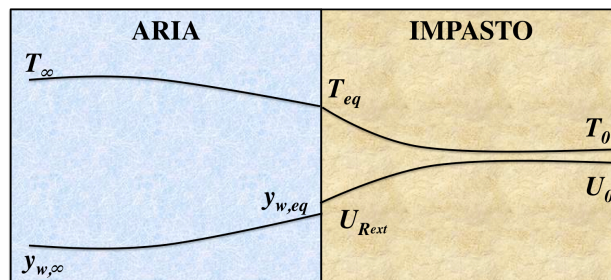
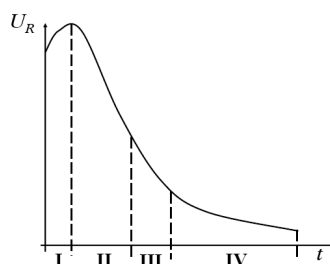


Figure 2. Physical phenomena.

Pasta drying can be divided into a constant drying-rate period, where about 20% of water is removed, followed by a falling rate period. All the process is a result of transient mass and heat transfer phenomena occurring until a state of equilibrium between the pasta and dryer environment is reached. According to de Cindio et al. (2004) at the early stage of the process, when the water content inside the pasta is sufficiently high that the heat coming from air just equates the heat due to water evaporation, no water gradient inside pasta arises. In this case, the temperature remains constant at the so called “wet bulb conditions” and the controlling transport mechanism is the external mass transfer. This process period is usually called “constant evaporation rate period”, because water is removed at a constant rate

After this step a decrease of the evaporation rate is observed because the internal mass transfer becomes controlling and a moisture gradient inside the material appears, as shown in Figure 2. During this period water is transported inside material to the surface (internal diffusion).

It is generally considered that the mass transfer mechanisms involved are the diffusion of the water in liquid form to the surface of the product, followed by evaporation of the water on the surface [Migliori et al., (2005a); De Temmerman et al., (2007)], as shown in Figure 3.

**Figure 3.** Sketch of drying periods: moisture content versus time.

Internal resistance to the transport of water is assumed to be the limiting factor. Consequently, during drying, moisture diffusion develops inside the product, which is normally described using Fick-type laws [Andrieu and Stamatopoulos,

(1986); Migliori et al., (2005a); De Temmerman et al., (2007)]. However, non-Fickian behaviour was observed around the state of glass transition [Xing et al., (2007)].

Finally, when water content becomes even lower, the external shell of pasta becomes dry and a moving evaporation front must be considered. Under this condition, a third slower drying period is attained. According to de Cindio (2004), usually, this condition is reached when humidity becomes lower than 8%.

4. Geometry of system

The format of pasta chosen for the drying model is the "vermicellone", which can be schematized as a long cylinder of radius R and length L , as shown in Figure 4.

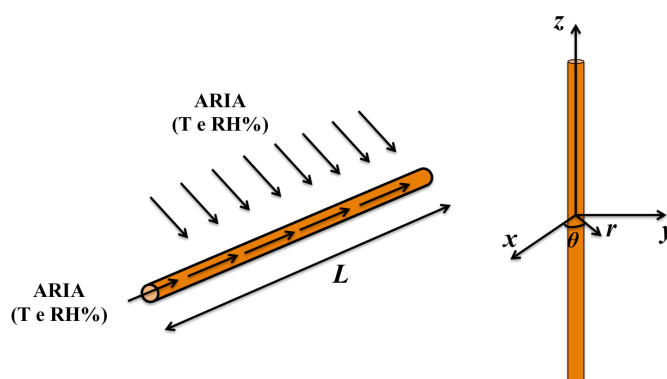


Figure 4. "Vermicellone": shape pasta geometry.

The schematized system is symmetric, and then the mathematical modeling of the process can be performed in a smaller region.

The vermicellone is a long spaghetti and also it is symmetric along the z -axis. To simplify the study, it is possible to identify eight symmetrical elements between them, as shown in Figure 5. The study is carried out in one of these eight part, because what is happening in this region is exactly equal to what is happening in the regions symmetrical to it.

5. Balance equation of system

The transport equations written to 3D model the drying phenomenon are the equations of energy and mass transport in Cartesian coordinate

It is used for the transport of energy, a mechanism purely conductive, while for the mass transport, a purely diffusive mechanism, which obeys Fick's law:

$$\rho_d C_d \frac{dT}{dt} = \nabla(k_d \nabla T) \quad (1)$$

$$\frac{dC}{dt} = \nabla(D_d \nabla C) \quad (2)$$

where T is the sample temperature expressed in K , C is the molar concentration of water in $[mol/m^3]$ inside the product, k_d $[W/m^2/K]$, ρ_d $[kg/m^3]$, c_d $[J/kg]$ and D_d $[m^2/s]$ are the thermal conductivity, density, specific heat and the diffusivity of water in the dough and are functions of temperature and humidity.

The fact that some properties are a function of temperature and water content, leading to a non-linear system of partial differential equations coupled, which must be solved with the correct boundary conditions.

6. Boundary and initial conditions

In this study, the transport phenomena in the game have been modeled through the budgets of matter and energy in transition, in a reference system in cylindrical coordinates.

On the base of this model, can be considered the following hypothesis:

- initial moisture and temperature profile are uniform;
- inside the sample mass and heat transport are purely diffusive, while they are only convective in the drying fluid;
- diffusive mass transfer is described by Fick's law;
- there is equilibrium at the air-paste interface.

As regards the external transport, it can be assumed the hypothesis of the "film theory" [Bird et al., (1960)]. The model idealizes the transition between the fluid properties and those at the wall as occurring entirely within a thin film next to the wall. The fall of temperature and water concentration occurs in a layer of fluid near of the surface, while the fluid phase unchanged within in the "bulk". In this film, the influence of convection parallel to the wall is furthermore neglected.

This assumption allows to focus the exchange in this layer and to obtain, so the equations that expresses flows outside.

Defining the appropriate initial and boundary conditions can solve the system of differential equations. The flow of material gas side, $N_{w,surf} [kg \text{ di acqua}/m^2/s]$ can be written as a function of a coefficient of exchange of material.

$$N_{w,surf} = -n \cdot (D_d \nabla C) = k_c \cdot M_w \cdot (C_\infty - C_{eq}) \quad (3)$$

where $k_c [m \cdot s^{-1}]$ is a mass coefficient for gas; C_∞ and C_{eq} are respectively the interfacial concentration and the concentration inside in the fluid for gas and D_d is the mass diffusivity in the dough.

For the transport of energy, the surface temperature is the temperature of balance T_{eq} :

$$T_{surf} = T_{eq} \quad (4)$$

In analogy to the mass transfer, the boundary condition on the flow of energy can be written in the following way:

$$q = h \cdot (T_\infty - T_{eq}) = -k_d (T_\infty - T_{eq}) + \lambda \cdot k_c \cdot M_w \cdot (C_\infty - C_{eq}) \quad (5)$$

where $h [W \cdot m^{-2} \cdot K^{-1}]$ is the rate of exchange of energy, λ is the latent heat of vaporization of water [$J \cdot kg^{-1}$] and T_∞ e T_{eq} are the temperature of the heat carrier fluid and the drying temperature and the balance shall be assessed on the basis of the hypothesis of thermodynamic equilibrium at the air-mixture in the form of an equality of chemical potentials.

This report is written in terms of water activity:

$$P \cdot y_w^{eq} = p_w^0 \cdot a_w \quad (6)$$

where $P [atm]$ is the pressure of the system, $p_w^0 [atm]$ is the vapor pressure and a_w is the activity of water in the dough. In the equation 6, it is assumed, for the gas phase, a behaviour type solution for the liquid phase; it is considered a real mixture whose behaviour deviates from Raoult's solution.

The value of a_w is expressed by one of the constitutive equations that bind the water activity to the content of water present in the dough, U_w , which is the percentage quantity of water inside the mixture expressed on a wet basis (w.b.) defined as:

$$U = \frac{\text{peso dell'acqua [kg]}}{\text{prso dell'acqua+peso della semola [kg]}} \cdot 100 \quad (7)$$

The initial conditions were obtained from the experimental data of temperature and humidity provided by the company “RUMMO” S.p.A. (Benevento, Italy). The humidity values were decoded in terms of the concentration of water within the model in Comsol.

7. Thermodynamic and transport properties

The following paragraph reports all the material parameters necessary for the simulation of the baking of a crunchy biscuit, relative to material and energy transport. Many of these were obtained from the literature data, while for the density value, surface tension, void fraction, number of bubbles and water activity laboratory tests were performed.

7.1 Activity water

From an engineering point of view, the water present in the sample of fresh pasta can be classified in three forms: free, partially and strongly bounded [de Cindio et al., (1992)], in relation to its position within system composed of gluten and starch.

Through the adsorption isotherms [Lewicki, (2000)] detects a system’s sensitivity to variations in water concentration in terms of variation in the activity a_w .

The most common ones used in describing sorption on food are the Langmuir equation, the Brunauer-Emmett-Teller (BET) equation, Oswin model, Smith model, Halsey model, Henderson model, Iglesias-Chirife equation, Guggenheim-Anderson-de Boer (GAB) model and Peleg model.

The equation models are shown in Table 1.

| Model | Equation | Parameters | Reference |
|----------|---|---------------|------------------------------|
| Langmuir | $a_w \left(\frac{1}{U} - \frac{1}{U_0} \right) = \frac{1}{CU_0}$ | U_0, C | Langmuir (1918) |
| BET | $U = \frac{U_0 C_B a_w}{(1 - a_w)(1 - a_w + C_B a_w)}$ | U_0, C_B | Brunauer et al. (1938) |
| Oswin | $U = C_0 \left(\frac{a_w}{1 - a_w} \right)^{n_0}$ | C_0, n_0 | Oswin (1946) |
| Smith | $U = A - B \ln(1 - a_w)$ | A, B | Smith (1947) |
| Halsey | $U = U_0 \left(-\frac{A}{RT \ln(a_w)} \right)^{1/n}$ | U_0, A, n_0 | Crapiste and Rotstein (1982) |

| | | | |
|-------------------------|--|----------------------|-----------------------------|
| Henderson | $U = \left[-\frac{\ln(1 - a_w)}{C} \right]^{1/n}$ | C, n_0 | Henderson (1952) |
| Iglesias-Chirife | $\ln[U + (U^2 + U_{0.5})^{1/2}] = C_1 a_w + C_2$ | $U_{0.5}, C_1, C_2$ | Iglesias-Chirife (1978) |
| GAB | $U = \frac{U_0 C_G K_G a_w}{(1 - K_G a_w)(1 - K_G a_w + K_G C_B a_w)}$ | U_0, C_G, K_G | Van den Berg & Bruin (1981) |
| Peleg | $U = C_1 a_w^{C_3} + C_2 a_w^{C_4}$ | C_1, C_2, C_3, C_4 | Peleg (1993) |

Table 1. Models of isothermal adsorption, where U=humidity d.b. [%] and a_w =water activity [-].

In this work the semi-empirical model used is equation of Oswin [Schuchmann et al., (1990)].

This equation provides good results when the activity water does not exceed 0.7. Being a two-parameter equation, the equation can be modified to obtain a linear form. The fitting of this equation provides slope and intercept values that identify the parameters of equation.

The parameters of desorption isotherms equation can be obtained by experimental measures.

Dry pasta process is realized in an oven using hot air with the following operative conditions $T_{inf}=60^\circ\text{C}$ and $v_{inf}=3\text{mm/min}$ and for a time of 60 minutes.

The water loss measurements have been carried out using a thermogravimetric balance, as shown in Figure 6 (HB43 Mettler Toledo, Germany).

It is a thermal analysis, in which the weight loss of sample is monitored as function of temperature and time.

The sample is heated up with halogen lamp in order to evaporate water.

The water activity is determined with Novasina AW Sprint TH500 (Novasina, Switzerland) using the hygrometric instrument method, as shown in Figure 7.



Figure 5. Balance thermogravimetric.



Figure 6. Water activity instrument.

In order to obtain the isothermal desorption curve and to control the rate of evaporation during the first phase of the process, it is decided to make a sampling measurement every 5 min during the first hour and after every 15 min until to end of the test.

The test starts when sample has value moisture of 34% and it finishes when sample has value of 10%.

7.2. Transport of coefficients

Within the cell of drying, the air flows investing the sample of pasta along the radial and axial direction (Figure 4). Therefore the calculation of the coefficients of heat and mass transport must take account of this condition.

The coefficient of energy transport is calculated using the Colburn factor J_h defined in terms of dimensionless numbers:

$$J_h = \frac{Nu}{Re \cdot Pr^{1/3}} \quad (8)$$

where Re is the Reynolds number and that Nu Nusselt.

Along the direction r , the system is considered as a cylinder invested by a flow of air, while along the z -direction as a flat. Therefore, the following definitions have been used for the Nusselt and Reynolds number:

$$Nu_{flat\ plate} = 0.664 \cdot Pr^{1/3} \cdot Re_{flat\ plate}^{1/2} \quad (9)$$

$$Nu_{cylinder} = 0.683 \cdot Pr^{1/3} \cdot Re_{cylinder}^{0.466} \quad (10)$$

$$Re_{flat\ plate} = \frac{\rho_a \cdot v_{inf,ext} \cdot L}{\mu_a} \quad (11)$$

$$Re_{cylinder} = \frac{\rho_a \cdot v_{inf,ext} \cdot R}{\mu_a} \quad (12)$$

where ρ_a is the density of air and $v_{inf,ext}$ is the air speed of 5 cm/s.

The equation 9 is valid for values of $Re < 5 \cdot 10^5$ and for values of $Pr > 0.1$, while the equation 10 is valid for values of Re between 40 and 4000 and for values of $Pr > 0.6$. The number of Pr is estimated as:

$$Pr = \frac{\mu_a \cdot c_{p,a}}{k_a} \quad (13)$$

where k_a [$W \cdot m^{-2} \cdot K^{-1}$] is the thermal conductivity of air, μ_a [$Pa \cdot s$] is the viscosity air, $c_{p,a}$ [$J \cdot kg^{-1} \cdot K^{-1}$] is the specific heat air.

The transport coefficient h is determined as:

$$h_{flat\ plate} = \frac{flat\ plate \cdot k_a}{L} \quad (14)$$

$$h_{cylinder} = \frac{Nu_{cylinder} \cdot k_a}{R} \quad (15)$$

For the mass transfer coefficient can use the analogy of Chilton-Colburn:

$$J_h = J_m \quad (16)$$

where J_m is defined:

$$J_m = \frac{Sh}{Re \cdot Sc^{1/3}} \quad (17)$$

where Sh is the number of Sherwood:

$$Sh_{flat\ plate} = \frac{k_{c,flat\ plate} \cdot L}{D_a} \quad (18)$$

$$Sh_{cylinder} = \frac{k_{c,cylinder} \cdot R}{D_a} \quad (19)$$

where D_a is the water diffusivity in the air e Sc is the number of Schimidt defined as:

$$Sc = \frac{\nu_a}{D_a} \quad (20)$$

where ν_a is the coefficient of thermal diffusivity of air.

The mass transfer coefficient was calculated using the following equations:

$$k_{c,flat\ plate} = \frac{h_{flat\ plate}}{\rho_a \cdot c_{p,a}} \cdot \left(\frac{Pr}{Sc}\right)^{2/3} \quad (21)$$

$$k_{c,cylinder} = \frac{h_{cylinder}}{\rho_a \cdot c_{p,a}} \cdot \left(\frac{Pr}{Sc}\right)^{2/3} \quad (22)$$

In all correlations, the calculations were performed under the conditions of "film", considering an average temperature between the surface conditions and the properties of bulk fluid phase:

$$T_{film} = \frac{T_{\infty} + T}{2} \quad (23)$$

The model thus formulated can be used for physical modeling of an object invested by an air current, but according to Migliori et al. (2005), the drying condition in the pasta cell is quite different. In fact, in the drying cell there is the presence of a high number of pasta samples, arranged in a contiguous manner between them. They are transported in different areas of the plant through a suitable transport system, which changes according to the size of the dough.

These conditions affect the amount of surface area available for the exchange of heat and material, thus resulting in a decrease in the speed of water evaporation [Migliori et al., (2005)].

Therefore, as reported in literature (Migliori et al., 2005), the mass transfer coefficient should be multiplied by an empirical factor β ($\beta = 0.0085$) to account for what has been said before:

$$k_{c, sheet\ plate_opt} = k_{c, sheet\ plate} \cdot \beta \quad (24)$$

$$k_{c, cylinder_opt} = k_{c, cylinder} \cdot \beta \quad (25)$$

8. Material parameters

The temperature and the relative humidity of the air inside of the cell drying of the values are not constant but is a function of time and the scheme has been provided by Rummo S.p.A..

The drying process is divided in 11 zones and the conditions have been specified in Table 2.

| zone | t [min] | T [°C] | RH [%] |
|------|---------|--------|--------|
| 1 | 4.375 | 49 | 48 |
| 2 | 12.5 | 54 | 56 |
| 3 | 18.75 | 61 | 68 |
| 4 | 40 | 80 | 67 |
| 5 | 66.25 | 68 | 70 |
| 6 | 108.75 | 90 | 71 |
| 7 | 225 | 85 | 76 |
| 8 | 375 | 78 | 78 |
| 9 | 406.25 | 75 | 80 |
| 10 | 428.125 | 45 | 55 |
| 11 | 446.25 | 28 | 70 |

Table 2. Data of the drying process divided into the various areas of the production line “vermicellone”.

The profiles of temperature and relative humidity have been implemented within the model using a function consists of cycles

8.1 Properties of air

The physical properties of air, thermal conductivity, specific heat and viscosity were calculated by polynomial equations of T_f in the program simulation:

$$k_a = \frac{2.3340 \cdot 10^{-3} \cdot T_{film}^{1.5}}{164.54 + T_{film}^2} \quad (26)$$

$$c_{p,a} = 1030.5 - 0.19975 \cdot T_{film} + 3.9734 \cdot 10^{-4} \cdot T_{film}^2 \quad (27)$$

$$\mu_a = \frac{1.4592 \cdot T_{film}^{1.5}}{(109.19 + T_{film})} \cdot 10^{-6} \quad (28)$$

The diffusivity of air is being evaluated instead with the following correlation taken from the literature [Perry and Green, (1997)]:

$$D_a = \frac{10^{-3} \cdot T_{film}^{1.75} \cdot \left(\frac{M_a + M_w}{M_a \cdot M_w}\right)^{0.5}}{P \cdot [(\sum v)_a^{1/3} + (\sum v)_v^{1/3}]^2} \quad (29)$$

where P is the external pressure [atm], M_x is the molecular weight of air and water and $(\sum v)_x$ is a material parameter, which depends on the atomic diffusion to the air and water and is:

$$(\sum v)_a = 20.1 \quad (30)$$

$$(\sum v)_b = 12.7 \quad (31)$$

The air density was calculated assuming the validity of ideal gas law:

$$\rho_a = \frac{P \cdot M_a}{R \cdot T_f} \quad (32)$$

8.2 Properties of dough

The physical properties of the dough, thermal conductivity, specific heat, density and diffusivity were evaluated using equations taken from the literature.

The thermal conductivity, in a mixture, is given by the sum of two contributions: the wet phase and dry phase [Saravacos et al. (2001)]. It is assessed through the use of a model based on two structural phases:

$$k_d(x, T) = \frac{1}{1+x} \lambda_0 \exp \left[-\frac{E_0}{R} \left(\frac{1}{T} - \frac{1}{T_{rif}} \right) \right] + \frac{x}{1+x} \lambda_i \exp \left[-\frac{E_i}{R} \left(\frac{1}{T} - \frac{1}{T_{rif}} \right) \right] \quad (33)$$

where x is the water content in the dough on a dry basis (d.b.) calculated as:

$$x = \frac{\text{massa d'acqua}}{\text{massa di secco}} \quad (34)$$

and $\lambda_i, \lambda_0, E_i$ e E_0 are characteristic parameters of the material and are respectively:

$$\lambda_i [\text{Wm}^{-1}\text{K}^{-1}] = 0.8 \quad (35)$$

$$\lambda_0 [\text{Wm}^{-1}\text{K}^{-1}] = 0.273 \quad (36)$$

$$E_i [\text{kJmol}^{-1}] = 2.7 \quad (37)$$

$$E_0 [\text{kJmol}^{-1}] = 0.0 \quad (38)$$

T is the temperature of the mixture, expressed in Kelvin [K], while t_{rif} is the reference temperature that is assumed equal to 333 K.

The heat capacity can be calculated as the weighted average on the compositions of the main components of the mixture [Andrieu et al. (1992)]:

$$c_d = \sum_i c_i \cdot x_i \quad (39)$$

The semolina used has the following composition:

| x_i | % |
|--------|------|
| Gluten | 11.9 |
| Fat | 1.4 |
| Starch | 86.7 |

Table 3. Semolina composition.

The following values were used for the individual components [de Cindio et al. (1992)]:

$$C_{\text{water}} = 4.184 \left[\frac{\text{J}}{\text{gK}} \right] \quad (40)$$

$$C_{\text{starch}} = 5.737 \cdot T + 1328 \left[\frac{\text{J}}{\text{gK}} \right] \quad (41)$$

$$C_{\text{gluten}} = 6.329 \cdot T + 1465 \left[\frac{\text{J}}{\text{gK}} \right] \quad (42)$$

$$C_{\text{fat}} = 2000 \left[\frac{\text{J}}{\text{gK}} \right] \quad (43)$$

The density of the mixture was calculated as a function of humidity [de Cindio et al. (1992)]:

$$\rho_d(U) = \frac{1}{(3.02 \cdot U + 6.46) \times 10^{-4}} \left[\frac{\text{kg}}{\text{m}^3} \right] \quad (44)$$

where U is the moisture wet basis [w.b.].

The value of the vapour pressure that appears in the equation 6 has been calculated using the following correlation [Perry and Green, (1997)]:

$$p_w^0 = 10^{8.07131 - \left(\frac{1730.631}{T_\infty - 273.15 + 233.426} \right)} \quad (45)$$

where T_∞ [K] and p_w^0 [torr].

With regard to the water content in the bosom of the fluid phase, C_∞ , is calculated in relation to the moisture content:

$$C_\infty = \frac{RH \cdot p_w^0}{R \cdot T_\infty} \quad (46)$$

so as to obtain a concentration profile in the bulk fluid phase.

The quantity of water in the bulk, C_{eq} , is instead calculated with the following expression:

$$C_{eq} = \frac{a_w \rho_w^0}{R \cdot T_\infty} \quad (47)$$

where a_w is the water activity that has been evaluated experimentally.

The experimental data of activity and moisture were obtained by performing tests of drying pasta. The data were obtained using the equation of Oswin:

$$a_w = \frac{\left(\frac{x_w}{a}\right)^{1/b}}{1 + \left(\frac{x_w}{a}\right)^{1/b}} \quad (48)$$

where $a=0.106$ and $b=0.55$.

The diffusivity of water was evaluated by the following correlation [Waananen et al. (1996)]:

$$D = \frac{1}{1+X} D_0 \exp\left[-\frac{E_0}{R} \left(\frac{1}{T} - \frac{1}{T_r}\right)\right] + \frac{X}{1+X} D_i \exp\left[-\frac{E_i}{R} \left(\frac{1}{T} - \frac{1}{T_r}\right)\right] \quad (49)$$

where D is the diffusivity in m/s^2 , X is the moisture on a dry basis (d.b.), D_0 is the diffusivity in m/s^2 to $X=0$ and $T=T_r$, D_i is the diffusivity in m/s^2 $X=\infty$ and $T=T_r$, E_0 is the activation energy for the conduction of heat in the dry materials to $X=0$ and is expressed in $kJ/kmol$, E_i is the activation energy for the conduction of heat in materials dried at $X=\infty$ and is expressed in $kJ/kmol$, R is the ideal gas constant, and it is expressed in $kJ/mol /K$ and T_r is the critical temperature expressed in K . The values are reported in Table 4:

| | |
|-----------------|----------------------|
| $D_0 [m/s^2]$ | 0.0 |
| $D_i [m/s^2]$ | $1.39 \cdot 10^{-9}$ |
| $R [kJ/mol/K]$ | 0.0083143 |
| $T_r [K]$ | 333 |
| $E_0 [kJ/Kmol]$ | 2.0 |
| $E_i [kJ/Kmol]$ | 16.2 |

Table 4. Parameters for calculating the diffusivity water.

9. Shrinkage

The phenomenon of pasta breaking is closely related to the variations of the viscoelastic properties of the dough. Below a certain percentage of water, in fact,

in the mixtures prevails a solid behaviour which, coupled to the deformations associated with the dimensional shrinkage, determines the onset of stress thermoelastic which, if not relaxed, may cause surface cracks, or even the breaking of the piece.

During the drying, in fact, the product is dried to humidity values of about 11.5% w.b. in order to extend the shelf life, which, generally, is three years.

The drying conditions, such as temperature, humidity and airflow, strongly influence the quality of the dough. Indeed, if the pasta is dried too quickly, will be obvious fracture lines or billing information on the product, with a consequent weakening of the structure and a poor final pasta quality. It is, therefore, proposed a predictive model of this phenomenon, coupled with the knowledge of the profiles of temperature and humidity of the treated piece, allows us to estimate the efforts that occur in the system, as well as providing a failure criterion which, when coupled with them, provides quantitative information about the integrity of the pasta after treatment and stabilization times during the drying process.

For this reason it is important to shape the dimensional change, which, obviously, is connected to decrease of water within the sample of pasta.

The dimensional change inevitably affects the efficiency of the process and introduces a complicating factor to the model.

This complication concerns not only the transport of matter, but also the preservation of the organoleptic characteristics of the product.

As a first hypothesis, one can think of using a proportional relationship between the reduction in size of the “vermicellone” and the humidity change during the process.

This relation is well known in the literature and assumed that the dimensional reduction of the material is only due to the loss of water and that this dependence is linear [Minshkin et al., (1984); Lang et al., (1994)]

$$V = V_0(1 + h_{sh}(U - U_0)) \quad (50)$$

where V_0 is the initial volume, U_0 is the initial moisture, U and V are respectively the value of moisture and volume over time, while h_{sh} is a parameter of proportionality and it is called coefficient of shrinkage.

In writing of the model in Comsol, the equation 52 was written for the x and y direction, whereas the variation nothing the z axis.

$$\Delta x = 0.42 \cdot (u_w - u_{w,0}) \cdot \cos(\text{atan2}(x > 0, y > 0)) \quad (51)$$

$$\Delta y = 0.42 \cdot (u_w - u_{w,0}) \cdot \sin(\text{atan2}(x > 0, y > 0)) \quad (52)$$

The reference system is cylindrical, so in writing the model, cylindrical coordinates were transformed into Cartesian coordinates.

10. Method of calculation

The system of nonlinear partial differential equations is solved using commercial software (Comsol Multiphysics 4.3, Comsol, Sweden), based on the use of finite element method. Using a PC with an Intel (R) Xeon (R) CPU ES-2650C, 2.00 Ghz (2 CPU) and 64 GB of RAM.

In order to follow more precisely the curvature of the domain, the discretization has been carried out through the use of a mesh defined by the user with the following parameters: 288929

The volume control in question was discretized into 1896395 elements, the solver used in the calculation is Pardiso and the solution was obtained in 1 hour and 24 minutes.

Figure 7 shows a schematic representation of the total domination of integration in the xy plane.

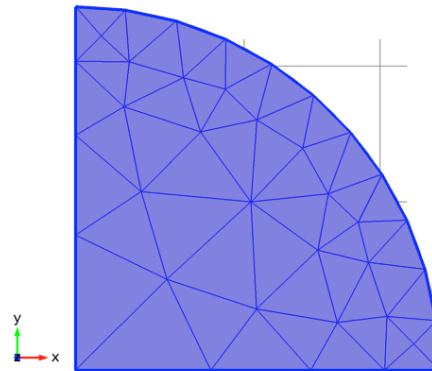


Figure 7. Schematic representation of the total domination of integration in the xy plane.

11. Results and discussion

The company Rummo gave the following experimental values in terms of diameter [mm] and humidity [w.b.], as shown in Table 5:

| <i>time [min]</i> | <i>diameter [mm]</i> | <i>moisture [w.b]</i> |
|-------------------|----------------------|-----------------------|
| 0 | 2.2 | 0.32 |
| 55 | 2.14 | 0.19 |
| 125 | 2.1 | 0.14 |
| 265 | 2.07 | 0.115 |
| 480 | 2.07 | 0.115 |

Table 5. Experimental values.

The model was simulated for a time of 480 min.

In the simulation program was therefore introduced the report which allows to model the reduction in volume of the dough.

The first mathematical modelling is simulated using the coefficient shrinkage found in the literature, $h_{sh}=0.42$. The comparison between the model and the experimental data gave the following result, as shown in Figure 8:

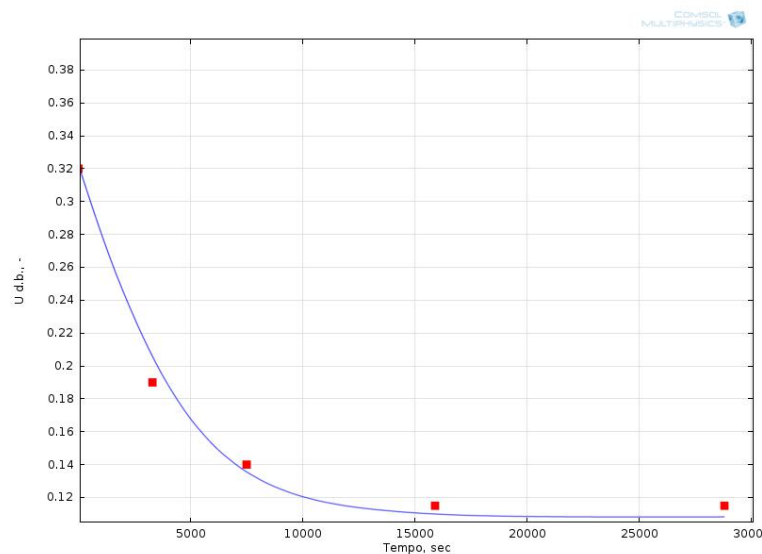


Figure 8. “Vermicellone”: experimentals data vs models data.

From figure 8, it can be seen that the model is in good agreement with the experimental data.

11.1 Sensitivity Analysis

Therefore, we proceeded to a validation of the model ensuring, however, before the sensitivity thereof to the important operating parameters.

The coefficient of shrinkage was made to vary with respect to values known in the literature [Mayor and Sereno, (2004)] and was also calculated from the experimental data available from industrial tests, as reported in Figure 8. The calculated value for the coefficient of shrinkage is equal to 0.27.

In the following figure shows the trend of the diameter as a function of shrinkage calculated coefficient (Figure 9).

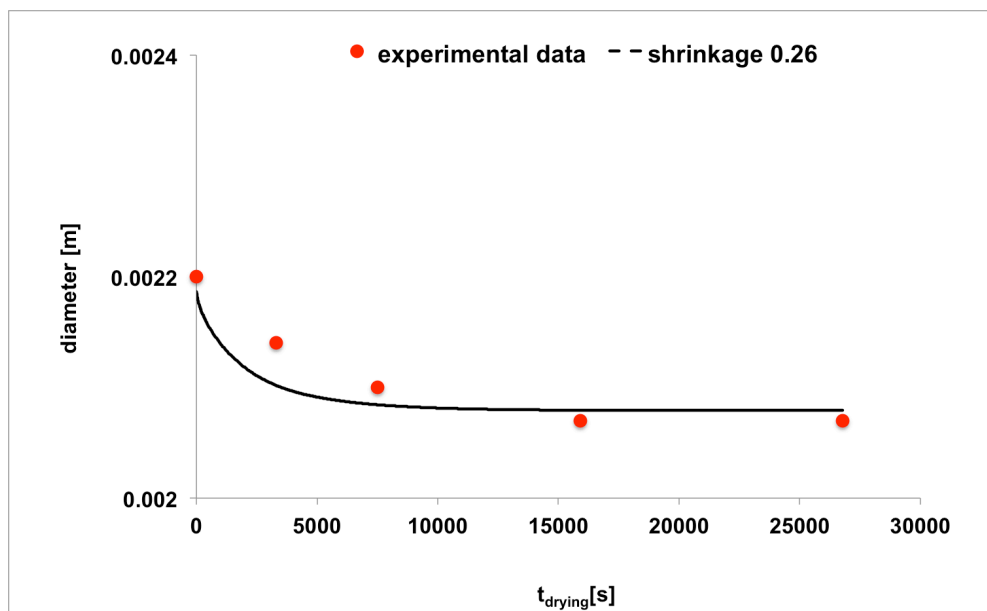


Figure 9. Performance of simulated diameter diameter vs experimental time.

This trend appears to be of crucial importance, because the volume reduction leads to a change in stress within the workpiece subjected to drying.

In this regard, were varied operating conditions, particularly the relative humidity, the temperature and the speed of the airflow used industrially in the production process of the paste, obtaining the following results shown in the Figure 10, 11 and 12.

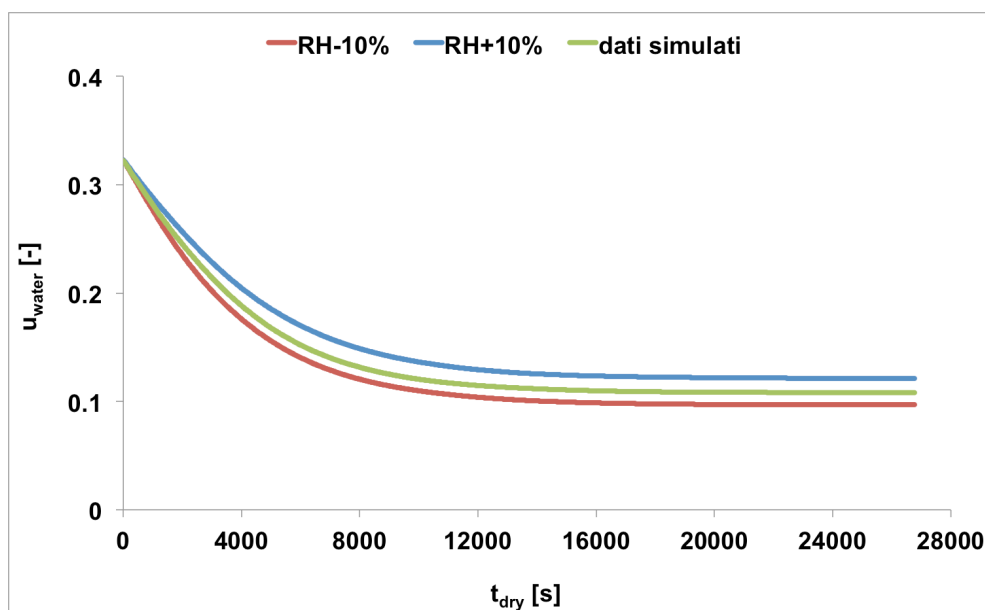


Figure 10. Comparing curve simulated with actual RH and RH increased and decreased by 10%.

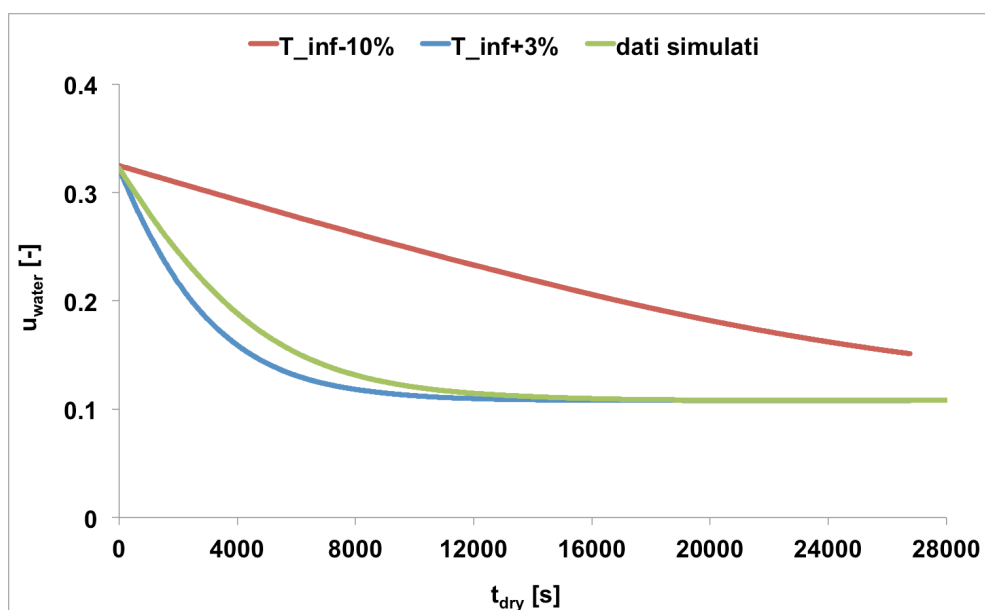


Figure 11. Comparing curve simulated with actual T_{∞} and T_{∞} increased by 3% and decreased by 10%

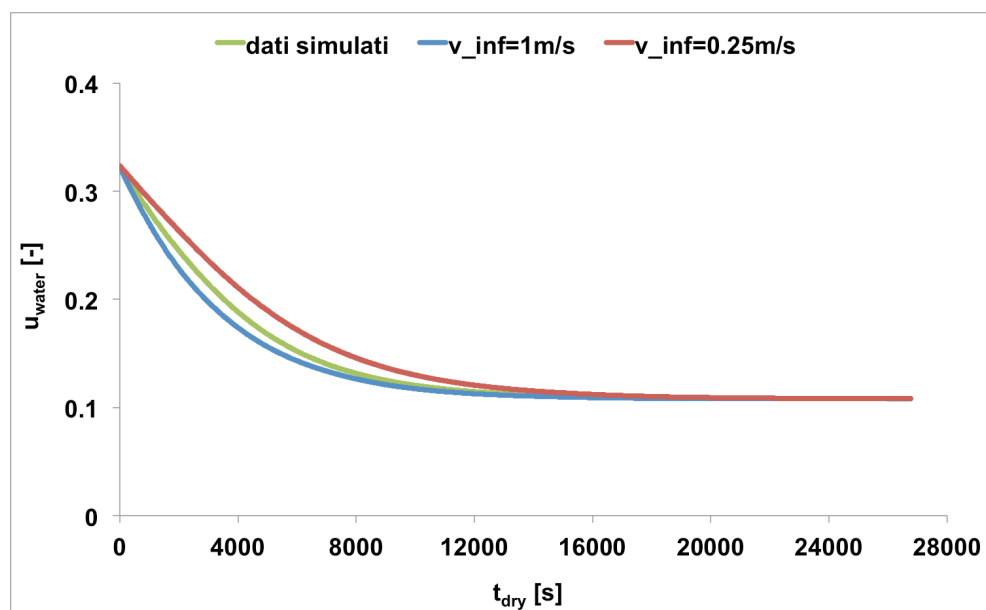


Figure 12. Comparing curve simulated with actual v_{∞} and v_{∞} increased by 1m/s and decreased by 0.25m/s

In the graph of Figure 10 the model sensitivity was performed comparing the simulated data with real operating conditions and then comparing with data obtained by increasing and decreasing by 10% the relative humidity. The model is sensitive to this parameter, and the curve moves downwards or upwards, lowering or raising the humidity conditions. This is due to different driving force that is established in the two cases. Decreasing, in fact, the relative humidity favours the exchange of matter between the flow of air and the sample for the entire duration of the process and is also observed in a last phase slope very low, for higher values, indicating an internal control the transport of matter, essentially diffusive and therefore a greater difficulty in removing the water from the matrix. In the second, increasing the relative humidity there is closer to equilibrium conditions going to disadvantage the exchange of matter and obtaining a product with a moisture content slightly lower than the initial moisture of the sample.

Even in the graph of Figure 11 depending on the increase or decrease in air temperature, the curve is shifted upwards or lower than the curve simulated with real operating conditions. The T_{∞} was decreased by 10%, the minimum driving

force is not capable of promoting the elimination of surface water going to establish, therefore, an equilibrium condition that is not conducive to the drying of the sample and consequently does not lead to decrease of its moisture. While for the temperature of air was possible to make only a 3% increase in that, for higher values the model is not converged. In this case, it is much more evident as the use of a higher T_{∞} go to affect most of the moisture content, as the sample is subjected to a force pushing very high, which favours an elimination faster water present on the surface.

In Figure 12 is varied by the rate of the flow of air is always decreasing and increasing. The mathematical model is simulated for two different airflow rate, $v_{\infty} = 1 \text{ m/s}$ and $v_{\infty} = 0.25 \text{ m/s}$. The value obtained it is compared to the airflow rate actually used, and also from here shows how, by increasing the rate, it reaches a humidity lower than the real conditions as it increases the drying capacity of the air. Naturally, the airflow rate variation affects the first phase of the process, because in this there is a flow of air capable of promoting the exchange of matter. In the second phase, in fact, the slope between the three curves remains almost constant, because it depends on the speed of the airflow. Decreasing the speed, it is known that there is not a net change in the first phase so disfavours the exchange of matter between the airflow and the sample.

Then, it is possible say tat the model is sensitive to the change of the principal operating conditions, and adequately reflect the reality of the industrial process.

REFERENCES

- 1) Andrieu J. and Stamatopoulos A. A., (1986). Moisture and heat transfer modelling during durum wheat pasta drying, *Drying*, (2), 492-498
- 2) Andrieu J. and Stamatopoulos A. A., (1986). Durum wheat pasta drying kinetics. *LWT, Food Science and Technology*, (19), 448-456
- 3) Bird R. B., Stewart E. W. and Lightfoot E. N., (1960). Transport phenomena. *John Wiley and Sons, London, UK*
- 4) de Cindio B., Brancato B. and Saggese A. (1992). Modellazione del processo di essiccamento di Paste Alimentari, *Università "Federico II" di Napoli, Final Report, IMI-PAVAN Project*
- 5) De Temmerman J., Verboven P., Nicolaï B. and Ramon H., (2007). Modelling of transient moisture concentration of semolina pasta during air drying, *Journal of food engineering*, 80, 892-903
- 6) De Temmerman J., Verboven P., Delcour J. A., Nicolaï B. and Ramon H., (2008). Drying model for cylindrical pasta shapes using desorption isotherms, *Journal of food engineering*, 86, 414-421
- 7) Hodge, J. E., (1953). Dehydrated foods, chemistry of browning reactions in model systems, *Journal of Agricultural and Food Chemistry*, (15), 928-943
- 8) Lang, W., Sokhansanj S., Rohani, S. (1994). Dynamic shrinkage and variable parameters in Bakker-Artema's mathematical simulations of wheat and canola drying, *Drying technology*, (13), 2181-2190
- 9) Lewicki P. P., (2000). Raoult's law based food water sorption isotherm, *Journal of Food Engineering*, (43), 31-40
- 10) Litchfield J. B. and Okos M. R., (1992). Moisture diffusivity in pasta during drying, *Journal of Food Engineering*, (17), 117-142
- 11) Mayor L. and Sereno A. M., (2004). Modelling shrinkage during convective drying of food materials: a review, *Journal of Food Engineering*, (61), 373-386
- 12) Mercier S., Villeneuve S., Mondor M., Drolet H., Ippersiel D., Lamarche F. and Des Marchais L. P., (2011). Mixing properties and gluten yield if

- dough enriched with pea protein isolates, *Journal of Food Research*, (1), 13-23
- 13) Migliori M., Gabriele D., de Cindio B. and Pollini C. M., (2005). Modelling of high quality pasta drying: mathematical model and validation, *Journal of Food Engineering*, (69), 387-397
- 14) Mishkin M., Saguy I. and Karel M., (1984). Optimization of nutrient retention during processing: ascorbic acid in potato dehydration, *Journal of Food Science*, (49), 1262-1266
- 15) Owens G., (2001). Cereal Processing Technology. London (UK): Woodhead Publishing
- 16) Ogawa T., Kobayashi T. and Adachi S.. (2012). Prediction of pasta drying process based on a thermogravimetric analysis, *Journal of Food engineering*, (111), 129-134
- 17) Perry R. H. and Green D. W., (1997). Perry's chemical engineering handbook, *McGraw-Hill 7th Edition*
- 18) Ponsart G., Vasseur J., Frias J. M., Duquenoy A., and Méot J. M., (2003). Modelling of stress due to shrinkage during drying of spaghetti, *Journal of Food Engineering*, (57), 277-285
- 19) Saravacos, G. D., and Maroulis, Z. B. (2001). Transport properties of food. New York-Basel (USA): Marcel Dekker Inc.
- 20) Schuchmann H., Roy I. and Peleg M., (1990). Empirical models for moisture sorption isotherms at very high water activities. *Journal of Food Science*, (55), 759-762
- 21) Van den Berg C., (1984). Description of water activity of foods for engineering purposes by means of the GAB model of sorption, *Engineering and Foods*, (1), 311-312
- 22) Veladat R., Ashtiani F. Z., Rahmani M. and Miri T., (2011). Review of numerical modeling of pasta drying, a closer look into model parameters, *Asia-Pacific Journal of Chemical Engineering*, (7), 159-170

- 23) Xing H., Takhar P. S., Helms G. and He B., (2007). NMR imaging of continuous and intermittent drying of pasta, *Journal of Food Engineering*, (78), 61-68
- 24) Waananen K. M. and Okos M. R., (1996). Effect of porosity on moisture diffusion during drying of pasta, *Journal of Food Engineering*, (28), 121-137

Chapter V

Thermo elasto-viscous stresses

1. Introduction

The phenomenon of breaking of the pasta is related to the viscoelastic properties of the dough to changes in humidity. Lower a percentage of water, in the dough prevails behaviour solid that coupled to the deformations associated with the dimensional shrinkage determines the start of stress thermo elasto-viscous which, if not relaxed, may cause surface cracks and the breakage of the piece.

It is, therefore, proposed a predictive model of this phenomenon, coupled with the knowledge of the profiles of temperature and humidity of the treated piece, allows to estimate the stresses that occur in the system, as well as providing a failure criterion which, when coupled with them, provides quantitative information about the integrity of the pasta after treatment and stabilization times during the drying. From latest studies [Phan-Thien et al. (1997)] in the dough prevails a long time the behaviour of solid, which is manifested by an inability to relax completely stresses.

The rheological behaviour varies significantly with the variations of the system. To decrease the humidity of the dough, the solid component increases its weight compared to the liquid, until reaching a value of “critical” moisture (around 15% w.b.), below which the behaviour is assailable to an elastic solid [de Cindio et al., (1992)], so that the rheological characterization of the material is done using the tensile stress mono-dimensional.

In elastic viscous materials, such as dough, three shear-rate-dependent material

functions are essential to complete the state of stress [Steffe, (1992)]. The scalar viscometric functions are: the viscosity function $\eta(\dot{\gamma})$ and the first and second normal stress coefficients $\Psi_1(\dot{\gamma})$ and $\Psi_2(\dot{\gamma})$, which are defined as:

$$\eta = f(\dot{\gamma}) = \frac{\tau_{yx}}{\dot{\gamma}} \quad (1)$$

$$\Psi_1(\dot{\gamma}) = f(\dot{\gamma}) = \frac{\tau_{xx} - \tau_{yy}}{\dot{\gamma}^2} = \frac{N_1}{\dot{\gamma}^2} \quad (2)$$

$$\Psi_2(\dot{\gamma}) = f(\dot{\gamma}) = \frac{\tau_{yy} - \tau_{zz}}{\dot{\gamma}^2} = \frac{N_2}{\dot{\gamma}^2} \quad (3)$$

where the first and second normal stress difference are N_1 and N_2 (measures of elasticity). In non-Newtonian materials it is assumed that $|N_2| \ll N_1$ [Steffe, (1992)]. In Newtonian fluids N_1 and N_2 are zero, which is also valid for viscoelastic materials in the linear region [Kraft, (1999)].

Models for describing viscoelastic behaviour are the two parametrical Maxwell or Kelvin-Voigt model. These combinations are shown in Figure 1.

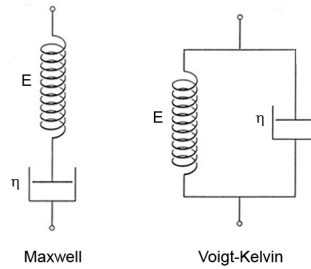


Figure 1. Models uses for approximating creep-recovery response.

2. Mariotte Analysis

In order to reduce the time of the operation of drying and increase the production, it operates in conditions of very hot air and dried.

For the purpose of realizing the drastic conditions within the system, which on one hand improve the transport phenomena, while on the other hand cause a fast drying of the product, causing wrinkling and cracking of the material.

The progressive decrease in volume that occurs inside the mixture is due to the presence of layers with different moisture.

It extends along the radial thickness of the cylindrical system, a reduction that occurs in a diversified manner.

The outer layers, more exposed to the fluid desiccant, show a more rapid contraction compared to the inner layers, which exchange matter with difficulty. Therefore, the shrinkage induced stresses within the structure of the piece: the outer layers dry and pressed on those still moist, more internal. There are thermo-viscoelastic stresses.

The model referred to provide for the abrupt transition of the mechanical properties of the work piece, reached the critical humidity, induces the formation of a crust around a central core, which tends to contract.

The reduction in volume gradually produced in the inner layers during the heating process, it falls with a tension on the outer layer.

If the process is such as to completely break down the water content of said layer, it cannot dissipate more deformation energy.

Thermo viscoelastic stress remains frozen in the elastic layer and remains capable, also in time, to overcome the threshold of breakage. This is the condition of mechanical failure of the structure.

During drying, the occurrence of a layer makes dry spaghetti similar to a tube of thin wall thickness δ , which contains in its interior an elastic-viscous material. The effect of the drying of the layers still moist is a dimensional reduction, which tends to subject the crust, deformable, to a pull inwards which can be schematized as a radial load P_M .

Applying the analysis of Mariotte according to which, for systems with axial symmetry, the average angular $\sigma_{\theta\theta}$ component of the stress tensor is obtainable by imposing the equilibrium condition on the crust itself can treat this problem:

$$\sigma_{\theta\theta} \cdot 2L\delta = P \cdot (2R) \cdot L \quad (4)$$

where L is the length and R the radius of the circular sample.

From this relation it is easy to obtain an expression for the stress as a function of the applied load during the retreat:

$$\sigma_{\theta\theta} = \frac{P_M \cdot R}{\delta} \quad (5)$$

In this analysis we neglect the radial force σ_{rr} , which is zero on the outer surface of the layer dry and is equal to P_M load on the inner surface of the same layer.

The angle stress is greater by a factor R/δ , and is therefore permitted the hypothesis of neglecting σ_{rr} than $\sigma_{\theta\theta}$.

The constitutive equation of the dry material of the crust is elastic type, and the form of proportionality between stress and strain can be assumed to be equal to the transverse modulus G [Pa]:

$$P_M = G(U) \cdot \varepsilon \quad (6)$$

where ε can be calculated as the sum of all the local variations in volume associated with each interior point.

To simplify the calculation, it calculates the sum of the changes in radius associated with each point of calculation used in the modeling:

$$\varepsilon = \sum \Delta(\Delta r_i) \quad (7)$$

In order to determine the stress it is subjected to the contact surface, it is first necessary to analyze the effects of compression of the wetland.

In tracing the state of stress of the points, it is necessary to consider the weight of the components $\sigma_{\theta\theta}$ and σ_{rr} deviatoric tensor of stress.

The thickness of the material in which they develop the stress of interest is and considering negligible the weight force, the mechanical equilibrium of an infinitesimal element of the layer wet, is expressible through the component along the coordinate r :

$$\frac{d\sigma_{rr}}{dr} + \frac{\sigma_{rr} - \sigma_{\theta\theta}}{r} = 0 \quad (8)$$

The load distribution is symmetric about the z -axis, so that the entire terms derivative with respect to θ cancel out, as well as the shear stress σ_{rr} .

As the stresses cannot be determined directly, we resort to the hypothesis of small deformations, which allows assuming an elastic behaviour for the material. Denoted by $E(U)$, the modulus of elasticity and ν the Poisson's ratio for the material wet, it can be assumed the validity of linear elasticity coupled with those of compatibility:

$$e_{\theta\theta} = \frac{1}{E(U)} [\sigma_{\theta\theta} - \nu(\sigma_{rr} + \sigma_{zz})] \quad (9)$$

$$e_{rr} = \frac{1}{E(U)} [\sigma_{rr} - \nu(\sigma_{\theta\theta} + \sigma_{zz})] \quad (10)$$

$$e_{zz} = \frac{1}{E(U)} [\sigma_{zz} - \nu(\sigma_{\theta\theta} + \sigma_{rr})] \quad (11)$$

$$e_{\theta\theta} = \frac{u_r}{r} \quad (12)$$

$$e_{rr} = \frac{\partial u_r}{\partial r} \quad (13)$$

$$e_{zz} \neq e_{zz}(r) \quad (14)$$

where e_{ij} are the strain tensor components and u_r is the r-component of the displacement vector. The coupling relations of compatibility, elasticity and the equation for the equilibrium, neglecting the dependence of E from r and after it is obtained to a differential equation that can be integrated to obtain the following equations (for $\sigma_{zz} \neq 0$):

$$\sigma_{rr} = \frac{-P}{1 + \left(\frac{1-\nu}{1+\nu}\right)} \left[1 + \left(\frac{r_0}{r}\right)^2 \left(\frac{1-\nu}{1+\nu}\right) \right] \quad (15)$$

$$\sigma_{\theta\theta} = \frac{-P}{1 + \left(\frac{1-\nu}{1+\nu}\right)} \left[1 + \left(\frac{r_0}{r}\right)^2 \left(\frac{1-\nu}{1+\nu}\right) \right] \quad (16)$$

The tension P , due to shrinkage, is defined by the equation linear constitutive that binds the stress to deformation, identified only by the volume change.

It is therefore a function of the volumetric compression modulus $K(U)$ on the wet material, and true strain ε_R only due to the increase of the inner radius of r_0 :

$$P = K(U) \cdot \varepsilon \quad (17)$$

where the compression module for a volumetric isotropic linear elastic material is defined as:

$$K(U) = \frac{E(U)}{3(1-2\nu)} \quad (18)$$

where ε_R , being nothing axial deformation, can be written as:

$$\varepsilon_R = \frac{V-V_0}{V_0} \quad (19)$$

Such constitutive equation can be improved by introducing within the module and the time dependence, the memory of the material, according to the following equation:

$$P(t) = \int_0^t M(t-t') dP(t') \quad (20)$$

where

$$dP_M(t) = E(U) \cdot \varepsilon(t) \quad (21)$$

and $M(t-t')$ is a function memory characteristic of the material that allows for addressing the problem in the single time interval with an elastic approach, but with a law of relaxation of elastic-viscous over the entire period.

The value of $K(U)$ is derived viscoelastic constitutive equation and the time-dependence is implicitly contained in the dependence on U that varies over time. As already described, during the drying evaporation triggers shrinkage radial outwards as much inwards. When the outer part to proceed to drying reaches the limit of formation of the crust, it becomes very rigid and therefore can no longer move to follow the shrinkage. As evaporation continues towards the inside, it generates a value of the stress tensor $\sigma_{\theta\theta}$ crust internally to the crown, the normal function of the elastic modulus for the dry material.

This can be identified by calculating the stress state caused by the stress σ_{rr} , b_0 of the inner part to the calculated radius b_0 side pasta obtaining:

$$\sigma_{\theta\theta_{crosta}} = \frac{-2E(U) \cdot (r_0) \cdot \varepsilon_r}{3\delta(1-2\nu)[(1-\nu)+(1+\nu)]} \quad (22)$$

The condition of breakage of the rigid shell along z is due to the attainment of the threshold of rupture by the component $\sigma_{\theta\theta}$ crust.

3. Material and methods

The model just proposed in final form only requires knowledge of the material parameter elastic modulus E as a function of T and U . Although the module represents one of the most widely used parameters to characterize the material, this does not apply to food substances, in particular type of cereal doughs.

In order to derive the elastic modulus of a dough of semolina for pasta industry, has been used a Dynamic Mechanical Analyser (TTDMA, Triton Technology, UK) using the configuration of the type "3-Point Bending", as shown in Figure 2.



Figure 2. TTDMA, 3-point bending clamps configuration

The TTDMA is a material-testing instrument used to characterise the properties of materials. The instrument combines the measurement head and the analysis electronics into one self contained unit.

The measurement head generates sinusoidal forces up to 9N peak, to deform a test sample, and an enclosure around the sample provides heating and cooling to achieve a sample temperature of -150°C to $+600^{\circ}\text{C}$. The medium for heating is electrical power applied to a resistive heater element fabricated from Thermo-Coax. The voltage level for heating is 48Vdc into the 13-ohm element, delivering a maximum of 177W.

The typical frequency range of such instruments is 0.001 to 1000 Hz. Any measurements below 0.01 Hz take too long for most analytical experiments, especially if data are required as a function of temperature and resonance often occurs at frequencies > 100 Hz, depending upon the sample stiffness.

In a dynamic mechanical test it is the sample stiffness and loss that are being measured. The sample stiffness will depend upon its modulus of elasticity and its geometry or shape.

The modulus measured will depend upon the choice of geometry, Young's (E^*) for tension, compression and bending, shear (G^*) for simple shear and torsion. The modulus is defined as the stress per unit area divided by the strain resulting from the applied force. Therefore it is a measure of the material's resistance to deformation, the higher the modulus the more rigid the material is.

Dynamic mechanical testers apply a periodic stress or strain to a sample and measure the resulting strain or stress response. Due to the time-dependent

properties of polymers the resultant response is out-of-phase with the applied stimulus. The complex modulus E^* is defined as the instantaneous ratio of the stress on the strain. To understand the deformational mechanism occurring in the material this is resolved into an in-phase and out-of-phase response.

This is equivalent to a complex number, where E' is the in-phase or elastic response this being the recoverable or stored energy.

E'' is the imaginary or viscous response, this being proportional to the irrecoverable or dissipated energy. The angle δ is the measured phase lag between the applied stimulus and the response. $\tan(\delta)$ is given by ratio E''/E' and is proportional to the ratio of energy dissipated on the energy stored. This is called the loss tangent or damping force. This is of the key parameters in dynamic mechanical testing, since it is seen to increase during transitions between different deformational mechanisms.

This is one of the key parameters in dynamic mechanical. It is possible to obtain the real and imaginary form:

$$E' = \left| \frac{\sigma}{\varepsilon} \right| \cos \delta \quad (23)$$

$$E'' = \left| \frac{\sigma}{\varepsilon} \right| \sin \delta \quad (24)$$

The samples are cut in order to obtain the ideal size for the rheological analysis. Indeed, in a test of this type the geometry and the shape also influence the measured parameters, stiffness and loss. The samples are then dried at 40°C in an oven for the time necessary to reach the moisture to be investigated, and after being lubricated with the silicon oil, they are subjected to analysis.

DMA tests have been performed at different humidity and temperature values.

The sample length in 3 point bending is the distance between the midpoint of the driveshaft clamp and the midpoint of either of the fixed clamps (which is half length of the sample supported between the two fixed clamps). Three-point bending depends on the specimen being a freely moving beam, and the sample should be about 10% longer on each end than the span. The four sides of the span should be true parallel to the opposite side and perpendicular of the neighbouring sides.

There should be no nicks or narrow parts. The sample is loaded so the three edges of the bending fixture are perpendicular to the long axis of the sample.

Before the test, pretension is necessary in order to maintain the sample under a net tension to prevent buckling that would otherwise occur.

The modulus E is calculated using

$$E = \frac{S}{k} \quad (25)$$

where S is the measured stiffness in N/m and k is the geometry constant in m^{-1} .

The geometry constant (k) is calculated using the following basic equations where w is the width, t is the thickness and l is the free length. In 3 point bending, k is calculated as:

$$k = \left(\frac{w}{2}\right) \cdot \left(\frac{t}{l}\right)^3 \quad (26)$$

4. Relaxation mechanism

The complete model requires the definition of the relaxation function $M(t-t')$, which appears in the equation 20. To specify this function can be used to the analysis of material evidence rheological *Creep-Recovery*.

The test is completed with the phase of Recovery, in which the applied stress is removed and is studied the recovery exhibited by the material in terms of decrease of $J(t)$ in time. The curve thus obtained provides useful information about the relaxation of the efforts made by the material and, generally correlate the experimental data using a series of models of Voigt [Lapasin & Pricl, (1995)] with a shape of the type:

$$\frac{J(t'')}{J(t'')|_{t''=0}} = W_0 + \sum_i P_i e^{-t/\lambda_i} \quad (27)$$

This equation contains essentially a series of pairs (W_i, λ_i) , which provide delay times (λ_i) and the rate of deformation relaxed in these times (P_i). With this logic, P_0 represents that part of residual deformation, which, therefore, the material never recovers.

The delay time is the time beyond which the material does not recover the deformation applied and, therefore, exhibits behaviour predominantly "liquid-

like". The relaxation time of the system, which corresponds to the moment beyond which the material, by relaxing the whole or in part, the effort applied exhibits a behaviour from "fluid", can be considered reasonably coincident with the delay time obtained by the analysis the creep-recovery.

Tests of Creep-Recovery have been performed, at different stress values, between 10 and 200 Pa, and the result of the phase of Recovery has been correlated with the equation 32, limited to two elements of Voigt.

$$M(t) = W_1' e^{-t/\lambda_1} + W_2' e^{-t/\lambda_2} \quad (28)$$

5. Result and discussion

Dynamic mechanical analyser and creep recovery tests are carried out for the sample S1. A typical result the TTDA analysis is shown in Figure 3.

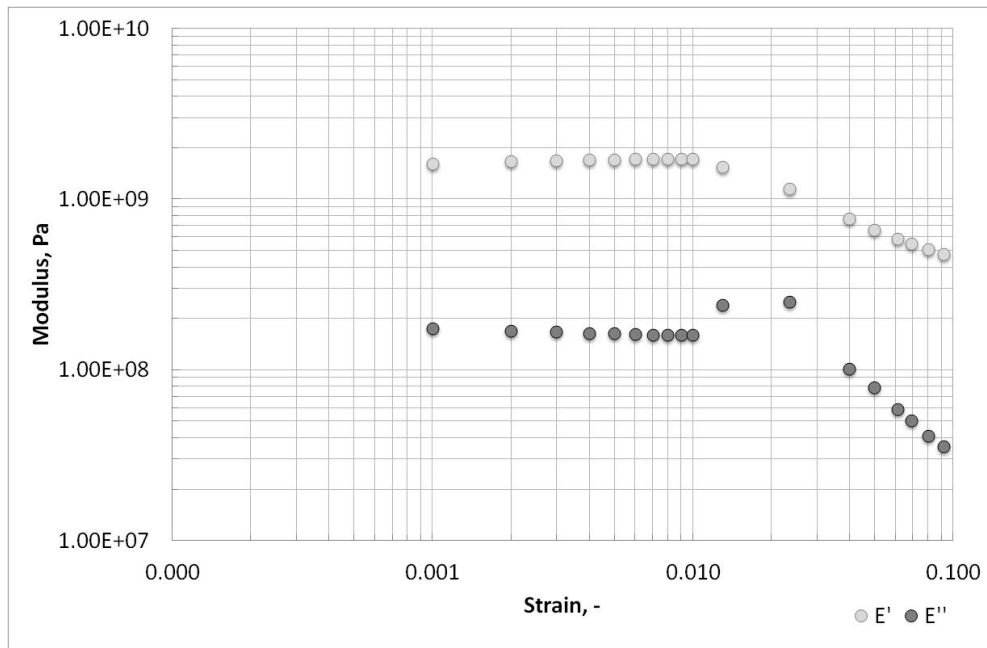


Figure 3. E', E'' vs strain at T=25°C and U=14.7% [w.b.]

It can be observed as $E' \gg E''$ throughout the analysis and then as the sample moisture investigated show a solid behaviour.

In Table 1 is showed results for TTDA tests.

| $E [N*mm^{-2}]$ | | $Umidità [\% w.b.]$ | | | | | |
|-------------------|---------------|---------------------|--------------|--------------|-------------|-------------|--------------|
| $Temperatura [K]$ | | 10.84 | 11.41 | 12.94 | 13.1 | 14.6 | 15.12 |
| | 298.15 | 1700 | 1575 | 1699 | 1543.5 | 1435.5 | 1189 |
| | 323.15 | 1000 | 1050 | 992 | 929 | 864 | 762 |
| | 343.15 | 600 | 580 | 590 | 559 | 413 | 383 |

Table 1. Elastic modulus for the sample S1. Experimental values are representing as functions of moisture and temperatures.

To facilitate the use of the data in the numerical model, the values shown have been correlated with an interpolation curve, which takes into account both functionality with temperature and moisture:

$$E(T, U) = A(T) \cdot U^2 + B(T) \cdot U + C(T) \quad (29)$$

The interpolation is carried out through the use of software Table Curve 3D and shown in Table 2

| $Temperatura [K]$ | $A [N*mm^{-2}]$ | $B [N*mm^{-2}]$ | $C [N*mm^{-2}]$ | r^2 |
|-------------------|-----------------|-----------------|-----------------|---------|
| 298.15 | -39.175 | 924.52 | -3781.2 | 0.837 |
| 323.15 | -15.775 | 364.78 | -1106.3 | 0.951 |
| 343.15 | -27.438 | 659.28 | -3322 | -27.438 |

Table 2. Parameter values at different moisture

The data in Table 2, are correlated, in order to obtain the functionality of A, B and C with the temperature T through the correlations of the type

$$A(T) = A_1 \cdot T^2 + A_2 \cdot T + A_3 \quad (30)$$

$$B(T) = B_1 \cdot T^2 + B_2 \cdot T + B_3 \quad (31)$$

$$C(T) = C_1 \cdot T^2 + C_2 \cdot T + C_3 \quad (32)$$

Results are showed in Table 3.

| A_1 [N*mm ⁻² *K ⁻²] | A_2 [N*mm ⁻² *K ⁻¹] | A_3 [N*mm ⁻²] | r^2 |
|---|---|--------------------------------|-------|
| -0.0338 | +21.91 | -3571 | 0.996 |
| B_1 [N*mm ⁻² *K ⁻²] | B_2 [N*mm ⁻² *K ⁻¹] | B_3 [N*mm ⁻²] | r^2 |
| 0.8248 | -534.82 | 87064 | 0.992 |
| C_1 [N*mm ⁻² *K ⁻²] | C_2 [N*mm ⁻² *K ⁻¹] | C_3 [N*mm ⁻²] | r^2 |
| -4.8396 | +3113.8 | -501962 | 0.995 |

Table 3. Values of the parameters of the Equation 33 in function of temperature

Creep recovery tests are performed for differences samples. A typical example, for sample S1, is shown in Figure 4.

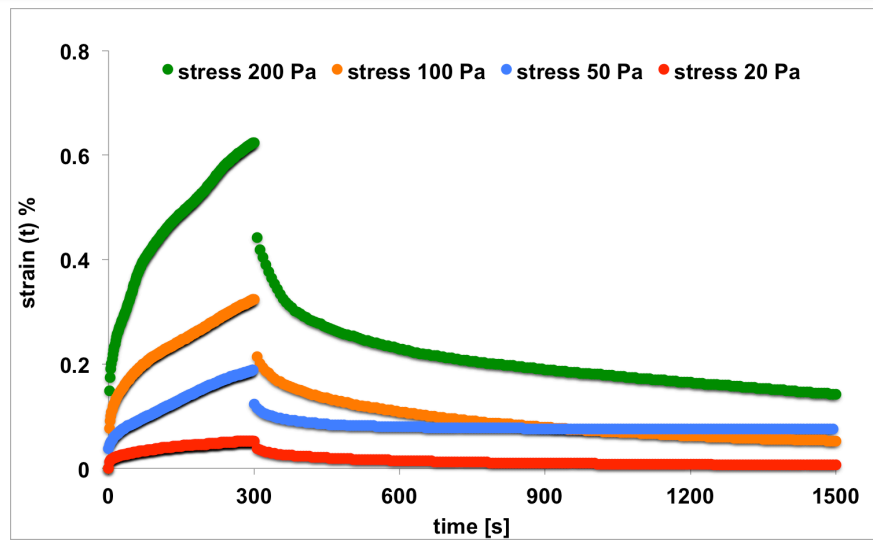


Figure 4. Creep-Relaxation of mixtures of durum semolina at different values of strain imposed, for the sample S1.

The element parameters of Voigt are reported in Table 4.

| <i>Parameters element of Voigt</i> | <i>Value</i> |
|--|--------------|
| $W'_1[-]$ | 0.590 |
| $W'_2[-]$ | 0.40 |
| $\lambda'_1[s]$ | 400 |
| $\lambda'_2[s]$ | 40.7 |

Table 4. Parameters with 2 element of Voigt.

After this, it is evaluated the stress of rupture σ_{rupt} . This parameter is important and is used as quality control index and different temperature-humidity profiles, in order to distinguish critical operating conditions [de Cindio B. et al (2002)]. During the test, the stress of rupture is evaluated extending the test over the limit of rupture.

The values of rupture are been obtained from literature Pollini et al. (1992), as function of temperature and moisture. Data are shown in Table 5.

| $\sigma_{rupt} [N \cdot mm^{-2}]$ | | <i>Umidità [%w.b.]</i> | | | | | | |
|-----------------------------------|------------|------------------------|--------------|--------------|--------------|--------------|--------------|-------------|
| | | 9.23 | 10.13 | 11.56 | 11.98 | 13.13 | 13.82 | 14.5 |
| <i>Temperature</i> [K] | 298 | 20.4 | 18.1 | 10 | 10.2 | 7.5 | 6.3 | 3.5 |
| | 323 | 9.4 | 4.7 | 3.9 | 3.1 | 2.3 | 1.9 | 1.6 |
| | 343 | 5 | 3.0 | 2.5 | 2.2 | 2.0 | 1.6 | 1.6 |

Table 5. Value of the stress of rupture [Pollini et al., (1992)].

This data can be fitting with this equation in which there is express functionally with moisture and temperature:

$$\sigma_{rupt} = M(T) \cdot U^{N(T)} \quad (30)$$

Data $M(T)$ and $N(T)$ are showed in Table 6.

| <i>Temperatura [K]</i> | $M [N \cdot mm^{-2}]$ | <i>Errore M [N·mm⁻²]</i> | <i>N[-]</i> | <i>Errore N [-]</i> | R^2 |
|------------------------|---|-------------------------------------|--------------|---------------------|-------|
| 298 | 66070 | 14 | -3.52 | 0.43 | 0.93 |
| 323 | 25700 | 24 | -3.62 | 0.31 | 0.96 |
| 343 | 812 | 12 | -2.35 | 0.26 | 0.94 |

Table 6. Values of parameters of Eq. (30), $M(T)$ and $N(T)$.

The values of $\sigma_{\theta\theta}$ are compared with σ_{rupt} . If $\sigma_{\theta\theta} > \sigma_{rupt}$, the sample of pasta is broken, otherwise the final product maintains its high characteristics for sale.

The thermo viscoelastic stress and the stress of rupture are representing as function of time. The cross of two curves is identified as the condition of broken of vermicellone. An example is shown in Figure 5.

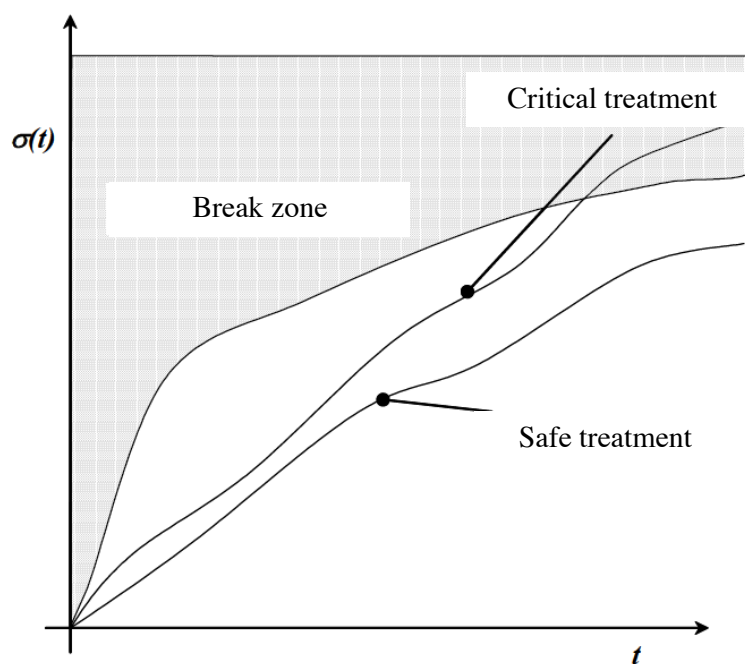


Figure 5. Example of the application of the principle of rupture.

The mathematical model of the stress is assembled in the structure of drying pasta model. This model is function of moisture, temperature and shrinkage data and it can calculate the module, the stress of rupture and the deformation necessary. This information is evaluated in the rheological model that estimates the internal stress with the Mariotte analysis and the possibility that this stress exceeds the threshold of breakage.

The result is showed in Figure 6 and 7.

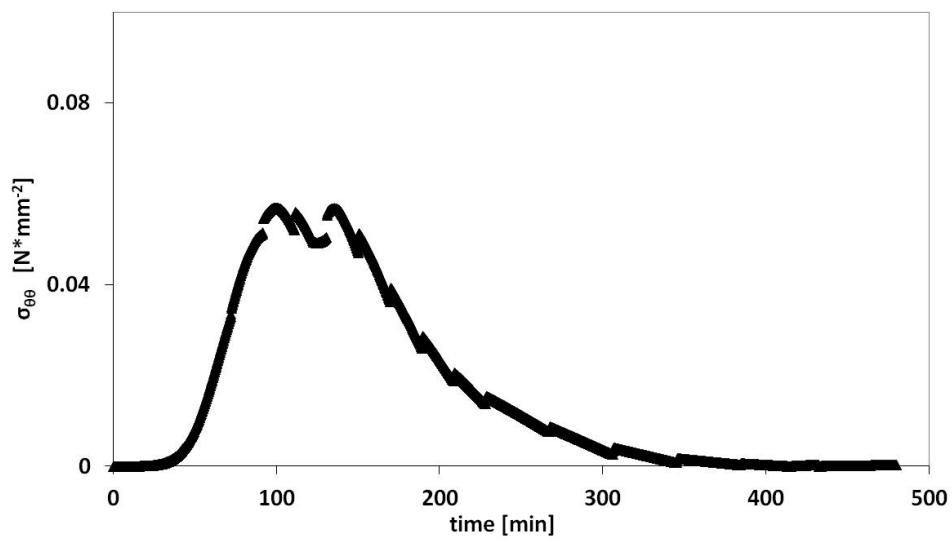


Figure 6. Curve of thermo viscoelastic stress as function of time.

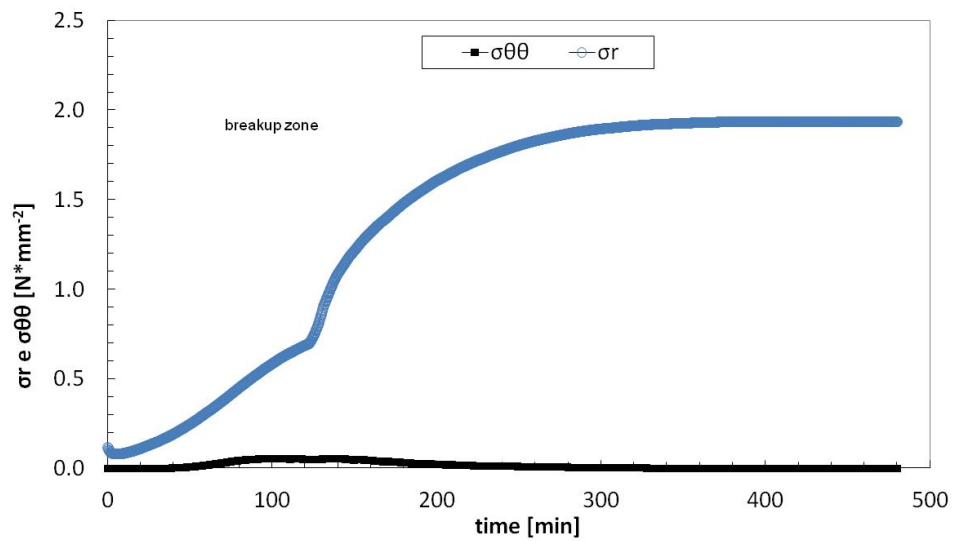


Figure 7. Curves of the stress of rupture and the thermo viscoelastic stress as function of time.

From the Figure 6 and 7, it is clear, as the $\sigma_{\theta\theta}$ inside of the sample of pasta never exceed the stress of rupture. From this point of view, it is reasonable optimization the time of drying process in function of the stress of the rupture. Because during the whole drying process, the stress of rupture is of and order of magnitude higher than the internal stress if the sample.

REFERENCES

- 1) de Cindio B., Brancato B. and Saggese A., (1992). Modellazione del processo di essiccamento di Paste Alimentari, *Università "Federico II" di Napoli, Final Report, IMI-PAVAN Project*
- 2) de Cindio B., Gabriele D., Migliori M. and Pollini C. M., (2002). Modelling of drying for high quality pasta production, 3^o International symposium on food rheology and structure, 635-636
- 3) Kraft M., Meissner J. and Kaschta J., (1999). Linear viscoelastic characterization of polymer melts with long relaxation times, *Macromolecules*, (32), 751-757
- 4) Lapasin R. and Priel S., (1995). Rheology of polysaccharide systems, Springer US, 250-494
- 5) Phan-Thien N., Safari-Ardi M., Morales P. A., (1997). Oscillatory and simple shear flows of a flour-water dough: a constitutive model, *Rheol Acta*, (36), 38-48
- 6) Pollini, C.M., de Cindio, B., Brancato, B., Lionetti, G. and Saggese, A. (1992). Misure delle proprietà meccaniche di spaghetti. *Atti del I Convegno RheoTech di Reologia Applicata*, Trieste 26-27 Novembre 1992, 50-53.
- 7) Steffe, J. F., (1992). Rheological Methods in Food Process Engineering Vol 2. Freeman Press, East Lansing

Conclusions

In the present PhD thesis has as end the study of mathematical modeling, experimental validation and optimization of transport phenomena that occur during the drying process in the production of dry pasta and as the different operating parameters used in the mixing step and in the drying of the dough (time of mixing, the initial amount of protein, water temperature, mixing, etc.) can influenced the process.

The aim of this thesis is to obtain a more accurate and predictive of the process and therefore an improvement in the quality of the final production.

To this purpose is analysed semolina with different fraction of protein.

In order to investigate the optimum network formation for high quality pasta dough during mixing, dough rheological properties are measured with the dynamic oscillatory test and in uniaxial extension, respectively analysed in according the model of weak gel and the Hollomon equation.

The rheological characterization of the samples in kinematic oscillatory are performed for the time of mixing, the temperature of mixing and the temperature of measure.

At the low temperature of mixing, the dough is only partially developed.

The dough structure changes between 20 and 40°C, because of the higher mobility and the unfolding of some semolina molecules, possibly linked to the transformation of some proteins from a vitreous to a rubbery stage.

At the increasing the temperature of measure, the temporary network becomes weaker, after the occurrence of the gelatinisation the network became stronger and therefore both dynamic moduli must increase. The loss tangent is the same, because the temperature has no effects on the extension of network as evidenced by almost constant value of z . On the contrary a reduction of the network strength is observed by the decrease of G' and G'' .

For the sample S1, a parity of the temperature of mixing can be seen as the parameter A has a slight increase with the time of mixing, while the extension z is constant. The analysis conducted on other durum semolina not show particular differences between the different stresses analysed, while the measurements

performed in uniaxial elongation showed a dependence on the conditions of mixing by the protein content.

The use of Hollomon equation has identified a dependence of the index of strain hardening by the protein content and the process temperature.

The uniaxial elongation tests of the samples are performed for the time of mixing, the temperature of mixing and the rate of elongation.

The index of strain hardening has been well correlated to the optimum mixing time, which would seem to decrease with increasing the protein content and temperature. This result is verified by SEM analysis.

The index of strain-hardening, for a mixing temperature of 20°C, does not show a significant trend with the time of mixing, due to the fact that low temperatures do not favour hydration of starch and consequently entail a delay in the development of gluten chain. For mixing temperature of 30 and 40°C, the index of strain hardening increases as the mixing time. At the increasing the rate of elongation the index of strain hardening increases.

In order to optimize the time industrial drying of the paste, it has been carried out writing of a mathematical model of the process that requires writing the balance equations of momentum, of energy and matter coupled with the appropriate boundary conditions, which through the use of appropriate dimensionless analysis.

In the simulation program is introduced the stress within pasta format laundry during the drying and the problem is resolve with analysis of Mariotte.

The σ_{00} inside of the sample of pasta never exceed the stress of rupture. From this point of view, it is reasonable optimization the time of drying process in function of the stress of the rupture. Because during the whole drying process, the stress of rupture is of and order of magnitude higher than the internal stress if the sample.

Conclusions

In the present PhD thesis has as end the study of mathematical modeling, experimental validation and optimization of transport phenomena that occur during the drying process in the production of dry pasta and as the different operating parameters used in the mixing step and in the drying of the dough (time of mixing, the initial amount of protein, water temperature, mixing, etc.) can influenced the process.

The aim of this thesis is to obtain a more accurate and predictive of the process and therefore an improvement in the quality of the final production.

To this purpose is analysed semolina with different fraction of protein.

In order to investigate the optimum network formation for high quality pasta dough during mixing, dough rheological properties are measured with the dynamic oscillatory test and in uniaxial extension, respectively analysed in according the model of weak gel and the Hollomon equation.

The rheological characterization of the samples in kinematic oscillatory are performed for the time of mixing, the temperature of mixing and the temperature of measure.

At the low temperature of mixing, the dough is only partially developed.

The dough structure changes between 20 and 40°C, because of the higher mobility and the unfolding of some semolina molecules, possibly linked to the transformation of some proteins from a vitreous to a rubbery stage.

At the increasing the temperature of measure, the temporary network becomes weaker, after the occurrence of the gelatinisation the network became stronger and therefore both dynamic moduli must increase. The loss tangent is the same, because the temperature has no effects on the extension of network as evidenced by almost constant value of z . On the contrary a reduction of the network strength is observed by the decrease of G' and G'' .

For the sample S1, a parity of the temperature of mixing can be seen as the parameter A has a slight increase with the time of mixing, while the extension z is constant. The analysis conducted on other durum semolina not show particular differences between the different stresses analysed, while the measurements